Estimating and monitoring the phenological cycle of bracken fern *(Pteridium Aquilinum)* using remote sensing

Trylee Nyasha Matongera

215081306

A thesis submitted in the fulfillment for the Degree of Doctor of Philosophy in Environmental Sciences, under the School of Agricultural, Earth and Environmental Sciences, University of KwaZulu-Natal.

Supervisor: Professor Onisimo Mutanga

Pietermaritzburg, South Africa

January 2022

Bracken fern, '*the problem plant*'

Global climate change has become entangled with the problem of alien invasive species. A warmer climate could allow some invaders to spread further, while causing native organisms to go extinct in their traditional habitats and making room for invaders.

-

Richard Preston

Abstract

Bracken fern is an invasive alien plant that has caused serious disturbances in many ecosystems due to its ability to encroach into areas of biological importance rapidly. Adequate knowledge of the phenological cycle and the associated morphological and physiological traits of bracken fern is required to serve as an important tool in formulating management plans to control the spread of the fern. The focus of this study was to estimate and monitor the phenological cycle of bracken using remotely sensed data. The first objective of the study focused on reviewing the progress and challenges in the remote sensing of Land Surface Phenology (LSP) in rangelands. The review provided a synopsis of developments in plant phenology studies using remote sensing. The study documented the evolution of satellite sensors and interrogates their properties as well as the associated indices and algorithms in quantifying plant phenological characteristics. Findings from the literature show that the Normalized Difference Vegetation Index (NDVI) pioneered LSP investigations and most other spectral vegetation indices were developed to address the weaknesses and shortcomings of the NDVI. New spectral indices continue to be developed based on recent sensors such as Sentinel-2. The Sentinel-2 sensor is characterized by unique spectral channels and fine spatial resolutions and its successful usage is catalysed by the development of cutting-edge algorithms for modelling the LSP profiles.

The second objective of the study characterized the phenological cycle of bracken fern using NDVI and the two band Enhanced Vegetation Index (EVI2) time series data derived from Sentinel-2 multispectral sensor. The TIMESAT program was used for removing low quality data values, model fitting and extraction of bracken fern phenological metrics. Findings from the study revealed that bracken fern phenological metrics estimated from satellite data were in close agreement with ground observed phenological events with R^2 values ranging from 0.53 -0.85 ($p < 0.05$). Although they were comparable, findings from the study revealed that NDVI and EVI2 differ in their ability to track the phenological cycle of bracken fern. Overall, EVI2 performed better in estimating bracken fern phenological metrics as it related more to ground observed phenological events compared to NDVI. The third objective of the study estimated the spatial distribution of bracken fern during the green up stage using the One Class Support Vector Machine (OCSVM) and Biased Support Vector Machine (BSVM) algorithms. The results show that in all data set combinations, the BSVM algorithm outperformed OCSVM with average overall accuracies of 0.89 and 0.93 respectively. The data sets which combined spectral bands, vegetation indices and topographic variables yielded the highest accuracies compared to all other datasets based on the two algorithms. Generally, the accuracy trends

revealed by the models show that as vegetation indices and topographic variables were added, the overall model performance improved significantly by an average of 2-4% accuracy.

The fourth objective optimized the Transformed Difference Vegetation Index (TDVI) for mapping bracken fern phenology. Five variants of the Optimized Transformed Difference Vegetation Index (OTDVI) were developed based on the ratios of spectral bands that showed maximum discrimination between bracken fern and other land cover classes. The optimal features selected by the SFS algorithm were used to map bracken fern at its four phenological stages. The findings from the current study revealed that there was a positive correlation ($r <$ 0.51) between the OTDVI variants trends and ground measured LAI. The $OTDVI_3$, developed using red edge (Band 7) and Near Infrared (NIR) was the most influential index in mapping bracken fern during green up and green peak stages. The $OTDVI_4$ that was calculated using SWIR (Band 11) and NIR was ranked as the best feature for mapping bracken fern during the dormancy phenological stage. Generally, the bracken fern classification results were good across all phenological stages, with an average overall accuracy of 90%.

The fifth objective assessed the spatial variability of bracken fern during the dormancy phenological stage using. An object-based classification approach was proposed for the assessment of the spatial variability of the fern during the dormancy phenological stage. The study also quantified the spatial variability of bracken fern across the landscape and its relationship with topographic variables. The Simple Non-Iterative Clustering (SNIC) was used to identify the spatial clusters while the Gray-Level Co-occurrence Matrix (GLCM) was employed for the computation of textural indices on a cluster basis. The findings from the current study shows that the object-based classification approach which included bracken fern texture information yielded the highest overall accuracy (89%). The major topographic variables influencing the spatial variability of bracken fern during the dormancy phenological stage were elevation, Topographic Wetness Index (TWI), valley depth and positive openness. Overall, the study has characterized bracken fern as a serious invasive species in KwaZulu-Natal, South Africa from both phenological and spatial dimensions. This is critical for providing important decision support tools on rangeland management in the face of climate change.

Keywords: Remote sensing; Phenology; Sentinel-2; Bracken fern; Vegetation indices; Phenology metrics; Rangelands

Preface

This study was conducted in the School of Agricultural, Earth and Environmental Sciences, University of KwaZulu-Natal, Pietermaritzburg, South Africa, from June 2017 to December 2021, under the supervision of Professor Onisimo Mutanga.

I declare that the work presented in this thesis has never been submitted in any form to any other institution. This work represents my original work except where due acknowledgments are made.

Student: **Trylee Nyasha Matongera**

Signed ……………………………   Date…10/01/2022…….

As the candidate's supervisor, I certify the statement and have approved this thesis for submission.

Supervisor: **Professor Onisimo Mutanga**

Signed……………   Date……10/01/2022……..

Declaration 1: Plagiarism

I Trylee Nyasha Matongera, declare that:

1. The research reported in this thesis, except where otherwise indicated is my original research.

2. This thesis has not been submitted for any degree or examination at any other institution.

3. This thesis does not contain other person's data, pictures, graphs or other information, unless specifically acknowledged as being sourced from other persons.

4. This thesis does not contain other persons writing, unless specifically acknowledged as being sourced from other researchers. Where other written sources have been quoted:

    a. Their words have been re-written and the general information attributed to them has been referenced.

    b. Where their exact words have been used, their writing has been placed in italics inside quotation marks and referenced

5. This thesis does not contain text, graphics or tables copied and pasted from the internet, unless specifically acknowledged, and the source being detailed in the thesis and in the references section.

Signed:……………………………   Date……10/01/2022…..

Declaration 2: Publications

1. **Matongera, T. N.,** Mutanga, O., Odindi, J, and Sibanda, M. (2021): 'Estimating and monitoring Land Surface Phenology in Rangelands: A review of progress and challenges', <u>MDPI Remote Sensing Journal</u>, 13: 48-67.

2. **Matongera, T. N.,** Mutanga, O, and Sibanda, M. (2021): 'Characterizing bracken fern phenological cycle using time series data derived from Sentinel-2 satellite sensor', <u>PLOS ONE: Remote Sensing</u>, 16:10 -23.

3. **Matongera, T. N.,** Mutanga, O., Sibanda, M., and Mutowo. G. 'Estimating the spatial distribution of bracken fern during the green up phenological stage using limited ground sample data, <u>IEEE Journal of Selected Topics in Applied Earth Observations and Remote Sensing,</u> Under Review, Manuscript ID: JSTARS-2021-01075.

4. **Matongera, T. N.,** and Mutanga, O. 'Optimization of the Transformed Difference Vegetation Index for mapping and monitoring of bracken fern phenology', <u>International Journal of Remote Sensing,</u> Submitted to Journal.

5. **Matongera, T. N.**, Mutanga, O, and Omosalewa, O. 'Assessing the spatial variability of bracken fern during dormancy phenological stage using object-based image analysis', In preparation.

Dedication

I dedicate this dissertation to all the fearless frontline health workers who have been bravely fighting against the COVID-19 pandemic globally.

Acknowledgments

Table of Contents

List of Tables

List of Figures

List of Acronyms

ABI	Advanced Baseline Imager
AG	Asymmetric Gaussian
ASTER	Advanced Spaceborne Thermal Emission and Reflection Radiometer
AVHRR	Advanced Very High-Resolution Radiometer
BRT	Boosted regression trees
BSVM	Biased Support Vector Machine
DEM	Digital Elevation Model
DL	Double Logistic
EOS	End of Season
ESA	European Space Agency
EVI	Enhanced Vegetation Index
FAPAR	Fraction of Absorbed Photosynthetically Active Radiation
FPR	False Positive Rate
GEE	Google Earth Engine
GIS	Geographic Information Systems
GLCM	Gray-Level Co-occurrence Matrix
GPS	Global Positioning System
GRVI	Green-Red Vegetation Index
IDE	Integrated Development Environment
IGSO-RF	Improved Grid Search Optimization Random Forest
ILTER	International Long Term Ecological Research Network
KZN	KwaZulu-Natal
LAI	Leaf Area Index
LSP	Land Surface Phenology
MAB	Mean Absolute Bias
MERIS	Medium Resolution Imaging Spectrometer
MODIS	Moderate Resolution Imaging Spectroradiometer
MSI	Multispectral Instrument
MTCI	MERIS Terrestrial Chlorophyll Index
MTMF	Mixture Tuned Matched Filtering
NDPI	Normalized Difference Phenology Index
NDVI	Normalized Difference Vegetation Index
NDWI	Normalized Difference Water Index
NIR	Near-infrared
OA	Overall Accuracy
OCC	One Class Classification
OCSVM	One Class Support Vector Machines
OTDVI	Optimized Transformed Divergence Spectral Index
PA	Producer Accuracy
PI	Phenology Index
POS	Peak of Season
PPI	Plant Phenology Index
PVI	Perpendicular Vegetation Index
RBF	Radial Basis Function

RF	Random Forest
RMSD	Root Mean Square Difference
ROC	Receiver Operating Characteristic
RVI	Ratio Vegetation Index
SAC	Semi-Automatic Classification
SANBI	South African National Biodiversity Institute
SAVI	Soil-Adjusted Vegetation Index
SEVIRI	Spinning Enhanced Visible and InfraRed Imager
SFS	Sequential Forward Selection
SG	Savitzky-Golay
SIF	Solar-Induced Chlorophyll Fluorescence
SNIC	Simple Non-Iterative Clustering
SOS	Start of Season
SPOT	Satellite Pour l 'Observation de la Terre
SR	Simple Ratio
SRTM	Shuttle Radar Topography Mission
SVM	Support Vector Machines
SWI	Shortwave
TDVI	Transformed Difference Vegetation Index
TM	Thematic Mapper
TPR	True Positive Rate
TWI	Topographic Wetness Index
UA	User Accuracy
UAVs	Unmanned Aerial Vehicles
VIIRS	Visible Infrared Imaging Radiometer Suite
VOD	Vegetation Optical Depth
WDRVI	Wide Dynamic Range Vegetation Index

Chapter One: General Introduction

1.1 Introduction

Human activities continue to facilitate the spread of invasive species through increased global mobility, leading to alteration of the rangelands and changes in the global climate (Václavík and Meentemeyer, 2012, Rocchini et al., 2015). The encroachment of invasive alien plants is largely associated with environmental, economic and cultural costs (Andrew and Ustin, 2008). Bracken fern has been one of the problematic invasive alien plants invading rangelands globally (Matongera et al., 2021a). The invasion of bracken fern has caused huge agricultural losses in many countries around the world. In severe circumstances such as in Mexico (Schneider and Geoghegan, 2006b), farmers abandoned agricultural land due to the uncontrollable spread of the fern. Additionally, livestock consuming bracken suffer from poisoning and cancers (Marrero et al., 2001). Bracken also produces toxic compounds that exert allopathic effects on other plant species (García-Jorgensen et al., 2021). The fern reduces water quality and yield in infested catchments that are used by the public, leading to high water scarcity and collection costs (García-Jorgensen et al., 2021). In South Africa, bracken fern has been a problematic invader in the Drakensberg Mountains, causing a threat to the rangeland biodiversity (Matongera et al., 2017). According to the South African National Biodiversity Institute (SANBI), bracken fern is amongst the red list of the most dangerous plants in South Africa (Raimondo et al., 2015). Although it is not clear how bracken fern was introduced in the Drakensberg, Finch et al. (2021) noted that archeological evidence suggests that the existence of bracken fern in the Drakensberg montane grasslands can be traced back to as far as 1840 Common Era (CE).

According to the Biodiversity Act 10 of 2004, it is specified that landowners are under legal obligation to control bracken fern occurring on their properties (Lukey and Hall, 2020). The control methods of alien invasive plants can be broadly classified into three categories: mechanical, chemical and biological (McDonald et al., 2003). The successful eradication of bracken fern in rangelands largely depends on the ability of the rangeland managers to develop and implement effective management plans. Evidence from literature reveals that the current bracken fern control approaches mainly emphasize the use of spatial and temporal data (Odindi et al., 2014, Schneider, 2006, Ngubane et al., 2014). However, advancing the knowledge on the phenological cycle and spatial dynamics of bracken fern will assist in decreasing the probability of future invasion at local and regional scales (Bradley and Mustard, 2006).

Bracken fern phenological information can be used to build models that predict future invasions, areas that are at risk of future bracken fern invasion. Additionally, understanding the dynamics in the phenological cycle of bracken fern is the key point in the restoration and reconstruction of the rangelands infected by the problematic fern. For instance, information on the start of the bracken fern season will help rangeland managers when to begin to implement control strategies while data on the end of the fern cycle will give them a chance to clear and uproot the residuals from the previous season. Due to the detrimental effects of bracken fern on the socio-economic environmental and ecological infrastructure, there is a need to understand the phenological cycle of the fern. Browning et al. (2019) defined phenology as the study of cyclic and seasonal variations of vegetation and their relationship to local and global environmental factors. Phenology has been documented in literature as one of the major influencers of carbon recycling, succession, ecosystem productivity and health (Sun et al., 2022, Kross et al., 2014, Migliavacca et al., 2015). Phenology is a valuable diagnostic tool that can be used to assess rangeland productivity and healthy (Clinton et al., 2010).

Previous efforts to understand the phenological cycles of bracken fern were more focused on traditional approaches such as direct human observation by botanists, farmers and volunteers at a local scale (Pakeman et al., 1994). However, the use of locally based data collection methods in phenology is limited by the spatial extent to which the plant phenological events are collected (Matongera et al., 2021b). The collection of plant phenology data using ground-based methods is expensive, tedious and time consuming (Matongera et al., 2021b). Remote sensing offers better prospects to estimate and monitor the phenological cycles of vegetation at both local and global scales (Berra and Gaulton, 2021, Bolton et al., 2020, Cheng et al., 2020). Remotely sensed data provides an opportunity to track and monitor the dynamics of terrestrial vegetation and it delivers important insights into rangeland monitoring and biodiversity conservation (Xue and Su, 2017). Remote sensing of plant phenology as an indicator of climate change and mapping land cover has received significant scientific interest recently (Misra et al., 2020). Over the past four decades, time series measurements derived from satellite platforms have been tracking the changes in annual and inter-annual greenness conditions of vegetation (Kumari et al., 2021). The time series data is important in characterizing and quantifying the biophysical characteristics of invasive species such as bracken fern. However, remote sensing does not observe vegetation only because it captures whatever is in the area covered by the field of view of the satellite sensor, thus the move to use the phrase 'Land Surface Phenology (LSP)' is seen in the remote sensing literature (Helman,

2018). LSP is described as the estimation of the phenological cycles of different vegetation species using data acquired from satellite sensors (Helman, 2018).

The most common satellite sensors that pioneered LSP studies include Landsat series (Justice et al., 1985, Haralick et al., 1980), Advanced Very High-Resolution Radiometer (AVHRR) (Norwine and Greegor, 1983, Justice et al., 1986), Moderate Resolution Imaging Spectroradiometer (MODIS) (Huete et al., 1997, Reich, 1995) and SPOT Vegetation (Delbart et al., 2005, De Wit and Su, 2005, Bartalev and Belward, 2002). The AVHRR and MODIS provided a series of earth observing satellite missions with global coverage free of charge daily (Matongera et al., 2018). While AVHRR and MODIS' temporal resolution was high enough for sufficient detection of vegetation activities, the spatial resolutions for the two sensor remains a limitation especially for phenology studies conducted at a local scale. Although Landsat has an improved 30 m spatial resolution, the key limitation of the utility of Landsat satellites in phenology studies is its 16-day long return interval which is not sufficient to capture vegetation activity (Helman, 2018). Additionally, the missing data due to high cloud cover and technical related sensor problems such as scan line errors for Land sat 7 also significantly reduces the quantity of usable Landsat images per year (Berra and Gaulton, 2021). The launch of new generational satellite platforms such as Sentinel-2 Multispectral Instrument (MSI) with a higher observation frequency at 10 - 60m spatial resolution presents a new opportunity in the extraction of bracken fern phenological metrics at various scales.

Sentinel-2 MSI is a constellation of two sensors 2A and B that provides freely accessible optical imagery with additional red-edge bands that are more sensitive to vegetation characteristics (Li and Roy, 2017). The long-term archives of satellite data enable the retrieval of bracken fern LSP metrics at different spatial and temporal scales. Through the availability of multi-spectral sensors such as Sentinel-2, LSP has made significant progress in extracting ecologically meaningful phenological variables (Bolton et al., 2020, Descals et al., 2020, Vrieling et al., 2018). Satellite data enables the large scale extraction of phenological variables that are referred to as phenometrics or phenological metrics in remote sensing literature. Some of the common phenometrics estimated from satellite data include the start, peak and end of the vegetation season (SOS, POS and EOS respectively) (Jayawardhana and Chathurange, 2016, Araya et al., 2018). These phenometrics are associated with the timing of specific biological events of a particular plant, hence it is possible to validate them. For instance, the start of the season may be associated with biological events such as leaf unfolding (Vitasse et al., 2009), while leaf fall is attributed to the end of the season (Chmielewski and Rötzer, 2001).

The mapping of bracken fern spatial and temporal distribution at its different phenological stages presents a wide range of challenges in the remote sensing community. Studies have shown that bracken fern is mostly found in mountainous areas (McGlone et al., 2005, Marrs et al., 2000a, Reimann et al., 2007). Due to the rugged terrain and poor road networks, some of the sections of the landscape of interest will be inaccessible. Consequently, the collection of land cover data which represents all land cover classes in the study area becomes costly, labour intensive and time consuming. To remedy this challenge, One Class Classification (OCC) algorithms was proposed to avoid the cost and labour of collecting representatives of all land cover classes. The OCC methods have been successfully tested in agricultural surveys (Xu et al., 2018), change detection (Räsänen et al., 2019, Zhang et al., 2021) and document classification (Manevitz and Yousef, 2001). The same OCC concept coupled with Support Vector Machines (SVM) and Random Forest (RF) machine learning algorithms has the potential to map the spatial distribution of bracken fern at any phenological stage using limited field data.

The large-scale mapping of invasive alien plants has been less effective due to the spatial variability in the expansion of these species (Pepin et al., 2019). The spatial variability of bracken fern across the infested landscapes compromises the application of remotely sensed data in mapping bracken fern at various phenological stages. For example, at the end of the season, the bracken fern patches across the landscape may not senesce at the same time, some remnant patches may be still at the green up stage due to various environmental factors (Schneider and Geoghegan, 2006b). Consequently, mapping approaches that assume homogeneity of the spatial distribution of the fern during a particular phenological stage become less effective. Moreover, it is also important to understand the environmental factors that influence the spatial variability of bracken fern. Cloud-based data processing and analysis platforms such as Google Earth Engine (GEE) provide an opportunity to track the spatial variability of the fern. The freely accessible GEE platform provides users with powerful data processing tools via the web-based Integrated Development Environment (IDE) code editor without downloading the data sets to a local computer (Shelestov et al., 2017a, Liu et al., 2018, Shelestov et al., 2017b).

The successful mapping, estimation and monitoring of the phenological cycles of vegetation rely on the demonstrated sensitivity of several satellite-based greenness proxies which are also known as spectral vegetation indices in remote sensing literature (Xue and Su, 2017). The vegetation indices enhance the sensitivity of the spectral feature which is correlated to

4

biophysical variables such as Leaf Area Index (LAI) while minimizing soil background effects (Pôças et al., 2020). The confounding distortions minimized by vegetation indices include external effects such as sun viewing angle and atmospheric composition while internal effects include soil background variation, topography and canopy background differences (Dorigo et al., 2007). The first generation of spectral vegetation indices were ratios indices such as the Simple Ratio (SR) (Birth and McVey, 1968), Ratio Vegetation Index (RVI) (Pearson and Miller, 1972) and the Normalized Difference Vegetation Index (NDVI) (Rouse Jr, 1972). Despite their contribution in vegetation dynamics assessment, the first-generation indices were limited by their sensitivity to effects of soil brightness, cloud shadow and their saturation in environments with high canopy cover (Matongera et al., 2021b). The second generation of indices such as the Soil-Adjusted Vegetation Index (SAVI) (Huete, 1988b) Transformed Difference Vegetation Index (TDVI) (Bannari et al., 2002) was designed to reduce the effects of soil background and atmospheric distortions when working with remotely sensed data in various applications. As more satellite sensors with wide spectral channels were launched, the development of new vegetation indices also increased significantly (Matongera et al., 2021b). Furthermore, the new sensors enable the optimization of the existing spectral indices and the development of new indices specifically designed to understand the phenological patterns of bracken fern and how they relate to ecosystem processes. The conclusions of this work will provide rangeland managers, farmers and conservationists with insights on the phenological information of bracken fern from a remote sensing perspective and how it can be integrated into rangeland management.

1.2 Aim and objectives

The main aim of this study was to estimate and monitor the phenological cycle of bracken fern using remote sensing. To achieve this, the following objectives were set:

1. To review the progress and challenges in estimating and monitoring Land Surface Phenology in rangelands

2. To characterize the phenological cycle of bracken fern using time series data derived from the Sentinel-2 sensor

3. To estimate the spatial distribution of bracken fern during the green up phenological stage using limited ground sample data

4. Optimization of the Transformed Difference Vegetation Index for mapping and monitoring of bracken fern phenology

5. To assess the spatial variability of bracken fern during the dormancy phenological stage

1.3 Description of the study site

The study was conducted at the Cathedral Peak Nature Reserve located at NW, Lat = −28.97360039, NW Long = 29.20739937, SE Lat = −29.01429939; SE, Long = 29.2670020 in the Drakensberg Mountains of South Africa (Figure 1.1). The nature reserve covers an area of approximately 200 km^2 and it falls under the protection of the KwaZulu-Natal (KZN) Ezemvelo Wildlife (Shoko and Mutanga, 2017). The Drakensberg climate is a result of a combination of factors such as altitude, topography as well as the Agulhas current in conjunction with atmospheric pressure system patterns over and adjacent to South Africa (Irwin and Irwin, 1992). The dominant weather patterns are orographic, with warm moist air moving in over the continent from the Indian Ocean, rising in the escarpment and cooling down while creating rainfall. The mean annual rainfall in the Drakensberg is approximately 1800mm (Nel, 2007). The maximum daily temperatures exceed 25 °C while the minimum daily temperatures may drop below 0°C during winter (Henzi et al., 1992). During the coldest periods, snow has been recorded in the upper part of the catchment. Low intensity frost is experienced almost every year. The light summer winds blow from east to west while summer thunderstorms are characterized by strong winds which usually blow from south or west. The Drakensberg elevation ranges from 800 to 3050m above sea level (Shoko and Mutanga, 2017).

Drakensberg rocks comprise Karoo Sequence geological formations. The Tarkastad formation of rocks is dominant in the Cathedral Peak area (Asmal, 1995). The sandstones and the shale's dominant parent rocks are positioned in horizontal beds underneath the earth's surface. The sediments from the rivers in the Drakensberg formed part of a dense layer of rocks that are presently known as the Karoo supergroup (Catuneanu et al., 2005). The soils within the catchment vary from shallow to deeply weathered saprolite, with intervening hardcore stones in Winterton. Drakensberg has a profusion of vegetation and animal species and is regarded as a biodiversity hotspot (Matongera et al., 2017). The Drakensberg rangeland is mainly comprised of grasslands, woodlands and shrublands (Mucina and Rutherford, 2006). The rangelands provide forage, water and cover to grazing livestock and wildlife whose socio-economic value is substantial in South Africa. The area is characterized by a mountainous

environment that is largely dominated by C_3 and C_4 grass species such as *Festuca costata* and *Themeda triandra* respectively (Adjorlolo et al., 2014). The Cathedral Peak landscape is also characterized by invasive species that are increasingly encroaching into the grasslands. Nearly seventy five categories of invasive alien plants have been recorded to exist in the Drakensberg (Sycholt, 2002). Bracken fern is amongst the commonly found invasive plants that have been invading rangelands in the Drakensberg.

Figure 1.1: Location of the study site

1.4 General structure of the thesis

Excluding the introduction and the synthesis chapters (1 and 7 respectively), the thesis comprises five research papers that answer each of the research objectives outlined in section 1.2. The literature review and methodology are entrenched within the mentioned papers.

Chapter Two reviews the progress and challenges in estimating and monitoring LSP in rangelands. The review provides a detailed overview of the satellite sensor developments and associated VIs in LSP studies. The study also interrogates the commonly used and recently developed LSP data processing software packages as well as proposing future research directions on the remote sensing of LSP in rangeland ecosystems.

Chapter Three characterizes the bracken fern phenological cycle using time series data derived from the Sentinel-2 sensor. Specifically, the bracken fern green up, green peak, senescence, and dormancy phenological metrics were estimated. The study also discussed the importance of land surface phenology studies in rangeland ecology and management in Africa and beyond.

Chapter Four estimated the spatial distribution of bracken fern during the green up phenological stage using limited field data. The study compared the accuracy of One Class Support Vector Machines (OCSVM) and Biased Support Vector Machine (BSVM) algorithms as they require positive and randomly generated unlabelled samples, thus reducing the amount of ground sampling required for the classification process. To assess the performance of the One Class Classification (OCC) algorithms, the study analyzed the effectiveness of (i) spectral bands, (ii) spectral bands plus vegetation indices, (ii) spectral bands plus topographic variables and (iv) all data sets combined in estimating the spatial distribution of bracken fern during the green up phase.

Chapter Five optimized the Transformed Difference Vegetation Index for mapping and monitoring bracken fern at its four phenological stages. The study developed five variants of the optimized TDVI (OTDVI) based on the ratios of spectral bands that showed maximum separation between bracken fern and other land cover classes. The optimal spectral regions which distinguished bracken fern from other land cover classes at each phenological stage were identified using the spectral curves and the Transformed Divergence Spectral Index (TDSI) statistical analysis.

Chapter Six assessed the spatial variability of bracken fern across the Cathedral Peak Nature Reserve landscape. The object-based classification approach which combines the Simple Non-Iterative Clustering (SNIC) was used to group spatial clusters, while the Gray-Level Co-occurrence Matrix (GLCM) was employed to compute bracken textural indices for the classification. The study also examined the key topographic factors influencing the spatial variability of bracken fern during the dormancy phenological stage.

Chapter Two

A review of progress and challenges in the estimating and monitoring Land Surface Phenology in Rangelands

This chapter is based on a paper:

Matongera, T. N., Mutanga, O., Odindi, J. Sibanda, M. 2021. Estimating and monitoring Land Surface Phenology in Rangelands: A review of progress and challenges; *MDPI Remote Sensing Jornal,* 13, 48-67. doi:10.3390/rs13112060

remote sensing

Submit to this Journal

Review for this Journal

Edit a Special Issue

Article Menu

Article Overview ⌃

- Abstract
- Open Access and Permissions
- Share and Cite
- Article Metrics
- Order Article Reprints

Open Access   Review

Estimating and Monitoring Land Surface Phenology in Rangelands: A Review of Progress and Challenges

by 🔵 Trylee Nyasha Matongera [1,*] ✉ 🔵, 🔵 Onisimo Mutanga [1] ✉ 🔵, 🔵 Mbulisi Sibanda [2] ✉ and 🔵 John Odindi [1] ✉

[1] Discipline of Geography, University of KwaZulu-Natal, Pietermaritzburg 3201, South Africa
[2] Department of Geography, Environmental Studies and Tourism, University of Western Cape, Cape Town 7535, South Africa
* Author to whom correspondence should be addressed.

Academic Editor: Arturo Sanchez-Azofeifa

View Full-Text   Download PDF   Browse Figures   Citation Export

Abstract

Land surface phenology (LSP) has been extensively explored from global archives of satellite observations to track and monitor the seasonality of rangeland ecosystems in response to climate change. Long term monitoring of LSP provides a large potential for the evaluation of interactions and feedbacks between climate and vegetation. The study reviews the progress, challenges and emerging opportunities in LSP as well as identifying possible gaps that could be explored in the future. Specifically, the review traces the evolution of satellite sensors and interrogates their properties as well as the associated indices and algorithms in estimating and monitoring LSP in rangelands. Findings from the literature revealed that the spectral characteristics of the early satellite sensors such as Landsat, AVHRR and MODIS played a critical role in the development of spectral vegetation indices that have been widely used in LSP applications. The Normalized Difference Vegetation Index (NDVI) pioneered LSP investigations and most other spectral vegetation indices were primarily developed to address the weaknesses and shortcomings of the NDVI. New indices continue to be developed based on recent sensors such as Sentinel-2 that are characterized by unique spectral signatures and fine spatial resolutions and their successful usage is catalyzed with the development of cutting-edge algorithms for modelling the LSP profiles. In this regard, the study documented several LSP algorithms that are designed to provide data smoothing, gap filling and LSP metrics retrieval methods in a single environment. In the future, the development of machine learning algorithms that can effectively model and characterize the phenological cycles of vegetation would help to unlock the value of LSP information in the rangeland monitoring and management process.

Keywords: Remote Sensing, Rangelands, LSP, Satellite data, Phenology metrics, Vegetation indices

2.1 Introduction

Rangelands are defined as landscapes that are mainly comprised of grasslands, woodlands, shrublands and wetlands (Cheng et al., 2020). Rangelands provide forage, water and cover to grazing livestock and wildlife whose socio-economic value is substantial in many countries (Coppock et al., 2017, Sayre et al., 2013). Globally, the state of rangelands has been threatened by many challenges such as biodiversity loss (Belnap et al., 2012), soil erosion (Mganga et al., 2015), frequent veld fires which destroy habitats (Rihan et al., 2021) and most severely, the encroachment of invasive alien plants (O'Connor and van Wilgen, 2020, Yapi et al., 2018, Liao et al., 2018). Invasive alien plants typically outcompete indigenous vegetation, often replacing palatable grasses with plants that are poisonous to livestock (Matongera et al., 2018). A better understanding of the phenological dynamics of the various vegetation types in the rangelands will enable us to assess how climate variability and management practices affect various functional groups (Cheng et al., 2020). Phenology data is essential for designing and planning rangeland management systems. For instance, phenology data can be used to adjust the timing of grazing or manage burns relative to the phenological cycles of vegetation species and for planning restoration actions, such as targeted grazing (Browning et al., 2019). The monitoring and modelling of the changes in phenological cycles of vegetation can also help rangeland managers to make suitable and cost-effective decisions on how to adjust management strategies to optimize livestock production and other ecosystem services provided by rangelands (Matongera et al., 2021b).

The assessment of changes in phenological cycles of vegetation in rangelands can be achieved using three main types of observations which include: human visual surveillance using phenology networks (Taylor et al., 2020b, Browning et al., 2019, Schwartz et al., 2012), near surface measurements such as Phenology Cameras (PhenoCams) (Cheng et al., 2020, Watson et al., 2019, Alberton et al., 2017); Unmanned Aerial Vehicles (UAVs) or drones (Assmann et al., 2020, Berra et al., 2016); and remote sensing measurements estimated from polar orbiting and geostationary satellite sensors (Lara and Gandini, 2016, Gong et al., 2015, Sankey et al., 2013). The monitoring of vegetation phenological cycles across regions was previously difficult to assess using ground observed phenological events due to limited spatial coverage (Zeng et al., 2020). The availability of remotely sensed data provided a long term opportunity as it is strengthened by the ability of the data sets to present the phenological trends of vegetation at large spatial and temporal extents (Tong et al., 2019, Davis et al., 2017).

The utility of several polar orbiting and geostationary satellite sensors has been explored in the estimation and monitoring of LSP in rangelands. The most common satellite data sources include Landsat (Tomaszewska et al., 2020, Nguyen et al., 2020), Advanced Very High Resolution Radiometer (AVHRR) (Fontana et al., 2008, Weiss et al., 2001), Moderate Resolution Imaging Spectroradiometer (MODIS) (Cao et al., 2015, Gong et al., 2015, Kawamura et al., 2005), Sentinel-2 (Vrieling et al., 2018), PlanetScope (Cheng et al., 2020) and Himawari Imager (Ma et al., 2020). However, the applications of each of these data sources present various challenges and opportunities in LSP research. For example, early sensors such as AVHRR and MODIS have a high temporal resolution sufficient to capture subtle changes in vegetation development but they have low spatial resolution insufficient to capture plant specific phenological changes (Shen et al., 2015). On the other hand, medium and high spatial resolution sensors such as SPOT and Sentinel-2 with a 3-10 day temporal resolution do not provide adequate time series data for the characterization of the phenological cycles of vegetation especially in areas with high frequent cloud cover (Misra et al., 2020). Recently, data fusion methods have emerged as a solution to minimize the trade-offs associated with the spatial and temporal characteristics of satellite sensors in LSP investigations (Bolton et al., 2020, Zhang et al., 2020, Pastick et al., 2020).

In LSP investigations, scientists do not use raw spectral bands to estimate the phenological trends of vegetation, instead, they use vegetation indices (VIs) and plant biophysical variables such as Leaf Area Index (LAI) (Xue and Su, 2017). Vegetation indices are calculated using spectral data in the visible and near-infrared (NIR) parts of the electromagnetic spectrum (Viña et al., 2011). The spectral data in the visible and infrared sections of the electromagnetic spectrum are commonly used as they are more sensitive to plant growth and development (Cleland et al., 2007). Long term satellite data archives present an opportunity to retrospectively extract phenological characteristics of vegetation using a wide range of vegetation indices (Fisher and Mustard, 2007). Although there is an abundance of spectral VIs that have been established for various functions, the current review focuses on the most used indices in LSP investigations. Specifically, this study included only vegetation indices that have been successfully tested by more than five LSP studies. These indices include but are not limited to the Normalized Difference Vegetation Index (NDVI) (Rouse Jr et al., 1974), Enhanced Vegetation Index (EVI) (Huete et al., 2002), two band Enhanced Vegetation Index (EVI2) (Jiang et al., 2008), Normalized Difference Water Index (NDWI) (Delbart et al., 2005), Wide Dynamic Range Vegetation Index (WDRVI) (Gitelson, 2004) and recently, new spectral

VIs such as the Normalized Difference Phenology Index (NDPI) (Wang et al., 2017a). Despite their successful application in LSP studies, the utility of these VIs is influenced by various factors such as sensor degradation, atmospheric impurities and snow affecting the quality of the data in the time series (Miura et al., 2019, Xue and Su, 2017, Lara and Gandini, 2016). To address these challenges, many LSP algorithms have been developed for noise reduction, gap filling, data smoothing as well as for retrieving vegetation phenological parameters from satellite data (Bolton et al., 2020, Duarte et al., 2018, Jönsson and Eklundh, 2004). However, there is no universal approach for estimating LSP that can be relevant in all applications. Although certain algorithms and data set combinations may produce good results in a specific land cover type, it may perform poorly in other LSP related applications (Matongera et al., 2021b). In this regard, the choice of data sets, sensors and processing methods depends on the feasibility and objectives of the LSP study.

One of the previous LSP related reviews focused on analyzing LSP as an indicator for global terrestrial ecosystem dynamics (Caparros-Santiago et al., 2021). The review provided a synthesis of the contributions of the global LSP to the development of environmental knowledge. LSP progress and challenges in temperate and boreal forests were also reviewed recently (Berra and Gaulton, 2021). The study uncovered an in-depth intercomparison of in situ and satellite phenological metrics in the boreal forest. A well detailed synthesis of the LSP phenological extraction methods using multispectral satellite data was recently published (Zeng et al., 2020). The review mainly uncovered the advantages and shortcomings of phenological metrics extraction methods. A sensor specific review investigated the utility of Sentinel-2 data in phenological research, unpacking the potential and drawbacks of the data set in LSP investigations (Misra et al., 2020). Their study discussed LSP developments using Sentinel-2 data only. However, preceding LSP reviews have two important aspects that require further attention. Firstly, the above mentioned reviews focused more on croplands and forests ecosystem, a comprehensive understanding of LSP developments in rangelands has largely remained elusive. Secondly, the phenological extraction methods covered in the previous reviews focused on the developments of various phenological extractions methods, with a particular focus on their strengths and limitations in LSP studies. However, the applications and suitability of LSP phenology packages that allow the processing of satellite time series data in a single environment were not extensively covered.

To the best of our knowledge, there is no comprehensive assessment of the progress and challenges in LSP studies with a key focus on rangeland environments. Consequently, there is

a need for a state-of-the-art review to establish the milestones that have been achieved in modelling LSP in rangeland ever since the availability of satellite data in the early 70s. Therefore, this study reviewed the progress and challenges in modelling LSP in tropical rangelands. The paper initially, provides a detailed account of the methodology used in selecting the literature examined in the study. Next, a detailed overview of the satellite sensor developments and associated VIs in LSP studies is provided. The paper also interrogated the commonly used and recently developed LSP data processing software packages as well as proposes future research directions on the remote sensing of LSP in rangeland ecosystems.

2.2 Literature search and selection of sources

The literature search was conducted using the Scopus and Web of Science electronic scientific databases. The search terms used were 'Land Surface Phenology', 'Remote Sensing', 'Rangelands' and only peer reviewed LSP literature that focused on rangelands between 1972 and 2021 were considered. Specifically, LSP studies from grasslands, savannah, shrubland, woodlands land cover types were included in this study. A total number of 120 English language publications from peer reviewed journals were retained from the search process. More studies were added to the gathered literature by reviewing the publications found in the reference list of the initially retrieved sources. A total of 37 articles from the references were included, bringing the total number of sources used in this study to 157. Since the majority of LSP studies cover a wide range of land cover types, studies that covered rangelands were included in the review. The retrieved literature sources comprised articles, reviews, book chapters, conference papers and letters.

2.3 Satellite sensor developments in LSP studies

Before the period of satellite sensors, vegetation phenology monitoring in rangeland ecosystems mainly relied on field surveys that collected phenological events of vegetation. Precisely, these surveys recorded distinct plant specific biological changes such as the emergence of first leaves, leaf expansion, flowering and fruiting (Borchert, 1980, Frankie et al., 1974, Berra and Gaulton, 2021, Muller, 1978). However, the major limitation of these field methods is the spatial extent to which the plant phenological events were collected. The plant phenological events were mostly collected at local scales by volunteers, farmers and botanists. Table 2.1 contains a summarized chronology of polar orbiting and geostationary satellite sensors commonly used in estimating and monitoring LSP in rangeland ecosystems. The spatial, temporal and spectral characteristics of the sensors are also presented while the

suitability of each of the sensors in estimating LSP in rangelands is discussed in the text. In the last two decades, satellite sensors have proven to be powerful and cost-effective tools for characterizing the phenological trends of vegetation at a larger scale (Zeng et al., 2020, Muller, 1978, Adole et al., 2018, White et al., 2014).

Table 2.1: Widely used satellite sensors used in estimating LSP in rangeland ecosystems

Satellite sensor	Spatial resolution (m)	Spectral bands	Swath width (km)	Acquisition frequency	Reference
AVHRR	1100	5	2600	12 hours	(Reed et al., 1994)
MODIS	250 -1000	36	2330	Daily	(Zhang et al., 2003)
VIIRS	375	22	3060	12 hours	(Yan et al., 2016a)
Landsat ETM	30	8	185	16 days	(Fisher et al., 2006)
SPOT VGT	1015	4	2250	Daily	(Guyon et al., 2011)
MERIS	300	15	115	3 days	(Boyd et al., 2011)
Sentinel-2	10-60	13	290	5 days	(Vrieling et al., 2018)
PlanetScope	3 -5	4	475	Daily	(Myers et al., 2019)
Himawari	500-2000	16	1000	10 minutes	(32)
SEVIRI	3000	12	980	15 minutes	(Yan et al., 2016a)
Advanced Baseline Imager	500 -2000	10	1000	15 minutes	(Zhang et al., 2019)

Earlier LSP studies in rangelands were pioneered by Landsat series satellite sensors with a 16-day revisit time at 30m spatial resolution (Rouse Jr, 1972). Since its official launch in 1972, The Landsat program provided a series of earth observing satellite missions with global coverage free of charge (Matongera et al., 2018). The Landsat data archive provides rangeland managers an opportunity to assess the long term phenological changes (multi-decadal studies) and how they affect rangeland productivity at local and regional scales. Although Landsat satellites pioneered LSP investigations, only 15% (Figure 2.2) of the sources used in this study explored the capability of Landsat data in rangelands. This could be explained by the sensor's low temporal resolution, which makes it ineffective in LSP applications since some plant phenological cycles change quicker than Landsat's 16-day revisit cycle. Additionally, the presence of cloud contamination in some of the satellite images further reduces the quantity

and quality of satellite data available for the characterization of phenological cycles of vegetation (Bolton et al., 2020, Melaas et al., 2013a, Busetto et al., 2008).
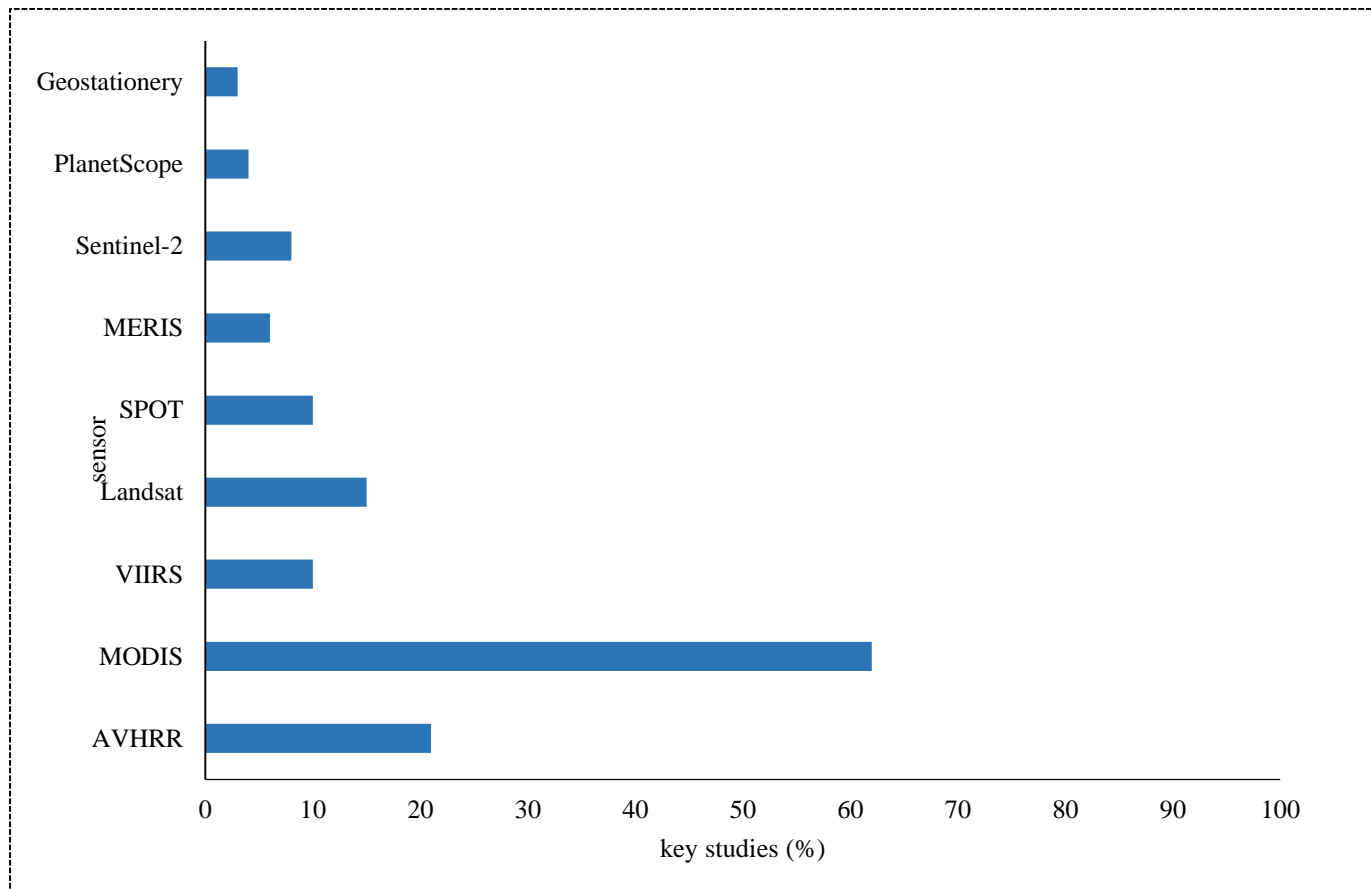
Figure 2.1 Polar orbiting and geostationary sensors used estimating and monitoring LSP

In the early 80s, LSP studies shifted more towards the use of the Advanced Very High Resolution Radiometer (AVHRR) sensor (Matongera et al., 2021b). The AVHRR data became one of the most widely used data sets for LSP investigations in rangelands around the world especially for large scale applications (Moulin et al., 1997, Justice et al., 1985, Reed et al., 1994) and has been proven to be well suited for long term phenological studies (Vrieling et al., 2017). Evidence from literature revealed that about 21% of LSP investigations in rangelands used the AVHRR data. The successful retrieval of phenological cycles of vegetation in rangeland ecosystems requires sensor platforms with a high quick return that is sufficient to capture the rapid changes of vegetation activity. Ample credit has been given to the AVHRR satellite platform for providing long term archives of 1 – 8 km spatial resolution of data with global coverage. In China, AVHRR data was used for the estimation of spring vegetation

green-up and the study reported that the onset of green up advanced at a rate of 0.4 to 1.9 days per decade (Zhang et al., 2017). Another study in Central Europe reported the successful application of AVHRR in multi-decadal studies, the phenological patterns of vegetation revealed a general shift to an earlier start of the season (−0.54 days per year) and extended growing seasons (0.96 days per year) in Central Europe (Stöckli and Vidale, 2004). However, the applications of AVHRR data in estimating and monitoring LSP in rangelands presented several challenges that primarily originated from the instrument's characteristics and sensor design. These characteristics include poor radiometric calibration, geolocation errors and broad spectral channels (Goward et al., 1991).

In the late 90s, The Satellite Pour l 'Observation de la Terre (SPOT) Vegetation was launched with a 10-day temporal resolution (Mhangara et al., 2020). About 10% of the research studies have used the SPOT Vegetation data for LSP applications in rangelands (Delbart et al., 2015, Wu et al., 2017, Verhegghen et al., 2014). Different from other scanner sensors like AVHRR, the SPOT instrument uses the linear array system which facilitates the production of good quality imagery at a coarse spatial resolution while it maintains a significantly reduced distortion (Chen et al., 2011). The utility of the SPOT vegetation satellites in retrieving LSP in rangelands is however limited by its low temporal resolution and atmospheric impurities such as clouds and snow (Matongera et al., 2021b). Due to the 10-day repeat cycle, the SPOT satellite's probability to capture cloud free satellite images over an entire growing season is reduced, leading to high temporal gaps in the time series. In the late 90s, The European Space Agency (ESA) deployed the Medium Resolution Imaging Spectrometer (MERIS) instrument with global coverage of 3 days at 300m spatial resolution (Rast et al., 1999). Although the instrument was mainly designed for ocean studies, 6% of studies have used the instrument in retrieving LSP in rangelands (Boyd et al., 2011, Dash and Curran, 2004b, Jin et al., 2012, Rodriguez-Galiano et al., 2015). Unfortunately, the mission ended in 2012, limiting long term monitoring of LSP. It was never possible to conduct multi-decadal LSP investigations using the MERIS instrument.

In the early 2000s, the Moderate Resolution Imaging Spectroradiometer (MODIS) satellite was launched, collecting daily reflectance data at 250 to 1000m spatial resolution (Justice et al., 2002). More than 60% (Figure 2.1) of the LSP studies in rangelands used MODIS data, making it the most used data set in LSP applications globally. Evidence from literature revealed that the availability of the MODIS sensor with substantively improved sensor characteristics enabled the estimation and monitoring of vegetation phenological cycles at various scales

(Zhang et al., 2006, Sakamoto et al., 2005, Yu et al., 2004). Since the MODIS instrument is now aging and its lifespan ending, the Visible Infrared Imaging Radiometer Suite (VIIRS) was launched towards the end of 2011 to enable the continuation of the MODIS data provision mission (Moon et al., 2019, Zhang et al., 2017). However, it is also imperative to note that there are technical errors linked to switching from the MODIS instrument to VIIRS (Skakun et al., 2018) such that users should consider adjustments to ensure consistent and good quality time series before phenological metrics can be extracted.

In 2015, ESA launched the Sentinel-2 satellite with a 5-day temporal resolution at 10-60m spatial resolution (Van der Meer et al., 2014). The applications of Sentinel-2 data in LSP have been gaining traction lately, 8% of the studies have tested the utility of the data set in rangeland applications (Bolton et al., 2020, Yu et al., 2004, Vrieling et al., 2018). At 10m spatial resolution, Sentinel-2 presents a huge potential for estimation of plant specific phenological cycles, which was previously difficult using early satellite sensors such as AVHRR, Landsat and MODIS (Matongera et al., 2021b). The estimation of plant specific phenological cycles, especially alien invasive species, is crucial for better management of rangelands (Matongera et al., 2021a). Nevertheless, since Sentinel-2 was launched in 2015, it lacks a global historical coverage of vegetation activity and possibly a greater impact of the sensor's contribution in LSP monitoring will be more evident in the next few decades. The new Sentinel-3 satellite also provides a greater potential for estimating and monitoring LSP on a global scale. The 1270 km swath width of the Sentinel-3 is well suited for global applications compared to its predecessor (Donlon et al., 2012).

Planet Labs an aerospace company launched PlanetScope, a constellation of more than 130 small satellites collecting multi-spectral images in 4 bands at 3m spatial resolution daily (Gašparović et al., 2018). The utility of PlanetScope data in estimating the phenology of short vegetation cycles was tested in Kenyan rangeland (Cheng et al., 2020). Their findings highlighted that the PlanetScope data set had more cloud free observations as compared to the Sentinel-2-time series, resulting in more reliable vegetation spatial patterns as compared to Sentinel-2. The PlanetScope data has a better quick return time which is sufficient to capture swiftly developing vegetation phenological transitions such as green up and peak. Like Sentinel-2, at 3 m spatial resolution, PlanetScope data presents a more refined potential for the estimation of plant specific phenological transition dates(Cheng et al., 2020). However, the acquisition of PlanetScope data from Sentinel Hub is not straightforward as compared to other freely available data sets such as Sentinel and Landsat that can be openly downloaded from the

public data archives such as earth explorer, Google Earth Engine and ESA. To obtain the data free of charge, the PlanetScope data acquisition process requires the submission of proposals and sponsorship applications via the Network of Resources (NoR) website (Matongera et al., 2021b). Consequently, the applicability of PlanetScope data sets in rangelands monitoring remains a challenge, especially in developing countries.

In addition to the previously discussed polar orbiting satellite sensors, high temporal resolution geostationary sensors have been increasingly used for estimating LSP in rangeland ecosystems. The most used sensors include the Himawari Imager (Ma et al., 2020), Spinning Enhanced Visible and InfraRed Imager (SEVIRI) (Yan et al., 2016b) and Advanced Baseline Imager (ABI) (Zhang et al., 2019). The new generation of geostationary sensors have the capability of imaging the earth at 10-15min intervals (Yan et al., 2019), and they have strategically positioned spectral bands that are appropriate for deriving a wide range of VIs, thus holding a huge potential in estimating the phenological cycles of vegetation in rangeland ecosystems. Since they have high frequency revisit time, geostationary sensors provide high cloud free observations, a key attribute that is crucial in tracking the phenological developments of vegetation when monitoring rangeland ecosystems in cloud contaminated regions (Matongera et al., 2021b). Despite the progress made by geostationary satellites in LSP studies, the sensors were recently launched and therefore do not have the data archives needed for the retrogressive extraction of LSP metrics. Combined, less than 5% of studies used geostationary sensors for extracting LSP metrics in rangeland ecosystems. Most of these studies were focused on specific areas of individual countries primarily in Japan, China and the United States of America.

2.4 Vegetation indices and biophysical variables in LSP

Table 2.2 shows a summary of the commonly used spectral VIs in LSP and their formulations. To assess vegetation cover dynamics, scientists developed spectral VIs derived from spectral data (Jiang et al., 2008, Huete et al., 2002, Fensholt and Sandholt, 2003). VIs are defined as mathematical calculations of various spectral bands that are in most cases located in the visible and NIR parts of the electromagnetic spectrum (Viña et al., 2011). The time series composites of VIs computed using satellite data have provided long term global coverage archives of valuable information on vegetation activity (Fensholt and Sandholt, 2003, Jin et al., 2017, Gonsamo et al., 2012a). The NDVI pioneered the estimation and monitoring of LSP on a global scale in the early 70s (Thompson et al., 2015). Over 62% of the studies have tested the utility of NDVI in modelling LSP in rangeland ecosystems. NDVI quantifies vegetation by measuring

the difference between visible red and NIR bands that are usually part of the most common multispectral sensors. The global coverage of NDVI could be useful for predicting the ecological impacts of environmental change in rangelands at various scales (Dunn and de Beurs, 2011). However, it can be argued that NDVI is not effective when extracting the start and end of the season especially in rangelands characterized by high levels of snow cover, since the onset of the NDVI normally coincides with the start of the snowmelt (Zuo et al., 2019). For this reason, the NDVI becomes less sensitive to slight changes in dense vegetation canopies and more sensitive to snow.

Table 2.2: Summary of widely used VIs and their formulation

Vegetation Index	Formulation	Characteristics and applications	Reference
NDVI	$\dfrac{NIR - Red}{NIR + Red}$	Large scale vegetation assessments, related to canopy structure and canopy photosynthesis	(Rouse Jr, 1972)
PVI	$\dfrac{NIR - a1 \times Red^{-a2}}{\sqrt{1 + a_1^2}}$	Characterizes vegetation biomass and filters the effects of soil background	(Richardson and Wiegand, 1977)
SAVI	$\dfrac{(1 + L)(NIR - Red)}{(NIR + Red + L)}$	Improves NDVI sensitivity to soil background effects	(Huete, 1988b)
NDWI	$\dfrac{NIR - SWIR}{NIR + SWIR}$	shows sensitivity to the changes in leaf water content	(Gao, 1996)
EVI	$G \dfrac{NIR - Red}{NIR + C_1\ Red - C_2\ Blue + L}$	Optimized to enhance sensitivity in high biomass environments	(Huete et al., 2002)
WDRVI	$\dfrac{a \times NIR - Red}{a \times NIR + Red}$	Enhances the dynamic range for high biomass regions	(Gitelson, 2004)
MTCI	$\dfrac{R_{753.75} - R_{708.75}}{R_{708.75} - R_{681.25}}$	Correlates strongly with chlorophyll content	(Dash and Curran, 2004a)
EVI2	$G \dfrac{NIR - Red}{N + \left(6 - \frac{7.5}{C}\right) R + 1}$	Enhances the dynamic range for high biomass regions without the blue band	(Jiang et al., 2008)
GRVI	$\dfrac{Green - Red}{Green + Red}$	Sensitive to land cover changes	(Motohka et al., 2010)
NDPI	$\dfrac{NIR - (\propto \times Red + (1-\propto) \times SWIR)}{NIR + (\propto \times Red + (1-\propto) \times SWIR)}$	Sensitive to changes in snow cover	(Wang et al., 2017a)
NDII	$\dfrac{NIR - SWIR}{NIR + SWIR}$	Sensitive to soil moisture storage	(Fensholt and Sandholt, 2003)
PPI	$-K \times In \dfrac{(NIR - Red)\max - (NIR - Red)}{NIR - Red)\max - (NIR - Red)soil}$	Detection of snow seasonality	(Jin et al., 2017)

The Normalized Difference Infrared Index (NDII) was developed for the detection of vegetation water stress using the shortwave infrared reflectance, which was reported to be negatively correlated to leaf water content because of the leaf's absorption capacity (Hunt Jr and Rock, 1989). The SWIR band is sensitive to land surface moisture; hence many studies have used the NDII for LSP investigations in rangelands at various scales (Thompson et al., 2015, Gonsamo et al., 2012a, Dunn and de Beurs, 2011). The Normalized Difference Water Index (NDWI), was proposed to be optimal in retrieving SOS metrics for areas with large snow cover (Gao, 1996). The NDWI utilizes the reflectance in the NIR and Shortwave (SWIR) sections, hence it becomes ideal for discriminating green up phenological stage from snowmelt. NDVI and NDII were combined to develop the phenology index (PI) (Gonsamo et al., 2012a). Specifically, the PI was developed to allow the capturing of subtle changes in the SOS and EOS transition dates. The combination of two or more vegetation indices improves accuracy in LSP retrievals since the amalgamation compliments the drawbacks of each vegetation index (Matongera et al., 2021b). Although some VIs are calculated from the same spectral bands, the phenological metrics retrieved by these indices may exhibit different trends (Zuo et al., 2019). For example, a study in Mongolia compared SOS and EOS estimated from NDVI and Simple ration (SR) which were calculated using NIR and Red spectral bands from MODIS data (Zuo et al., 2019). Their findings reported that different mathematical expressions used in these two indices would lead to the difference in vegetation phenology trends.

The Enhanced Vegetation Index (EVI) was developed as a typical satellite vegetation index for MODIS sensor (Huete et al., 2002). EVI was the second most used vegetation index in estimating LSP trends in rangelands. Originally, the EVI was designed to improve vegetation sensitivity in areas with high biomass and enhanced LSP estimation through de-coupling of the canopy background signal and a reduction in atmospheric influences (Vescovo et al., 2012). Following the successful applications of EVI in vegetation monitoring, many studies have used EVI time series in LSP applications (Adole et al., 2018, Shen et al., 2014, D'Odorico et al., 2015, Leinenkugel et al., 2013). Evidence reported from a plethora of LSP literature shows that the EVI has proven to be valuable in enhancing one-dimensionality with vegetation biophysical properties as well as reducing saturation effects normally experienced in high biomass areas, frequently experienced when using NDVI (Wang et al., 2018, Testa et al., 2018, Wardlow and Egbert, 2010). However, the blue band is a pre-requisite for the computation of EVI and some sensors do not have the blue band, limiting the consistency of EVI across different sensors (Jiang et al., 2007a). Subsequently, a two-band combination Enhanced Vegetation Index

(EVI2) was developed for sensors such as AVHRR without the blue band. The applications of EVI2 in LSP studies provided a long term EVI record that could potentially complement the NDVI record at a global scale. Several studies have reported the best similarity of the EVI2 with the 3 band EVI when extracting LSP metrics. The large scale application of EVI2 reported that the phenological patterns from EVI and EVI2 data did not show any significant differences at a global level (Jiang et al., 2008). The need to provide continuity with past and present sensors has been a critical topic in LSP literature over the past few decades. Interestingly, the EVI2 came in to bridge the gap and provided continuity of LSP data across sensors.

The Wide Dynamic Range Vegetation Index (WDRVI) is a simple modification of the widely used NDVI by enhancing the dynamic range while using the same spectral bands as NDVI (Gitelson, 2004). The WDRVI improves the robust characterization of crop physiological and phenological trends. Several other studies have used the WDRVI in LSP estimation (Zheng et al., 2016, Sakamoto et al., 2010) and have reported this index reduces saturation in high biomass regions which is a challenge that is commonly encountered by NDVI. However, when biomass is low, NDVI remains a better choice for vegetation characterization (Xue and Su, 2017). The Green-Red Vegetation Index (GRVI) has also been an important index in LSP investigations (Motohka et al., 2010, Nagai et al., 2012) and has been proven to show distinct changes in vegetation even in ecosystems that show subtle changes in plant phenological appearance. The Soil-Adjusted Vegetation Index (SAVI) was mainly developed to reduce sensitivity to environmental factors such as the effects of soil background on VIs (Huete, 1988a). Evidence from literature has shown that the application of SAVI in LSP is mostly suitable for areas with less vegetation cover, where the influence of soil brightness is high (Lu et al., 2015, Wu et al., 2014, Motohka et al., 2009). Similarly, the Perpendicular Vegetation Index (PVI) was also designed to decrease the sensitivity to soil reflectance; it has a higher signal to noise ratio compared to NDVI (Richardson and Wiegand, 1977).

The MERIS Terrestrial Chlorophyll Index (MTCI) is a sensor specific spectral vegetation index that has been used by numerous studies in LSP investigations (Rodriguez-Galiano et al., 2015, Motohka et al., 2009, Boyd et al., 2011, Jeganathan et al., 2010). Evidence gathered from the aforementioned studies shows that the MTCI is sensitive to chlorophyll changes, making it appropriate for phenology investigations. However, since the MERIS sensor ceased operation (Zhang et al., 2018a), no further developments or studies can be continued using the MTCI, a major disadvantage of sensor specific spectral indices. With the launch of more satellite sensors such as Sentinel-2, the number of spectral bands has increased leading to the development of

new VIs that can be widely utilized in LSP applications at various scales. New VIs are gaining traction in LSP studies. The Normalized Difference Phenology Index (NDPI), is a spectral index that is less affected by snow when extracting green up date (Xue and Su, 2017). The new NDPI significantly minimizes the influence of snowmelt on retrieving the phenological metrics ecosystems. The Plant Phenology Index (PPI) was designed to untangle vegetation start of season and snow seasonality (Jin et al., 2017).

While VIs remains the most used vegetation indicators, some vegetation physiological parameters have also been used to extract LSP in rangeland ecosystems. The most commonly used biophysical variables include the leaf area index (LAI) (Wang et al., 2017b, Ding et al., 2017, Cho et al., 2017), Fraction of Absorbed Photosynthetically Active Radiation (FAPAR) (Bórnez et al., 2017, Yao and Zhang, 2016), Solar-Induced Chlorophyll Fluorescence (SIF) (Dannenberg et al., 2020, Thenkabail, 2015) and Vegetation Optical Depth (VOD) (Tong et al., 2019). Evidence from literature shows that the parameters provide detailed information about the biophysical characteristics of vegetation and how they respond to climatic and environmental changes (Wang et al., 2017b). The LAI biophysical variable has been widely used in LSP applications because of the availability of numerous remote sensing products and its clear signal of the physical and biological processes that are related to vegetation phenological cycles at various scales (Chen et al., 2002, Fassnacht et al., 1994).

2.5 LSP software packages for data processing

The spectral reflectance from vegetation can be disturbed by a variety of atmospheric impurities such as ground and atmospheric conditions (Hird and McDermid, 2009), changes in the satellite sensor's illumination patterns and viewing angle (Matongera et al., 2017), causing inaccurate trends in the time series data. Figure 2 shows a detailed flowchart of LSP procedures. The widely used phenological metrics are shown in a schematic diagram under the phenological metrics retrieval section. The successful estimation of LSP involves three main steps in processing spectral VIs time series data. These stages include (1) preprocessing of VIs time series data by detecting and removing outliers, (2) data smoothing and gap filling, and (3) extraction of LSP metrics. The performance and limitations of LSP data smoothing methods have been extensively reviewed (Zeng et al., 2020, de Beurs and Henebry, 2010). Therefore, the developments and drawbacks of data smoothing techniques and phenological extraction methods will not be included in this section. The focus will be on reviewing the widely used LSP software packages that are designed to provide functions that perform data smoothing,

25

gap filling and LSP metrics retrieval in a single environment. The drive for developing such all in one LSP software packages was to avoid errors related to moving large amounts of time series data from one algorithm to another for further processing.

The Harmonic Analyses of NDVI Time-Series (HANTS) algorithm was proposed for the extraction of the characteristics of the vegetation dynamics. The HANTS algorithm has been extensively used in rangeland LSP investigations successfully (Li et al., 2019, Zhou et al., 2015, Jeganathan et al., 2010, Choi and Jung, 2014). The amplitude and harmonic components of the algorithm makes HANTS attractive for LSP studies (Zhou et al., 2015). However, HANTS limits the ability of users to specify phenological parameters and it also preserves year to year variations in the time series data as it filters atmospheric impurities such as clouds. The TIMESAT program provides tools for analyzing time series data for various LSP applications (Jonsson and Eklundh, 2002). The TIMESAT program has been extensively utilized by researchers to estimate and monitor LSP in rangelands (Stanimirova et al., 2019, Pan et al., 2015, Wei et al., 2012, Tan et al., 2010). The TIMESAT program offers three data filtering functions to remove noise from the time series data. These are asymmetric Gaussian (AG), double logistic (DL), and adaptive Savitzky-Golay (SG) filtering (Jönsson and Eklundh, 2004). One of the major advantages of using TIMESAT is that it enables the flexible tuning of thresholds and parameter settings compared to other algorithms such as HANTS. As a prerequisite, the TIMESAT program requires gap free time series data for successful characterization of the phenological cycles of vegetation cycles (Matongera et al., 2021a). The gap free pre-requisite limits the applications of the software package especially in circumstances where the data is of poor quality due to persistent cloud contamination. Consequently, TIMESAT was revised to produce temporally and spatially continuous time series data (Gao et al., 2008). The revised TIMESAT was later named enhanced TIMESAT in a study that estimated vegetation phenology metrics from MODIS data (Tan et al., 2010). The enhanced TIMESAT significantly improved the time series data quality by replacing the upper envelope function in the original TIMESAT software with the tuned data quality weightings whereby higher quality retrievals were assigned more influence than low quality retrievals (Matongera et al., 2021b).

TimeStats is a software package used for retrieving temporal patterns of vegetation activity from satellite data (Udelhoven, 2010). Unlike other packages such as TIMESAT that use various least-squares approaches for preprocessing time series data, TimeStats provides robust statistical methods such as cyclic, transient and stochastic for preprocessing of time series data

using a pixel by pixel approach (Udelhoven, 2010). Phenosat was developed as a semi-automated tool for the temporal analysis from satellite data (Rodrigues et al., 2011). The Phenosat tool can capture double growth season and is flexible in the selection of data interval process (Rodrigues et al., 2011), a limitation that was encountered using other software such as TimeStats and TIMESAT. Although TIMESAT, HANTS and Phenosat are freely available for use, they require Matlab software (Matongera et al., 2021b), which is a non-free environment to execute the analysis and therefore limits their applications in resource constrained region. An open source QPheno-Metrics software package was proposed for the extraction of vegetation phenological metrics (Duarte et al., 2018).

Recently, the utility of the Multisource Land Surface Phenology (MS-LSP) algorithm that combined data from fine spatial resolution Sentinel-2A and -2B (10m) and medium spatial resolution Landsat 8 (30m) was tested (Bolton et al., 2020, Soubry et al., 2021). The launching of the MS-LSP algorithm is a significant achievement in LSP investigations since the temporal frequency of Landsat 8 was not sufficient for the estimation of vegetation phenological changes (Helman, 2018). The current study shows that the successful estimation and monitoring of LSP in rangeland ecosystems re-lies heavily on the availability of robust algorithms that are capable of processing vegetation time series whilst minimizing atmospheric noise and sensor related errors. In developing countries, the availability of these software packages free of charge plays a crucial role in data modelling for the management of rangelands. Concerning the choice of LSP algorithm to use, it is important to note that each method has its strengths and weaknesses. Therefore, the suitability of each smoothing algorithm largely depends upon the objectives of that study and the targeted land cover types. The level of expertise demonstrated by the user in tuning parameters and settings during the data processing and phenology metrics extraction process influence the results.
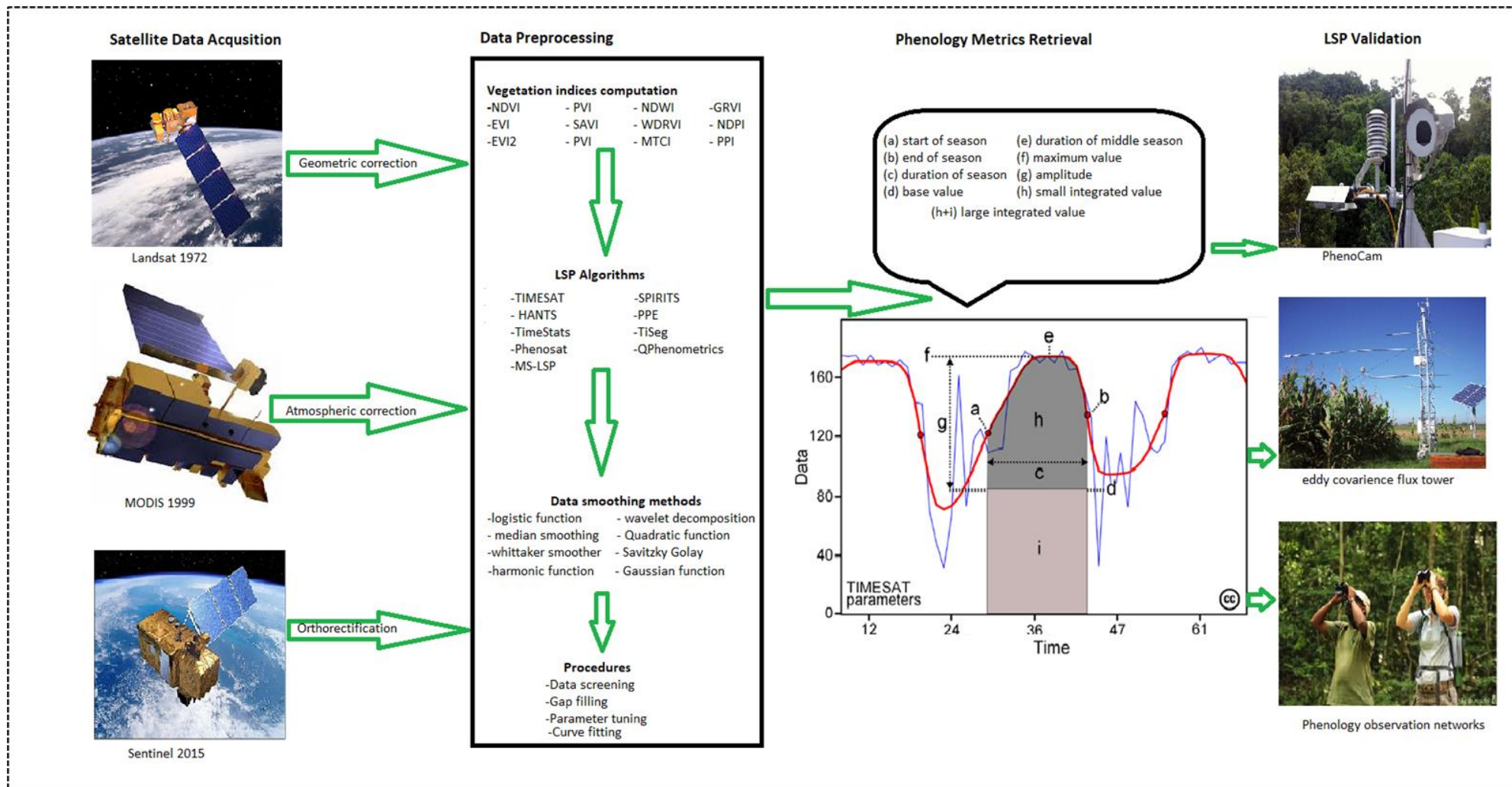
Figure 2.2: Summary of the common procedures followed in LSP investigations

2.6 LSP metrics validation

To evaluate the accuracy of remotely sensed time-series data in estimating the phenological cycles of vegetation in rangeland ecosystems, there is a need for comparisons between satellite-based phenological metrics and what can be observed or measured on the ground (Tong et al., 2019, Coops et al., 2012, Studer et al., 2007). The linking of ground-based phenological observations with satellite-based LSP retrievals provides a huge potential for tracking the response of vegetation to climatic changes in rangelands (Beaubien and Hall-Beyer, 2003). However, large samples of ground phenological observations or measurements are required to adequately validate LSP retrievals especially in cases where studies are conducted at a large scale (Liang et al., 2011). The widely used methodological approaches for LSP validation include the periodic recording and documentation of distinct plant specific biological changes such as the emergence of first leaves, leaf expansion, flowering and fruiting at a local scale (Dambreville et al., 2015, Fadón et al., 2015, Gougherty and Gougherty, 2018). The phenological stages are usually recorded by farmers, botanists, naturalists, volunteers as well as phenological observation networks such as the Nature Canada PlantWatch (Gonsamo et al., 2013) and the USA National Network (USA-NPN) (Peng et al., 2017). For hundreds of years, botanists and naturalists have been collecting a diversity of plant specimens in the world's herbaria (Davis et al., 2015, Panchen et al., 2012, Bolmgren and Lönnberg, 2005). Eventually, scientists and researchers recognized the potential use of herbarium specimens in detecting and modelling the phenological changes of plants in response to environmental and climatic changes (Pearson, 2019, Pearson et al., 2020, Zalamea et al., 2011). However, the collection of herbarium specimens data is labour intensive and time consuming, and this may lead to inconsistencies in the data collection protocols and methodologies (Nic Lughadha et al., 2019).

Some researchers and scientists defined the first appearance of green leaves as the green up date (Studer et al., 2007, Berman et al., 2020, Tang et al., 2016), which resembles the start of the season in LSP. However, due to scale mismatch and data uncertainties, the phenological phases observed and recorded on the ground may sometimes be inconsistent with satellite based LSP estimations (Fisher and Mustard, 2007). Furthermore, field based visual surveys have been reported to be costly and time-consuming (Sakamoto et al., 2010) making it difficult to effectively use them in validating large scale LSP retrievals. Digital repeat photography widely known in remote sensing

literature as Phenological Cameras (PhenoCams) have also been extensively used in validating LSP retrievals. For example, a study in Northern Japan used PhenoCam data from the Phenological Eyes Network to evaluate the LSP metrics from the Himawari Satellite Imager and MODIS (Yan et al., 2019). Their study highlighted that the Root Mean Square Difference (RMSD) between LSP metrics from MODIS and PhenoCam data was high in spring and fall (14 – 29 days). Similarly, another study in United States reported that LSP metrics estimated using VIIRS and MODIS showed an agreement with SOS and EOS metrics estimated from PhenoCam data with RMSDs ranging from 10.1 to 21days (Moon et al., 2019).

However, despite the successful application of PhenoCams in retrieving phenological metrics that are comparable to satellite-based retrievals, several other studies reported low or no correlation between the two data sources especially in rangelands (Richardson et al., 2018, Zhu et al., 2013). Generally, findings from the literature show that the inconsistencies that may arise between PhenoCams and satellite based LSP metrics are largely linked to discrepancies caused by differences in the scale of observation (Zhang et al., 2018b, Browning et al., 2017, Richardson et al., 2018). In some cases, the phenological changes of vegetation in small areas monitored by PhenoCams cannot accurately be representative of large-scale changes observed by satellite images (Matongera et al., 2021b). Other differences could emanate from the fact that PhenoCams do not acquire images in the NIR wavelengths (Yang et al., 2014), they only rely on information from the visible bands. Unlike satellite sensors which have global coverage, PhenoCams coverage is limited. The majority of PhenoCam networks have specific regions they cover, for instance, Phenological Eyes Network mainly covers Japan, the USA, China, Malaysia, and the United Kingdom (Yan et al., 2019) while the PhenoCam network (http://phenocam.sr.unh.edu) mostly focuses on the terrestrial ecosystems of North America (Seyednasrollah et al., 2019). Consequently, there is little or no PhenoCam coverage in rangelands that are geographically located in poor regions, making it becomes difficult to validate LSP retrievals in those under-resourced areas.

Unmanned Aerial Vehicles (UAVs), also referred to as drones in literature, have been an important data source for validating satellite based phenological metrics in many rangeland ecosystems (Browning et al., 2009, Berra et al., 2016). Carbon dioxide flux observations from FLUXNET stations have also been used to validate LSP retrievals in rangelands. For instance, a study in

Canada compared LSP retrievals from MODIS and SPOT with global FLUXNET derived phenological data (Wu et al., 2017). Their study reported that the satellite based LSP estimations had an overall low correlation ($R^2 < 0.30$) with the phenological timings obtained from the flux observations. On the contrary, another study highlighted that carbon flux phenology estimations were highly comparable to satellite-based LSP metrics, with R^2 values ranging from $0.43 - 0.78$ amongst the 4 biomes used in their study (Zhu et al., 2013). However, the use of carbon flux observations to estimate the phenological cycles of vegetation is more suitable in biomes with distinct and detectable seasonal cycles since it can be arduous to detect the start of carbon uptake in high biomass environments (Richardson et al., 2018). As widely reported in the literature, another limitation associated with the use of carbon flux data in validating LSP retrievals is the limited coverage of eddy covariance flux data collection sites in many biomes (Zhu et al., 2013, Gonsamo et al., 2012b, Churkina et al., 2005) thus the estimation of vegetation phenological cycles using carbon flux data remains challenging at a large scale. Another method of validating LSP retrievals involves the use of bioclimatic models which use precipitation and temperature data to track the phenological changes of vegetation (Schwartz and Reed, 1999, Schaber and Badeck, 2003). However, several studies have reported low correlations between satellite derived phenology and bioclimatic based phenology retrievals (Schwartz and Hanes, 2010, White et al., 2009). Evidence from the literature consulted in this review shows that the majority of the LSP validation methods lack detailed spatial and temporal ground phenological measurements and events which include species level field observations.

2.7 Challenges and future directions in rangeland LSP

LSP research has been hobbled by inconsistencies between remote sensing retrievals and vegetation phenological events recorded on the ground (Moon et al., 2019, Balzarolo et al., 2016, Liang et al., 2011). Evidence from literature has shown that the sources of disagreements in phenological metrics amongst different vegetation species may arise due to VIs used (Zuo et al., 2019, Liang et al., 2011) satellite sensor characteristics (Helman, 2018, Zhang et al., 2017) atmospheric conditions (Zhao et al., 2013) and algorithms used to smooth and estimate the LSP phenological metrics (Bornez et al., 2020, Lara and Gandini, 2016, Helman, 2018). The variations introduced by atmospheric impurities, absorption, and scattering, can considerably affect the precision of users when interpreting remote sensing images, especially for the detection of

vegetation dynamics at a landscape scale (Nguyen et al., 2015). Additionally, the impacts of bandpass and other sensor characteristics on the behaviour of the VIs causes errors when retrieving LSP metrics. Another common challenge in LSP investigations is mixed pixels. A pixel in the VIs time series may contain an unknown composition of vegetation species and may result in mixed signals (Chen et al., 2018) since vegetation species vary in their sensitivity to climatic fluctuations and changes.

Although they do exist, future LSP research should probably consider investing more in developing algorithms that fuse moderate and high spatial resolution sensors to improve LSP metrics retrieval at the species level. The extraction of phenological metrics in rangelands such as alpine grasslands remains a challenge due to subtle seasonal variation in VIs time series (Hmimina et al., 2013, Wu et al., 2014, Melaas et al., 2013b). To address saturation problems encountered when deriving phenology metrics, there is a need for further research on the reconstruction and regeneration of VIs that will adequately reduce the problem of saturation in high biomass regions. Specifically, the WDRVI was reported to be effective in dealing with saturation, a common problem encountered using NDVI (Gitelson, 2004). Ground based phenological observations provide reliable and accurate information on individual plant species, but LSP observes changes at a large scale, hence the use of species specific phenological phases observed on the ground to validate large scale satellite LSP retrievals becomes problematic. The current study suggests that international phenology research networks such as International Long Term Ecological Research Network (ILTER) have the potential to facilitate the regulation and standardization of phenology research protocols.

The compatibility of formats when linking LSP algorithms and remote sensing data processing software packages is a challenge. For instance, phenology packages such as TIMESAT (Eklundh and Jönsson, 2012) do not perform the preprocessing of satellite data and the computation of vegetation indices. Consequently, data conversion procedures may lead to the loss or deformation of valuable information in the time series. The development of LSP algorithms that can preprocess remotely sensed data and handle phenological analysis in the same environment will go a long way in addressing some of the technical errors encountered in LSP retrieval. Specifically, deep learning presents an opportunity to further develop robust software packages (Tian et al., 2020) with the abundance of data processing tools and techniques that can be used to better characterize

the phenological cycles of vegetation in rangelands. The validation of LSP metrics remains a challenge in many of the biomes covering the African continent.

To improve the LSP estimation and monitoring there is a need for the establishment of more phenology networks in Africa. While a plethora of LSP studies have focused on the investigation of croplands (Estrella et al., 2007, Haghverdi et al., 2018, Tao et al., 2006) and forests (Roberts et al., 2015, Dragoni and Rahman, 2012, White et al., 2014), the study of the phenological cycles of invasive alien plants in rangelands has largely lagged. The invasive species LSP modelling will enable understanding of the biological structure and timing of alien invasive phenology and lead to improving rangeland management using this knowledge to choose suitable treatment methods in zones infested by the invasive alien plants (Matongera et al., 2021b). The applications of medium spatial resolution sensors such as Landsat in LSP studies have been largely limited by the sensor's temporal resolution since some plant phenological appearance changes quicker than Landsat's 16-day temporal resolution (Helman, 2018). On the other hand, the high temporal resolution sensors such as MODIS lack spatial detail that can accurately track the phenological events of vegetation at the subspecies level (Peng et al., 2017). To tackle these challenges, the constellation of Planet sensors (Planet Scope) holds a huge potential in LSP applications. PlanetScope data have an appropriate quick return time to capture swiftly developing phenological transitions, such as green-up.

The effective management of rangelands requires timely, accurate and reliable information about vegetation activities and how they change over time due to changes in climate or environmental conditions (Browning et al., 2019). Based on the LSP developments discussed in this study, there is a huge potential of LSP data for future use in a wide range of applications for better management of rangeland ecosystems. User groups such as rangeland managers, ecologists and government agencies may use published LSP data sets for various objectives such as designing better management systems and planning restoration activities after ecosystem disturbances. A typical example of the relevance of LSP data is the forecasting of grass and invasive species reproduction based on phenological models that incorporates satellite data, climate data and phenological networks observation networks databases.

2.8 Conclusion

The current study has reviewed the literature on the progress of remote sensing in estimating land surface phenology in rangelands. Empirical evidence has shown that remote sensing offers invaluable data sources in the generation of phenological trends of vegetation at regional and global scales, a task that was previously impossible using ground based phenological observations. The application of remote sensing in LSP studies was pioneered by early satellites such as Landsat, AVHRR and MODIS. However, evidence from literature revealed that the applications of these data sets have been largely limited by the sensor's low spatial resolution, poor radiometric calibration and geolocation errors. Consequently, the launching of high spatial resolution sensors such as Sentinel-2 has significantly improved rangeland LSP investigations. Findings from literature revealed that NDVI pioneered LSP investigations in the early 70s, and many other indices were subsequently developed to address the shortcomings of NDVI. Although milestones have been achieved in the applications of VIs in the retrieval of LSP, the modelling of phenology from remote sensing remains a challenge since it is difficult to develop VIs models that can be used efficiently in all environments. Owing to the unique traits of many Vis and models, appropriate indices should be used to characterize vegetation phenological cycles at various growth stages and estimate phenology trends in different biomes. The successful retrieval of LSP metrics depends on the availability of robust algorithms that are capable of processing vegetation time series whilst minimizing atmospheric noise and sensor related errors.

The literature review uncovered the utility of remote sensing in estimating and monitoring LSP in rangelands. The review also noted that LSP rangeland studies have predominately focused on, grassland, shrubland and savannah. Not much work has been done to understand the phenological cycles of alien invasive species in rangelands from a remote sensing perspective. Thus, in the following Chapter 3, an approach is proposed to understand the phenological cycle of bracken fern, a destructive invasive alien plant using Sentinel-2 time series data.

Chapter Three

Characterizing the phenological cycle of bracken fern using time series data derived from Sentinel-2 satellite sensor

This chapter is based on a paper:

Matongera, T. N., Mutanga, O, and Sibanda, M. (2021). Characterizing bracken fern phenological cycle using time series data derived from Sentinel-2 satellite sensor, PLOS ONE Remote Sensing, 16:10 -23.

Abstract

Bracken fern is an invasive plant that has caused serious disturbances in many ecosystems due to its ability to encroach into new areas swiftly. Adequate knowledge of the phenological cycle of bracken fern is required to serve as an important tool in formulating management plans to control the spread of the fern. The study characterized the phenological cycle of bracken fern using NDVI and EVI2 time series data derived from Sentinel-2 sensor. The TIMESAT program was used for removing low quality data values, model fitting and for extracting bracken fern phenological metrics. The Sentinel-2 satellite-derived phenological metrics were compared with the corresponding bracken fern phenological events observed on the ground. Findings from our study revealed that bracken fern phenological metrics estimated from satellite data were in close agreement with ground observed phenological events with R^2 values ranging from 0.53 – 0.85 ($p < 0.05$). Although they are comparable, our study shows that NDVI and EVI2 differ in their ability to track the phenological cycle of bracken fern. Overall, EVI2 performed better in estimating bracken fern phenological metrics as it related more to ground observed phenological events compared to NDVI. The key phenological metrics extracted in this study are critical for improving the precision in the controlling of the spread of bracken fern as well as in implementing active protection strategies against the invasion of highly susceptible rangelands.

3.1 Introduction

The encroachment of invasive species in productive rangelands influences changes in nutrient cycles (Zhao et al., 2020), fire incidences and severity (Gharari et al., 2018) and alters the abundance of biodiversity (Linders et al., 2019), resulting in socio-economic implications on livelihoods. Bracken (*Pteridium Aqulinimun*) is one of the most problematic alien invasive ferns that encroach into new landscapes (Ngubane et al., 2014). Due to its vigorous growth and dense canopy, the fern has negative impacts on agricultural productivity (Berget et al., 2015), animal and human health (Senyanzobe et al., 2016), forestry and recreational potential (Ssali et al., 2017), leading to huge economic losses. Generally, farmers abandon the agricultural land once the fern heavily invades the land (Schneider and Geoghegan, 2006a) due to its persistent underground root system, which facilitates fast growth. The invasive fern invades grasslands and grazing pastures (Sato et al., 2017, Maya-Elizarrarás and Schondube, 2015, Hamer et al., 2013), while it also perseveres in woodlands and hedgerows, making it difficult for indigenous grass species to thrive (Odindi et al., 2014). The biochemical chemistry and morphology of bracken fern influence its spectral reflectance behavior (Matongera et al., 2017). Specifically, bracken fern has various pigments and carotenoid pigments that form part of the compound arrangement of the fern's cells which actively absorb and distribute radiation and different wavelengths (Matongera et al., 2018).

Understanding the biological structure and timing of bracken fern phenology improves rangeland management's knowledge and ability to choose the suitable treatment method in areas infested by the fern (Taylor et al., 2020a). The phenological information can be used to implement rapid response initiatives for the successful restoration of landscapes at different scales (Taylor et al., 2020b). In literature, the prediction of future invasions before their occurrence has been postulated as one of the most efficient strategies of managing rangelands (Fournier et al., 2019, Jazwa et al., 2018, Fletcher et al., 2016). Therefore, understanding the phenology of bracken fern can help to predict how the fern encroachment will change in time, and necessary proactive measures can be planned accordingly. Accurate and effective strategies in invasive species management save time and resources (Courtois et al., 2018, Baker and Bode, 2016). A well-documented phenological cycle of bracken fern will assist conservationists and farmers in determining the most effective methods and appropriate time for controlling the fern across its life cycle, to ensure the complete eradication of the fern with minimum costs. For instance, knowing the beginning of the bracken

fern season will help the rangeland managers with planning and implementation of the appropriate control measures at an early phenological stage before the spores have been dispersed. Furthermore, the information on bracken fern's phenology is vital in establishing the major drivers of its population dynamics and patterns of invasion. In this regard, an understanding of bracken fern's phenological cycle will provide spatial information on areas that are more threatened for informing policy decisions on deriving effective control and management strategies. Over the past decades, remote sensing has proved to be an invaluable data source suitable for characterizing the phenological profile of vegetation at the local, regional and global scale (Wang et al., 2020, Bolton et al., 2020, Small and Sousa, 2019). Therefore, the uncontrolled colonization of bracken fern in the Drakensberg (Matongera et al., 2017), ascertains the necessity to characterize its phenological cycle.

Earlier works on bracken fern phenology have used field-based studies (Pakeman et al., 1994, Williams and Foley, 1976) and Phenology Cameras (PhenoCams) (Granados et al., 2013) to understand the phenological cycles of the fern in different parts of the world. However, the major limitation of these locally based methods is the spatial extent to which the plant phenological events were collected (Matongera et al., 2021b). Remote sensing technology offers better prospects in providing archives of long term spatial data (Helman, 2018) required to understand the phenological cycles of bracken fern at various scales. The use of remotely sensed data sets in retrieving the phenological metrics of vegetation is referred to as Land Surface Phenology (LSP) in remote sensing literature (Bornez et al., 2020). The application of remotely sensed data in estimating and monitoring LSP was pioneered by early satellite sensors such as the Landsat series (Rea and Ashley, 1976), Advanced Very High Resolution Radiometer (AVHRR) (Justice et al., 1985), the Moderate Resolution Imaging Spectroradiometer (MODIS) (Zhang et al., 2003). The AVHRR and MODIS satellite sensors have a high temporal resolution and synoptic views which is appropriate for large-scale monitoring of land surface phenology (Justice et al., 1985, Reed et al., 1994, Tan et al., 2011). However, despite pioneering land surface phenology studies, the application of low spatial resolution sensors like AVHRR and MODIS is limited by their spatial resolution (Tsuchiya et al., 2003), calibration errors and poor geometric registration while Landsat is limited by its low temporal resolution.

The freely available Sentinel-2 Multi-Spectral Instrument (MSI) optical sensor is composed of two satellites; Sentinel-2A and 2B, hence its revisit time has been decreased from 10 to 3-5 days (Li and Roy, 2017). The sensor has improved sensor calibration with $10 - 60m$ spatial resolution which presents a potential for successful characterization of the phenological cycles of vegetation at the species level (Matongera et al., 2021b). LSP scientists have utilized numerous spectral vegetation indices derived from satellite data to estimate the phenological cycles of vegetation at various scales (Vrieling et al., 2018, Fernández-Manso et al., 2016, Michele et al., 2018, Zhang et al., 2018b, Gitelson, 2004). Over the past decades, vegetation indices were developed and used as indicators of change in vegetation structure, density, spatial extent and phenological timings. The Normalized Difference Vegetation Index (NDVI) and the Enhanced Vegetation Index (EVI2) have been commonly used to quantify the cyclical patterns of vegetation in different ecosystems (Adole et al., 2018, Richardson et al., 2018, Lumbierres et al., 2017, Yao et al., 2017, Liu et al., 2016). The NDVI is a commonly used spectral index regarded as a proxy indicator of vegetation canopy function and is directly associated with the absorption of photosynthetically active radiation by plant canopies (Xue and Su, 2017). The EVI2 was developed to enhance the vegetation signal with better sensitivity in areas with high biomass (Jiang et al., 2007b).

The characterization of the phenological profile of specific vegetation species using satellite data has mainly been done for crops (Sakamoto et al., 2005, Boschetti et al., 2009, Duchemin et al., 2006, Vina et al., 2004), whilst the estimation of the phenological cycles of specific invasive species such as bracken fern still requires more attention. To the best of our knowledge, there are no published studies that have used polar orbiting satellite data sets such as Sentinel-2 to extract the phenological metrics of bracken fern to improve its management approaches. Therefore, the first objective of this study was to characterize the phenological cycle of bracken fern using NDVI and EVI2 time series data derived from the Sentinel-2 satellite sensor. Secondly, the study sought to investigate the differences and similarities between NDVI and EVI2 data in estimating bracken fern phenological metrics. Finally, the study assessed the relationship between phenological metrics estimated from satellite data and the bracken fern phenological events recorded on the validation site, using Cathedral Peak World Heritage Site in the Drakensberg as the study site. This study is part of a continuing effort to craft an integrated approach to control the spread of invasive species in KwaZulu-Natal Nature reserves in South Africa.

3.2 Methods and materials

3.2.1 Ground observed phenology data

The ground phenology recordings included the collection of bracken fern patches locations using a portable Leica GS20 Global Positioning System (GPS). A total of 60 bracken fern patches were collected. The bracken fern patches that were recorded were larger than 10 by 10 m ($100m^2$) for them to match the Sentinel-2-pixel size as well as to account for geolocation errors of the GPS and the Sentinel-2 imagery. Purposive sampling was used to select bracken fern patches with more than 75% bracken percentage cover. The bracken fern phenological developments were recorded weekly from 1 January 2016 to 31 December 2018. Ferns like bracken develop fronds instead of leaves. For ground phenology observations in this study, the term 'fronds' was used instead of leaves. Specifically, we recorded the dates of bracken fern frond emergence, expanded frond growth, withering and frond drying and considered them as green up, green peak, senescence and dormancy respectively. Figure 3.1 shows the phenological transformation of bracken fern appearance from October 2016 to September 2017. The bracken fern photographs were captured weekly, but only monthly images were shown since they proved to be sufficient to show the change in the phenological appearance of the fern. For consistency, the photographs were captured in the same position, at a bracken fern patch located at 29°13'26.758"E 28°56'46.2"S.

Figure 3.1: Phenological transformation of bracken fern appearance from October 2016 to September 2017 captured in Cathedral Peak study site

3.2.2 Satellite data acquisition and pre-processing

Sentinel-2 Multispectral Instrument (MSI) satellite images were obtained from the European Space Agency (ESA) online platform (https://earthexplorer.usgs.gov/). Sentinel-2A and 2B satellite images were included in the time series data for bracken fern phenological analysis. The images were acquired at the processing level 1C. The images were atmospherically and geometrically corrected by ESA. A total of 108 images from January 2016 to December 2018 were acquired. Only Sentinel-2 images with less than 20% cloud cover were selected and included in the phenological analysis. The Function of mask (Fmask) 4.0 algorithm was used for detecting and removing clouds and shadows in the satellite images (Qiu et al., 2019).

The Normalized Difference Vegetation Index (NDVI) (Rouse Jr, 1972) and the two band Enhanced Vegetation Index (EVI2) (Jiang et al., 2008) were used to extract the bracken fern phenological metrics. The NDVI was chosen based on its long term successful applications in the phenology studies (Zhou et al., 2015, Wardlow and Egbert, 2010, Verhegghen et al., 2014). NDVI is suitable for both local and large-scale vegetation assessments, related to canopy structure and canopy photosynthesis, an attribute that is very crucial in the current study. EVI2 was also used based on its sensitivity to coherent inter-band (blue, red and NIR) atmospheric correction and thus may become much better over extreme bright or dark surfaces, such as subpixel clouds, desert playas, and inland water bodies, where the EVI values are usually problematic (Rocha and Shaver, 2009). Additionally, EVI2 has also been reported to solve resolve Leaf area Index (LAI) differences for vegetation with different background soil reflectance (Mourad et al., 2020). The NDVI and EVI2 indices were calculated using the 108 Sentinel-2A and 2B satellite images in the TerrSet Geospatial Monitoring and Modelling System (Version 18.21) software based on the following equations:

$$\text{NDVI} = \frac{NIR - RED}{NIR + RED} \qquad\qquad \text{Equation (1)}$$

$$\text{EVI2} = G \frac{NIR - Red}{N + \left(6 - \frac{7.5}{C}\right)R + 1} \qquad\qquad \text{Equation (2)}$$

where NIR, red and blue represents the quantity of NIR, red and blue light reflected by vegetation and measured by the satellite sensor (D'Allestro and Parente, 2015), 2.5 is the gain or scaling factor; 6 and 7.5 are coefficients of the aerosol resistance term while 1 represents the canopy

background adjustment for correcting the nonlinear, differential NIR and red radiant transfer through a canopy. G will be determined in accordance with the c value. The NDVI and EVI2 images were exported to TIMESAT program for further analysis.

3.2.3 Data smoothing and phenological metrics extraction

The current study used TIMESAT 3.3 program for processing vegetation indices time series data and estimating bracken fern phenological metrics. The TIMESAT program provides an understandable Matlab based user interface that facilitates the manipulation of data into vegetation phenological parameters (Jönsson and Eklundh, 2004). Specifically, three main processing stages were executed in TIMESAT: (1) preprocessing of NDVI and EVI2 time series data by detecting and removing outliers, (2) data smoothing and gap filling using the SG, DL and AG models based on the procedures which are described in detail by Tan et al. (2010) (3) extraction of bracken fern phenological metrics. To provide the most robust description of bracken fern seasonal dynamics, 10-fold leave one out cross validation was used to automatically select the smoothing parameters for the SG, AG and DL smoothing functions.

The TIMESAT program relies on the assumption that the growing seasons begin and end at a similar time annually. In principle, the start and end of the season for the targeted year are identified in the same period as the first and third years (Tan et al., 2011). The seasonal amplitude threshold method was used to extract bracken fern phenological metrics. The seasonal amplitude method is defined between the base level and the maximum value for each season (Eklundha and Jönsson, 2017). The principle of the seasonal amplitude method states that the start of the season occurs when the left section of the fitted curve has reached a specified fraction of the amplitude, which is counted from the base level. The end of the season is also defined similarly but using the right side of the fitted curve. The start of the bracken fern season was defined as the day of the year when the vegetation indices surpassed 10% of the distance between the left minimum level and the maximum, while the end of the season is defined in a similar way, but the opposite direction.

3.2.4 Statistical analysis

To assess the statistical relationships between satellite-derived phenological metrics and ground observed bracken fern phenological events, the coefficient of determination (R^2) (Kasuya, 2019), the Root Mean Square Deviation (RMSD) (Gonzalez-Dugo et al., 2009) and the Mean Absolute Bias (MAB) (Posselt et al., 2012) were computed. For comparison between satellite retrieved and ground observed phenological dates, the linear regression analysis was computed by using the ground observed phenological events as the independent variable and the satellite-derived vegetation indices as the dependent variable. The linear regression analysis was also conducted between NDVI and EVI2 phenological retrievals with NDVI and EVI2 retrievals as independent and dependent variables, respectively. The significance test for all the phenology models was conducted using the F-test with the standard 0.05 cut off indicating statistical significance between variables (*p<0.05*). Figure 3.2 shows the flow chart illustrating the research methodology that was adopted in this study.
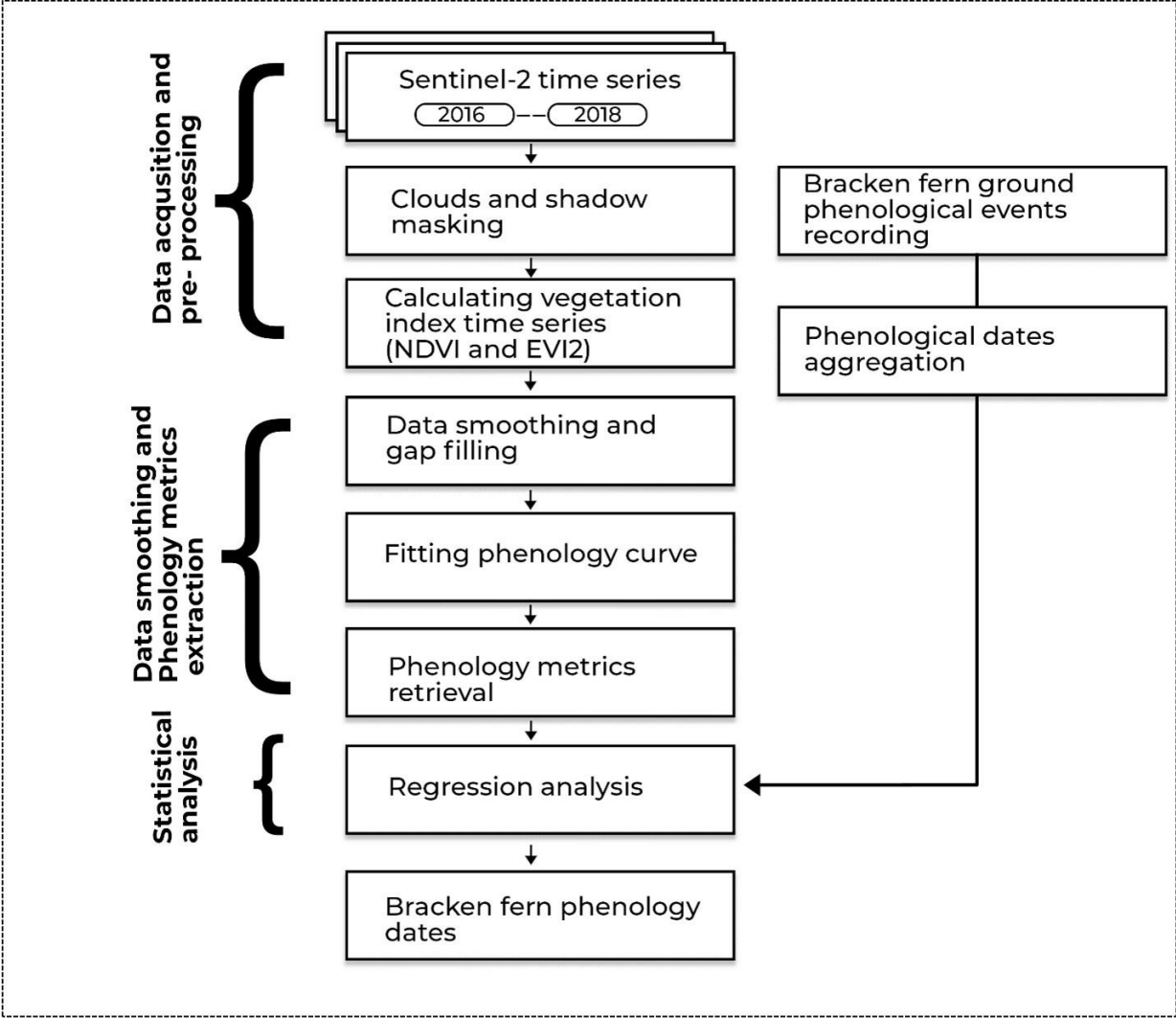
Figure 3.2: Schematic diagram illustrating the research methodology adopted in this study.

3.3 Results

3.3.1 Variation in TIMESAT models phenological retrievals

Table 3.1 shows a summary of bracken fern phenological metrics computed from the three models embedded in the TIMESAT program. Comparison of the mean phenological dates estimated using the three models revealed that bracken fern phenological dates from each model were different although their discrepancies were all less than 15 days. The statistical analysis revealed that the variance in the estimated phenological dates produced by the three models was statistically significant ($p < 0.05$) for all the bracken fern phenological stages based on both NDVI and EVI2 time series. Results obtained using NDVI phenological retrievals show that the mean bracken fern green up onset dates for the AG, SG and the DL was approximately around day 298, 296 and 294 while EVI2 dates were estimated to be around day 280, 288 and 284 respectively. Using the calendar dates, the average timing of bracken fern green up onset dates was towards the end of October 2016. The EVI2 green up onset dates were generally earlier than NDVI dates by an average of 11 days across the three models. For all the models, the standard deviations for the green up onset retrievals were consistent with a range of 2 to 5 days. Based on the NDVI phenological estimations, the DL model recorded the lowest deviation of 2.96 days while the SG NDVI model reported the highest deviation of 5.3 days.

Table 3.1: Mean phenological dates and standard deviations for the TIMESAT models

Model	Phenological metric	Mean (DOY)		Calendar Date	Standard Deviation (Days)	
		NDVI	EVI2		NDVI	EVI2
SG	GU	296	288	October; 2016	5.3	3.78
	GP	57	53	February; 2017	3.36	3.04
	SEN	101	88	April; 2017	5.36	3.91
	DM	176	196	July; 2017	2.03	2.52
DL	GU	294	284	October; 2016	4.96	2.96
	GP	56	54	February; 2017	3.86	2.56
	SEN	99	90	April; 2017	3.69	2.92
	DM	177	184	July; 2017	6.23	4.38
AG	GU	298	280	October;2016	3.76	4.73
	GP	54	44	February;2017	6.11	7.35
	SEN	96	88	April;2017	3.34	2.57
	DM	181	190	July;2017	5.59	3.82

where GU = green up; GP = green peak; SEN = senescence; DM = dormancy

The NDVI green peak onset dates for the AG, SG and the DL were estimated to have occurred around days 54, 57 and 56 while the EVI2 dates were predicted to be around days 44, 53 and 54 respectively. Using the calendar dates, the estimated bracken fern green peak dates were towards the end of February 2017. The NDVI green peak onset dates were later than EVI2 dates by an average of 8 days across the three models. Compared to the green up the phenological stage, the green peak standard deviations were higher across all the models ranging from 2 to 7 days. The

bracken fern green decrease was associated with the plummet in the vegetation index signal which signified the onset of the senescence phenological stage. Based on the AG, DL and SG the NDVI estimated date of senescence onset was around days 96, 99 and 101 while EVI2 retrievals estimated days 88, 90 and 81 respectively. The standard deviations ranged from 2 to 5 days across all models. The NDVI retrievals predicted the onset of dormancy stage to be around days 181, 177 and 176 for AG, DL and SG, while EVI2 retrievals were estimated to be around days 190, 184 and 196 respectively. For both NDVI and EVI2 phenological retrievals, the DL dormancy dates were earlier when compared to the other two models by an average of 16 days. The SG model had the lowest standard deviations (NDVI = 2.03 and EVI2 = 2.52), while the DL recorded the highest deviations (NDVI = 6.23 and EVI2 = 3.42).

3.3.2 Intercomparison of NDVI and EVI2 phenological retrievals

Findings from our study demonstrated that the phenological metrics estimated using NDVI and EVI2 across the four major bracken fern phenological stages were comparable. The statistical analysis in Figure 3.3 shows scatter plots depicting the agreement between bracken phenological metrics estimated using the two vegetation indices. The EVI2 and NDVI phenological metrics show significant linear relationships between each other amongst all phenological stages ($p < 0.05$) although the correlation coefficients were weak for some of the phenological stages with R^2 values ranging from 0.49 – 0.61. For the green up onset stage, the coefficient of determination ($R^2 = 0.58$) indicated a good correlation between NDVI and EVI2 phenological retrievals. The EVI2 phenological dates for green up onset were earlier than NDVI retrievals for most of the pixels across the study site. The green up onset RMSD was 8.2 days while a bias of 4.9 days was recorded.
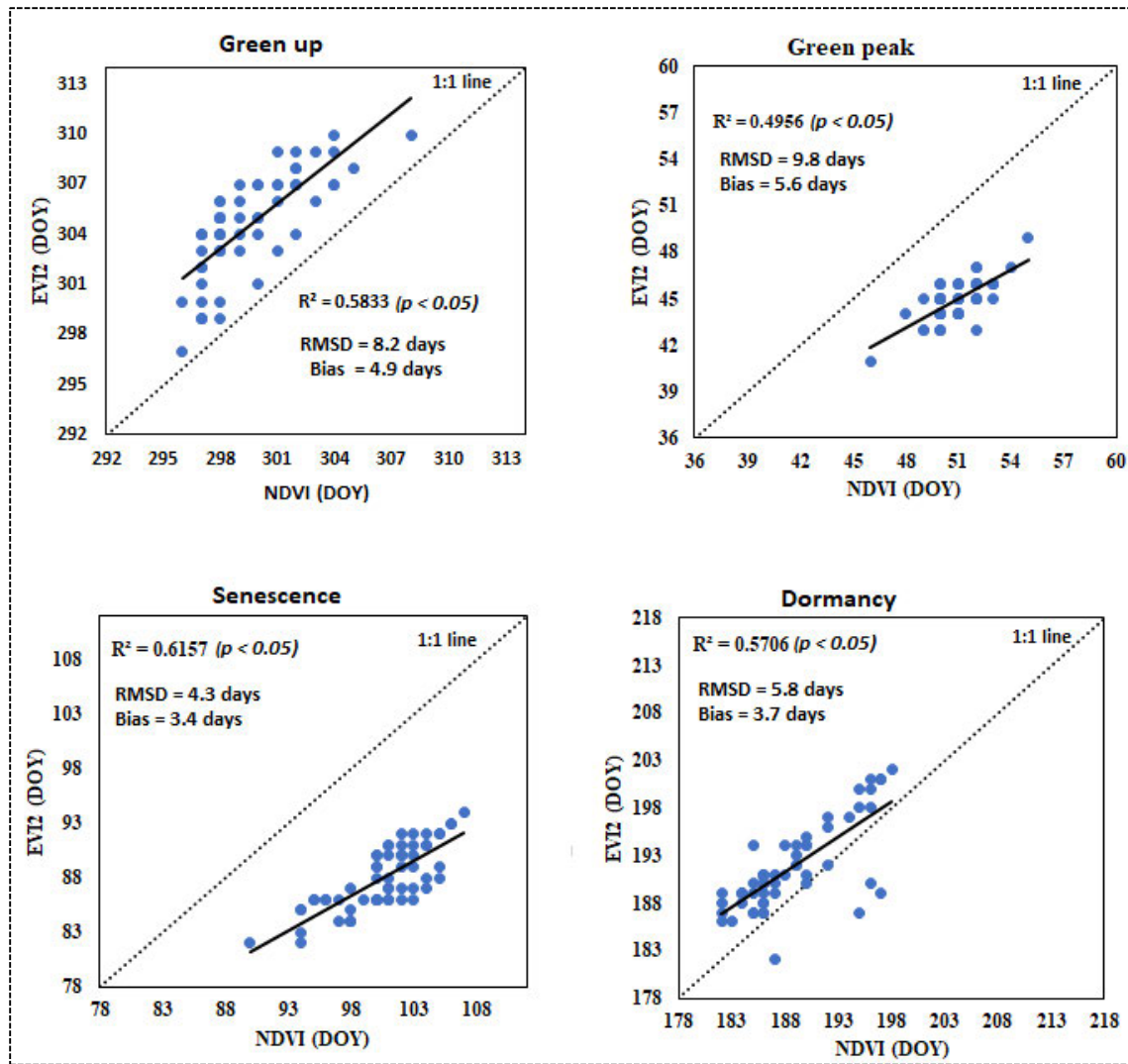
Figure 3.3: Statistical comparison between NDVI and EVI2 phenological dates

3.3.3 Comparison between satellite-based phenological retrievals and ground observations

Bracken fern phenological metrics estimated using NDVI and EVI2 generally showed a good agreement with phenological dates from ground observations. Both EVI2 and NDVI phenological metrics show significant linear relationships ($p < 0.05$) with bracken fern ground observed phenological events with varying correlations across all phenological stages. To provide a more comprehensive and quantitative assessment, Figure 3.4 shows scatter plots illustrating the statistical agreement between satellite-derived phenological metrics and ground observed transitional dates.

The coefficients of determination for both NDVI and EVI2 phenological retrievals indicated a correlation with ground observed onset dates, with R^2 values ranging from

0.53 – 0.85. The dormancy$_{EVI2}$ phenological retrievals recorded the highest correlation ($R^2 = 0.85$) with the ground observed frond drying and falling dates. The relationship between EVI2 retrieved dormancy onset dates and the ground observed bracken fern frond drying and falling showed a very strong correspondence for more than 75% of the pixels across the study site. The green peak $_{EVI2}$ also reported a strong correspondence ($R^2 = 0. 72$) with ground observed bracken fern expanded frond growth.

The RMSDs statistical values between satellite-based phenological retrievals and ground observed phenological transitional dates ranged from 2.5 to 6.4 days across the four bracken fern phenological stages. The RMSDs between NDVI and corresponding ground transitional dates were modestly higher (approximately one week) for senescence and dormancy phenological stages, while the EVI2 green peak and dormancy had the lowest RMSDs of 3.1 and 2.4 days respectively. The RMSDs between NDVI and ground recorded phenological dates were also higher (approximately one week) for green peak, senescence and dormancy while the green up phenological stage showed the lowest RMSD value of 4.6 days. The bias between satellite-based phenological retrievals and ground observed phenological events appeared to be very low as they ranged from 2.2 to 5.3 days. The largest bias (5.3 days) was recorded between green up $_{NDVI}$ bracken fern frond withering, while the lowest bias (2.2 days) was reported between green peak $_{EVI2}$ and bracken fern frond emergence. Generally, the EVI2 phenological retrievals corresponded more with bracken fern ground observed phenological events compared to NDVI phenological retrievals as shown by higher EVI2 correlation coefficients and lower RMSDs and Biases. Overall, the satellite-based bracken fern phenological estimates matched moderately well with the ground observed phenological events.
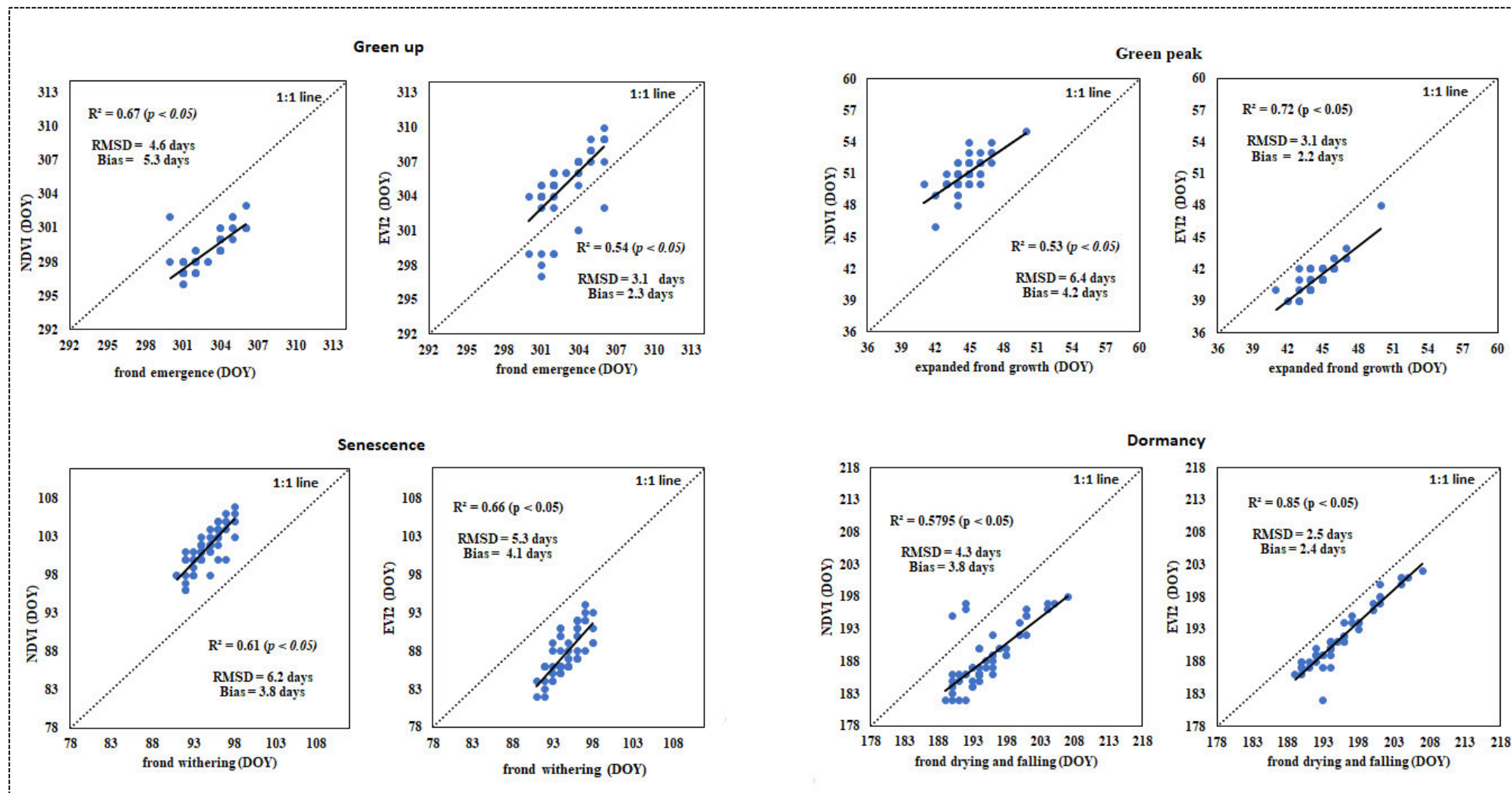
Figure 3.4: Statistical comparison between LSP dates and ground observed phenology

3.4 Discussion

3.4.1 The role of remotely sensed data in characterizing bracken fern phenology

The current study characterized the phenological cycle of bracken fern invasive species using NDVI and EVI2 time series data derived from the Sentinel-2 MSI sensor. The satellite-based phenological retrievals were compared with bracken fern ground observed phenological events. The Sentinel-2 sensor proved to be a reliable data source that could assist in improving the understanding of bracken fern phenological cycles, an aspect that could lead to better management of rangelands that are infected by the fern. Corresponding to our findings in this study, a plethora of scientific studies have also reported the capability of Sentinel-2 data in extracting the phenological cycles of vegetation at various scales (Descals et al., 2020, Pastick et al., 2020, Vrieling et al., 2018, Tian et al., 2021). The sensor's revisit time was sufficient to adequately capture the phenological changes of bracken fern. However, slight cloud coverage issues were experienced during the bracken fern green peak stage which coincided with the peak of the summer season. This could explain lower correlations between NDVI and bracken fern ground observed phenological events during the bracken fern green peak phenological stage.

The bracken fern phenological metrics estimated using the three models in the TIMESAT program were comparable across the bracken fern phenological stages. The shape of the fitted NDVI and EVI2 curves in Figure 3.2 shows a possible quick response to precipitation, followed by a slow decay as bracken fern fronds withered. Corresponding with findings reported by Eklundh and Jönsson (2015), the current study established that the DL and AG models produced phenological curves that were subsequently used to estimate bracken fern phenological metrics that were more correlated to ground observed phenological events as compared to the SG model. Similarly, the works of Cai et al. (2017) also concluded that the AG and DL models produced a more robust and accurate description of the phenological cycles of vegetation compared to the other methods tested in their study including the SG model. Although the AG and DL produced similar bracken fern phenological curves, it can be noted that the AG well adapts and performs better during vegetation indices peaks as compared to the DL model. Vrieling et al. (2018) reported that the AG is less affected by noise and has a great advantage if the time series data has missing data or if the satellite data is poor quality due to sensor calibration errors. SG is mostly affected by atmospheric impurities and subsequently produces erroneous phenological metrics especially during the peak of the season

where the data is characterized by clouds. Results from our study corresponded with previous findings by Li and Liu (2010) and (Khobkhun et al., 2013) who reported that the SG model works well for data that is unaffected by noise caused by atmospheric contamination. Generally, our study demonstrated that the three models in TIMESAT perform good and they can reduce noise, reconstruct, and fit time series data for the estimation of bracken phenological metrics. However, the tuning of parameters is essential in the extraction of phenological metrics using these three models. The inappropriate selection of parameters may lead to uncertainty and bias in phenological trends produced by data smoothing models. The tuning of parameters in phenological metrics extraction was also raised in literature by Stanimirova et al. (2019) who highlighted that the differences in tuning parameters such as the use of 10% or 15% of seasonal amplitude as a benchmark threshold to ascertain the phenological metrics will yield different results.

3.4.2 Comparisons with ground observed phenological events

The validation of phenology metrics is essential for the evaluation of satellite sensors' performance in estimating LSP. However, previous research studies have shown that the validation of remote sensing products is a huge challenge in LSP investigations (Wang et al., 2017b, Zhang and Hepner, 2017, Wang et al., 2018). Overall, the EVI2 performed better in estimating bracken fern phenological metrics that were correlated to ground observed phenological events. EVI2 proved to produce better estimates that are comparable to bracken fern ground observations during the green peak, senescence and dormancy phenological stages. Corresponding with our findings, Peng et al. (2021) noted that EVI2 significantly improves linearity with biophysical vegetation properties and reduces saturation effects found in densely vegetated surfaces, a challenge that is commonly encountered when using NDVI. Similarly, Zhang et al. (2018b) concluded that EVI2 is the better choice for detecting phenology than NDVI because EVI2 phenological retrievals were in close agreement with PhenoCam observations. The performance of EVI2 could also be attributed to its resistance to soil background effects which normally causes an artificial increase in NDVI as reported by (Rocha and Shaver, 2009). On the other hand, NDVI outperformed EVI2 in retrieving the bracken fern green up onset. The performance of NDVI in estimating the onset of bracken fern green up could be attributed to its ability to reduce topographic effects (Huete et al., 2002) and illumination conditions (Testa et al., 2018) much better as compared to the EVI2.

The NDVI showed poor correlation with ground observation during the green peak phenological stage, while the EVI2 retrievals performed well during the green peak stage. As the bracken fern fronds increased in size and the canopy expanded, NDVI tends to saturate and become less efficient in extracting phenological metrics during the green peak period. The differences in phenological retrievals between NDVI and EVI2 probably originated from various resistance levels to noise and sensitivities to spectral signals at different bracken fern stages of the growing season. The NDVI's poor performance in estimating the bracken fern green peak could probably be related to its loss of sensitivity when the vegetation canopy's leaf area index reaches a maximum as reported by Davi et al. (2006). Our results were consistent with Zuo et al. (2019) and Zhao et al. (2011) who reported that NDVI has more ability to track weak spectral signals in the early and end of vegetation growth season and tends to saturate at dense vegetation. Findings from the current study are consistent with previous work by Davi et al. (2006) who noted that false highs occur when high NDVI values are considered to give better estimations than low values, and the bias tends to break the assumptions of many standard statistical methods. The rapid changes of NDVI during the bracken fern green peak period make it complex for the determination of the phenological metrics. A study by Tan et al. (2010) confirmed that vegetation normally changes quickly during green up and green peak, making it difficult to accurately detect changes in NDVI fluctuations.

3.4.3 Implications to the control and management of bracken fern

Challenges in controlling the encroachment of bracken fern into areas of ecological importance due to inappropriate timing have been widely reported in the literature (Matongera et al., 2018, Schneider, 2004, Berget et al., 2015, Marrs et al., 2000a). Therefore, the accurate estimation of bracken fern phenological transition times will help in the appropriate timing control measures and efforts of controlling the invasive fern for better management of the rangelands. Furthermore, the information on bracken fern's phenology is vital in understanding the major drivers of its population dynamics and patterns of invasion. The effective management of rangelands requires continuous data sources that track the changes in various vegetation species that are within a landscape. Dawson et al. (2011) noted that an effective conservation response must be broadly coordinated and informed by a range of scientific approaches with diverse data sources. The free availability of high spatial and temporal resolution data sets such as Sentinel-2 enables rangeland managers to continuously monitor the changes that occur within areas of their jurisdiction.

The debate with regards to the most suitable methods of controlling the spread of bracken fern has received much attention in the literature (Douterlungne et al., 2010, Matongera et al., 2018, Levy-Tacher et al., 2015a). Findings from the current study suggest that the Sentinel-2 data is an invaluable tool that can be used as a foundation for decision-making particularly in controlling the spread of bracken fern in ecologically sensitive areas. The current study suggests that the development of bracken fern spores at the beginning of the senescence phase can be timely controlled using chemical measures such as spraying with asulum before they disperse. The application of chemicals on bracken fern during the senescence period significantly reduces the number of fronds that will be produced the following season (Pakeman et al., 1994). Asulum does not affect the year of application but kills almost all the buds on the rhizome which leads to less production of fronds in the following growing season. The mechanical control methods would probably be suitable during the green up phase when the bracken frond biomass is still low.

3.5 Conclusions

The current study focused on characterizing the phenological cycle of bracken fern using NDVI and EVI2 time series data derived from the Sentinel-2 sensor. The Sentinel-2 satellite-derived phenological metrics were compared with the corresponding bracken fern phenological events observed on the ground. Based on the results established at bracken fern's four phenological stages, the following conclusions were drawn;

- Sentinel-2 sensor was able to extract the phenological profile of bracken fern, making remote sensing technology a potential tool for effective bracken fern management.
- Inter-comparisons between NDVI and EVI2 based phenological metrics revealed that the two vegetation indices differ in their ability to track the phenological developments of bracken fern during its growing season. EVI2 is more suitable for retrieving LSP metrics than NDVI as it produced phenological metrics that were more related to bracken fern ground phenological events.
- The satellite-based phenological retrievals showed a good correlation with bracken fern ground observed phenological events.

Through this study, LSP has demonstrated to be an invaluable data source that can be used by conservationists, ecologists and rangeland managers in controlling and managing bracken-infested rangelands. To the best of my knowledge, not much work has been done to understand the spatial distribution of bracken fern during a specific phenological stage. Thus, in the following Chapter Four, a mapping approach is proposed to assess the spatial distribution of bracken fern using limited ground sample data during the green up phenological stage.

Chapter Four

Estimating the spatial distribution of bracken fern during the green up phenological stage using limited ground sample data

This chapter is based on a paper:

Abstract

Bracken is a problematic alien invasive fern that outcompetes indigenous vegetation and threatens their diversity while it is also reported to have adverse effects on water quality and possible incidences of some strains of human cancers. It is imperative to detect bracken fern invasion before it gets dominant and unmanageable. Mapping methods that demand extensive fieldworks are costly and time-consuming in mountainous areas, where the terrain is rugged and generally inaccessible. The aim of this study was to estimate the spatial distribution of bracken fern during green up phenological stage. The study compared the accuracy of One Class Support Vector Machines (OCSVM) and Biased Support Vector Machine (BSVM) algorithms as they require positive and randomly generated unlabelled samples, thus reducing the amount of ground sampling required for the classification workflow. To assess the performance of the One Class Classification (OCC) algorithms, the study analyzed the effectiveness of (i) spectral bands, (ii) spectral bands plus vegetation indices, (ii) spectral bands plus topographic variables and (iv) all data sets combined in estimating the spatial distribution of bracken fern during the green up phase. Results show that the BSVM algorithm outperformed OCSVM with average overall accuracies of 0.89 and 0.93 respectively. The data sets which combined spectral bands, vegetation indices and topographic variables yielded the highest accuracies compared to all other datasets based on the two algorithms. The spatial distribution maps produced in the current study can be used as baseline data when formulating intervention strategies for controlling the encroachment of bracken fern in rangelands.

Keywords: Bracken fern; OCC; Green up; Phenology; Sentinel-2

4.1 Introduction

The encroachment of invasive alien plants into farmlands, rangelands and forests has negatively affected the productivity of the infested environments globally (Agha et al., 2021, David et al., 2021, Birhanie et al., 2020, Sintayehu et al., 2020). Bracken fern has been documented to be one of the most aggressive invasive alien plants that invade agricultural land (Berget et al., 2015), poison grazing animals (Faccin et al., 2018), compromise water quality (Eyibio Olaifa, 2018), cause biodiversity loss (Maya-Elizarrarás and Schondube, 2015), increase fire risk and costs (Gill and Catling, 2002) as well as destructing native vegetation in ecosystems around the world. The fern produces allelopathic substances which trigger changes in soil composition, causing limitation and total inhibition of the growth of indigenous plants (Eastman, 2003). Additionally, the dense thickets formed by bracken fern disrupt the regeneration of other plants in many ecosystems (den Ouden, 2000). Bracken fern is ranked as one of the major threats to the vestige patches of the KwaZulu-Natal grassland (Ngubane et al., 2014). The continuous threats from hysterical encroachment of bracken fern in South Africa, predominantly in the Drakensberg Mountains of KwaZulu-Natal province require quantification. If uncontrolled at an early phenological stage, the fern could encroach into agricultural land in surrounding areas which could lead to the abandonment of cultivation and grazing land like what was reported in Southern Mexico by (Schneider and Geoghegan, 2006b). Therefore, the early detection and monitoring of bracken fern invasion is essential to avoid huge ecological and economic loss.

There has been a debate in the literature regarding the optimal phenological stage at which control measures can be effectively applied to curb the ramped spread of bracken fern into new landscapes. For instance, Lawton (1990) proposed the biological control of bracken using insects at the green peak phenological stage. Pakeman et al. (1994) argue that the cutting of full-grown bracken rhizomes once every three years will significantly reduce the fern's biomass. However, the bracken fern plant multiplies from dropped spores that fall from the feathery fronds. For effective management, the fern should be harvested during its early shooting when the fronds are still few, immature, and curled up. An attempt to control the fern at a later phenological stage such as green peak through cutting and rolling will require more resources (Lawton, 1988) while controlling it at the senescence stage will not be significant since the spores would have been dispersed already (Conway, 1957). It is critical to quantify the spatial extent of the fern during the green up phenological stage to improve efficiency in

developing control management strategies. The bracken fern green up phenological stage is observed in the field when the first bracken fern fronds appear (McGlone et al., 2005). The assessment of the spatial distribution of the fern at the beginning of its phenological cycle enables rangeland managers to deal with the invasion before the infestation becomes unmanageable.

Remote sensing has been used as a reliable tool for estimating the spatial distribution of invasive species at any phenological stage. For instance, Kazmi et al. (2022) mapped the spatial distribution of invasive alien species using remote sensing in Pakistan during green peak and dormancy phenological stages with an overall accuracy of 93%. Dube et al. (2020) estimated the spatial distribution of lantana camara in semiarid savanna rangeland ecosystems of South Africa during dormancy phenological stage with an overall accuracy of 78% and 66% for Sentinel-2 and Landsat 8 OLI sensors respectively. In another study, Odindi et al. (2014) compared the utility of WorldView-2 and SPOT 5 images in mapping bracken fern during senescence phenological stage with overall classification accuracies of 85% and 72% for Worldview-2 and SPOT 5 respectively.

Remote sensing provides reliable global coverage through its rich remotely sensed data sets acquired by satellite imagery at various spatial and spectral resolutions (Matongera et al., 2021b). Remotely sensing is better suited for landscape mapping since most of the data sets are freely available and have a wider spatial coverage (Gillanders et al., 2008, Foody, 2002). Remote sensing offers the opportunity to perform a temporal analysis of land cover changes in rangelands (Palmer and Fortescue, 2004). With a wide range of remotely sensed data sets and robust data processing algorithms, it is possible to evaluate the statistics of past change, relative to the present and depict major trends in land cover changes (Haque and Basak, 2017). In 2015, Sentinel-2 Multispectral Instrument (MSI) emerged as a reliable sensor suitable for monitoring landscapes at different scales. Sentinel-2 multispectral imager covers a wide swath of 290 km, with a 3-5 day revisit time, which make it suitable for use in numerous applications (Fauzan et al., 2017). The management of rangelands infected by bracken fern requires continuous mapping and monitoring based on spatially explicit datasets such as Sentinel-2 to evaluate the progress of its eradication.

Remote sensing image classification is the widely used approach to extract species distribution information from satellite data (Mngadi et al., 2020, Amani et al., 2020a, Rwanga and Ndambuki, 2017). Numerous multiclass supervised classification techniques have been

developed and tested over the past few decades. These include Artificial neural networks (Gopal and Woodcock, 1996), Random Forests (RF) (Pal, 2005), and Support Vector Machines (SVM) (Pal and Mather, 2005). Despite attaining good accuracies in several studies, the convectional multiclass classification procedures are inappropriate in cases where the research targets a specific land cover class. In principle, multiclass classification techniques require extensive training data for all classes to be effective and accurate in classifying (Deng et al., 2018). In mapping the spatial distribution of invasive species, where there is a specific class of interests, it is somehow unnecessary, time-consuming and resource-wasting to collect ancillary data that represents all the land cover classes within the study area. Literature shows that bracken fern is usually found in mountainous areas (McGlone et al., 2005, den Ouden, 2000, Matongera et al., 2018) in inaccessible locations where rugged terrain and poor road infrastructure renders field data collection to be a challenging task. The One Class Classification (OCC) is the most ideal approach for mapping invasive alien plants such as bracken fern in inaccessible mountainous locations (Piiroinen et al., 2018). Moreover, the OCC procedure is cost-effective because it can perform classification with limited ground sampling. The targeted class is regarded as the positive class while all the other classes are categorized as negative.

In remote sensing, the OCC approach was initially developed for anomaly detection (Moya and Hush, 1996). The OCC approach requires minimum field data, only reference data for the target class is required for the training and testing of the classification model (Liu et al., 2020). The parameters and thresholds in one class classification influence the performance of the algorithm (Seliya et al., 2021). In principle, OCC algorithms produce binary predictions for the test data set using thresholds that can be adjusted (Khan and Madden, 2014). The key to achieve good results in land cover classification using OCC methods relies on the ability of the user to define the kernel structure and to tune the free parameters (Mũnoz-Marí et al., 2010). The OCC methods have been successfully applied in document classification, texture separation, image classification, and environmental modelling (Foody et al., 2006, Muñoz-Marí et al., 2007). The OCC is efficient for mapping invasive species since only the invasive plant is the main target. Several machine learning OCC algorithms have been proposed and widely applied for image classification at various scales. The widely used algorithms include the Biased Support Vector Machine (BSVM) (Piiroinen et al., 2018), one-class Support Vector Machine (OCSVM) (Baldeck and Asner, 2014), Boosted regression trees (BRT) (Skowronek et al., 2016), Mixture Tuned Matched Filtering (MTMF) (Barbosa et al., 2016) and Maxent (Mack and Waske,

2017). Therefore, this study sought to estimate the spatial distribution of bracken fern during green up phenological phase using a One Class Classification approach. The secondary objectives compared the performance between OCSVM and the BSVM as well as assessing changes in the spatial distribution of bracken fern between 2015 and 2020.

4.2 Data and Methods

4.2.1 Ancillary data collection

The bracken fern locations were collected during two field campaigns in October 2015 and October 2020 during the green up phenological phase. Stratified random sampling was used to collect bracken fern, using elevation categories as strata. The elevation was graded into three categories which were low (1000 – 1500m), medium (1500 – 2000m) and high (above 2000m) elevation. A total of 40 bracken fern location were collected in each elevation category. The sampling approach was adopted to cover all relevant environmental gradients. The sampling points were located at least 50m away from each other to avoid autocorrelation. The bracken fern sampled locations were documented in a table format and later converted into a point map in ARCGIS 10.6.

4.2.2 Remotely sensed data acquisition and pre-processing

The Sentinel-2 satellite data was obtained from the European Space Agency (ESA) online platform. The cloud-free Level 1C Sentinel 2 scenes acquired in October 2015 and 2020 were downloaded. The sensor has four multispectral bands at 10m, six bands at 20m and three bands at 60m spatial resolution (Immitzer et al., 2016). Sentinel-2 has a 3–5-day revisit time at an orbital angular distance of 180km with a 290km swath width (Phiri et al., 2020). The thirteen spectral wavelengths of this multispectral sensor cover the visible, red edge and the short-wave infrared potions of the electromagnetic spectrum (Matongera et al., 2021a). However, the coastal aerosol and circus bands were not used in the analysis because they do not have useful information for bracken fern classification. Prior to the analysis, the images were pre-processed for atmospheric correction using the Semi-Automatic Classification (SAC) Plugin available in QGIS. The Function of the mask (Fmask) 4.0 algorithm was used for detecting and removing clouds and shadows in the satellite images.

4.2.3 Vegetation indices

Several spectral vegetation indices have been developed for various applications in vegetation mapping and monitoring on the terrestrial surface. Table 4.1 shows the summary of vegetation indices used in this study. VIs were included in the analysis because of their efficiency for mapping vegetation and to improve the dimensionality of Sentinel-2 data. In this study, vegetation indices were generated, as follows: Normalized Difference Vegetation Index (NDVI), Soil Adjusted Vegetation Index (SAVI), Enhanced Vegetation Index (EVI) and Transformed difference vegetation index (TDVI). The four vegetation indices were chosen based on their success in the diagnosis of vegetation biophysical parameters such as biomass (Silleos et al., 2006), percentage of land cover (Ayala-Izurieta et al., 2017) and photosynthetic activity (Wong et al., 2020).

Table 4.1: Description of the vegetation indices used in this study

Vegetation Index	Formulation	Characteristics and applications	Reference
NDVI	$\dfrac{NIR - Red}{NIR + Red}$	Large scale vegetation assessments, related to canopy structure and canopy photosynthesis	(Rouse et al., 1974)
SAVI	$\dfrac{(1 + L)(NIR - Red)}{(NIR + Red + L)}$	Improves NDVI sensitivity to soil background effects	(Huete, 1988b)
EVI	$G \dfrac{NIR - Red}{NIR + C_1\, Red - C_2\, Blue + L}$	Optimized to enhance sensitivity in high biomass environments	(Huete et al., 2002)
TDVI	$TDVI = 1.5 * \left[(NIR - Red) / \sqrt{NIR^2 + R + 0.5} \right]$	Reduce the effects of bare soil during land cover classification	(Bannari et al., 2002)

4.2.4 Topographic variables

Topographic variables have been documented as some of the key variables that influence vegetation diversity and variability at various scales (Zeferino et al., 2020). The topographic variables refer to the geomorphological attributes that match the Digital Elevation Model (DEM), plan curvature and slope. The DEM was generated from The Advanced Spaceborne Thermal Emission and Reflection Radiometer (ASTER) imagery, with a 30m spatial resolution. Elevation, slope, aspect and topographic wetness index (TWI) were included in the analysis based on their influence on the phenology and spatial distribution of vegetation (Piiroinen et al., 2018).

4.2.5 Classification

The selection of datasets to build the classification models was separated into four categories: (i) spectral bands, (ii) vegetation indices, (iii) topographic variables and (iv) combined data set with spectral bands, vegetation indices and topographic variables. Support Vector Machines (SVMs) have become significantly common for land cover classification and regression applications, owing to their ability to transform non-linear data using the kernel functions (Üstün et al., 2007). In principle, the SVMs find a hyperplane splitting the samples of the target class from the origin with the best possible separation (Nalepa and Kawulok, 2019). Ultimately, most of the samples that fall within the same hypersphere are considered to belong to the target class, while samples that are found outside the hypersphere are treated as outliers (Awad and Khanna, 2015). In this regard, the successful application of SVM models relies on the ability of the user to define the kernel structure and to tune the free parameters (Mũnoz-Marí et al., 2010). SVM models have a successful track record of processing high dimensional data using fewer training samples as input data (Li and Xu, 2010). By separating data using the best possible boundary, the model becomes robust and can process irregularities such as noisy test data or biased train data. The current study tested the utility of the OCSVM and BSVM algorithms in estimating the spatial distribution of bracken fern during the green up phenological phase. The OCSVM and BSVM were executed using the oneClass package in R statistical software.

4.2.5.1 One Class Support Vector Machine

Schölkopf et al. (2001) developed the OCSVM method for novelty detection and classification of specific phenomena. Given *n* training points, OCSVM tries to find a hypersphere to separate the training data from the origin with maximum margin in a multidimensional space (Li and Xu, 2010). The best values that are used for tuning the parameters were selected by a grid search which uses five reiterations of ten-fold cross-validation based on the training dataset. The positives were locations where bracken fern was present while negative samples meant the absence of bracken fern. The data set used to train the model contained 112 positive and 400 negative samples. The OCSVM free parameter and threshold tuning was executed using the procedure described in detail by (Li and Guo, 2013). If training data does not include negative data, only True Positive Rate can be generated (Mũnoz-Marí et al., 2010). Therefore, instead of using only labelled data, the current study also used negative data to train the OCSVM model.

4.2.5.1 Biased Support Vector Machine

In circumstances where there are very few training data samples available, the OCSVM may produce biased classification results (Li et al., 2010). To deal with this challenge, OCSVM can be revised in the context of the Biased Support Vector Machine (BSVM) to include not only labelled but also unlabelled samples in the classification workflow. The BSVM method was initially developed for text classification (Liu et al., 2003), using the ordinary binary SVM protocol. Instead of having negative samples, the BSVM classifier uses randomly generated samples, often called background data (Barbosa et al., 2016) or unlabelled samples (Piiroinen et al., 2018). The BSVM training data had 112 labelled samples and 1000 randomly generated unlabelled samples. Since the unlabelled class is randomly generated, it will also contain samples from the positive class. The unlabelled class sample was set to be large to balance a sizeable portion of the bracken fern positive samples.

4.2.6 OCC model assessment

To evaluate the accuracy of the OCC algorithms the standard accuracy indices were used. The overall accuracy, recall, precision, and F-score, for all data set combinations were computed for all data set combinations. Bracken fern presence class had the same number of positive (presence) cases and the negative (absence or unlabelled) cases were unequal for BSVM and OCSVM, the True Positive Rate (TPR), also known as Recall was computed to assess the

classification accuracy of the derived models. The TPR standard evaluates the probability of a positive pixel being identified correctly (Piiroinen et al., 2018). Since the focus of the study was to estimate the spatial distribution of bracken fern, it was essential to find the algorithm that can identify positive labels within the data set as accurately as possible. Therefore, in this study, the True Positive Rate (recall) performance metric was considered more important than the False Positive Rate (FPR) metric in assessing the model performance. The higher recall of 100% indicates that an algorithm managed to correctly identify bracken fern positive samples.

To improve the confidence in the model's performance in predicting positive samples, the precision performance metric was calculated. Precision is the proportion of true positives to total predicted positives (Zhao and Cen, 2013). The F-score metric was also computed to measure the accuracy of the model on the data set. The F-score combines the precision and recall of the model and is often called the harmonic mean of the model (Tchakounté and Hayata, 2017). Ideally, the F-score was chosen since it considers both precision and recall, it is known to be the harmonic mean of the precision and recall. The F-score is normally employed when the classes are not evenly distributed (Kulyukin and Blay, 2015), which is normally the case in applications where OCC methods are used. To ascertain the model with the best predicting power the Receiver Operating Characteristic (ROC) Curve was used. The findings on the performance of OCSVM and BSVM algorithms were presented using the averages of the results obtained from 2015 and 2020.

4.2.7 Changes in the spatial distribution of bracken fern

The total amount of pixels covered by bracken fern target species was calculated for the entire study site using the dplyr package in R. These were later converted to square kilometres and the percentage of change was calculated using the rgdal package in R. Comparison was made for the pixels covered in 2015 and 2020 to establish if bracken fern is rapidly encroaching into new areas. To visualize the spatial and temporal distribution of bracken fern based on the two one class algorithms, thematic maps showing the spatial distribution of the fern in 2015 and 2020 were produced.

4.3 Results

4.3.1 Comparison of OCC algorithms

Table 4.2 presents classification accuracies on the test data set for the OCSVM and BSVM algorithms based on the four data sets used in this study. Generally, the classification accuracies for the two algorithms were high (OA < 75%) based on the four categories of data sets used. Results show that in all data set combinations, the BSVM algorithm outperformed OCSVM with average overall accuracies of 89% and 93% respectively. The largest overall accuracy discrepancy between BSVM and OCSVM algorithms was exhibited by the model derived based on combined spectral bands and topographic variables while the spectral bands and vegetation indices model recorded 90% accuracies for both algorithms.

The BSVM model recorded the highest recall across all data set combinations with an average of 87%, while OCSVM recorded 85%. The BSVM algorithm correctly identifies bracken fern positive samples with 87% accuracy. On average, OCSVM achieved the highest precision (84%) while BSVM recorded 81%. On average, BSVM had the highest F-score of 83% while OCSVM recorded 79%. Overall, the classification performance measurements tested in this study revealed that BSVM outperformed OCSVM in estimating the spatial distribution of bracken fern during the green up phenological cycle.

Table 4.2: Accuracies based on the four data sets for the OCSVM and BSVM algorithms

Variable combination	Performance metric	OCSVM (%)	BSVM (%)	OCSVM (%)	BSVM (%)
		2015		**2020**	
Spectral bands	Overall accuracy	87	88	85	86
	Recall	78	84	75	79
	Precision	79	81	80	82
	F-score	75	82	76	81
Spectral bands + Vegetation indices	Overall accuracy	90	90	88	89
	Recall	87	76	86	87
	Precision	86	78	84	88
	F-score	86	76	85	82
Spectral bands +Topographic variables	Overall accuracy	90	94	88	90
	Recall	88	93	87	86
	Precision	89	76	86	88
	F-score	85	83	84	85
Spectral bands + Vegetation indices + Topographic Variables	Overall accuracy	92	95	88	90
	Recall	81	94	89	90
	Precision	84	89	85	86
	F-score	83	91	82	89

4.3.2 Comparing the performance of different variable combinations in discriminating bracken fern

The model that was produced by using the combination of spectral bands, vegetation indices, and topographic variables was the most accurate for both OCSVM (95%) and BSVM (97%) algorithms. The models built using spectral bands only produced the lowest overall accuracy for OCSVM (87%) and BSVM (88%). The model with spectral bands only had the lowest recall (78%), precision (79%) and F-score (75%) based on the OCSVM algorithm. Using BSVM, the spectral bands only model performed much better as indicated by its accuracy which was above 80%. The BSVM model with spectral bands only performed poorly as it recorded the greatest bracken fern misclassification rate exhibited by its recall. Interestingly, the OCSVM outperformed BSVM in the spectral bands and vegetation indices data sets as shown by the high recall, precision and F-score model performance indicators recorded in Table 4.2. Generally, the accuracy trends show that as more variables were added to the classification models, the accuracies also significantly increased in both OCSVM and BSVM algorithms. These results show that the inclusion of topographic variables and vegetation indices in classification models can improve the accuracy when estimating the spatial distribution of bracken fern during the green phenological stage.

4.3.3 Variable importance

Figure 4.1 shows the ranking of variables that were most significant in mapping the spatial distribution of bracken fern in 2015 and 2020 based on the best performing models. The most significant variables had rankings higher than 0.7 while variables with less than 0.55 were less significant. The most significant variables in classifying bracken fern were NIR (Band 8), red edge (Band 7), elevation, TDVI and TWI. Bracken fern was highly reflected in Bands 7, 8 and 8A, demonstrating the red edge and Near Infrared (NIR) as the most optimum wavelengths for detecting bracken fern spatial distribution during green up phase.
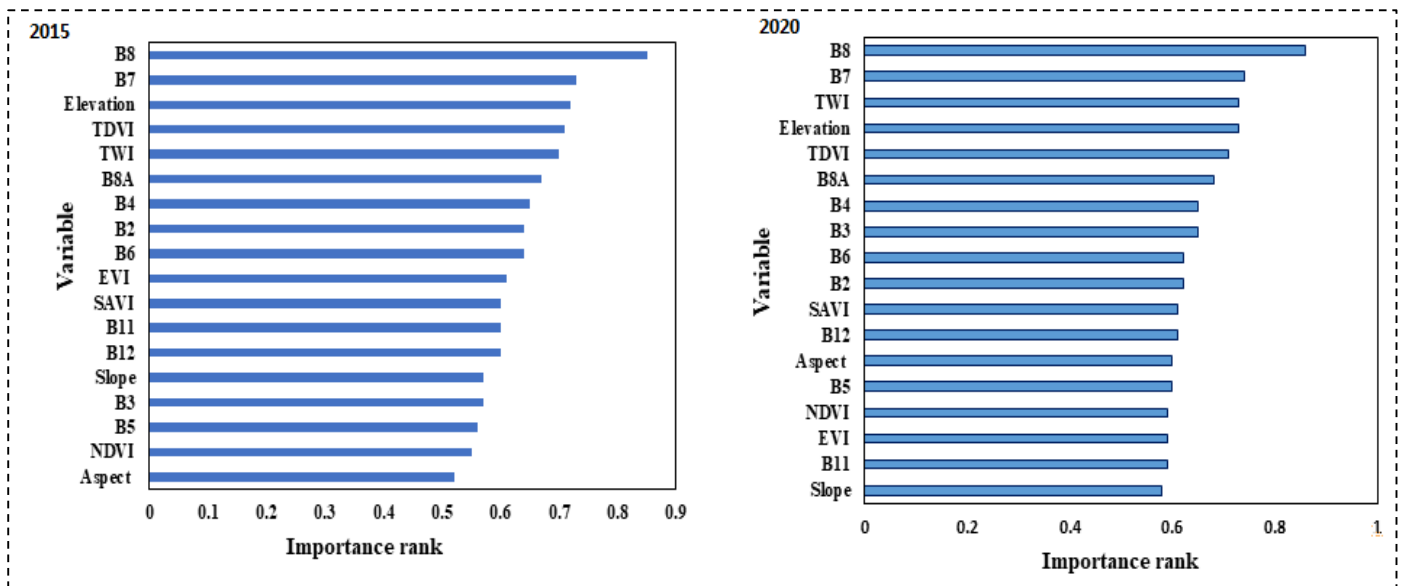
Figure 4.1: Important variables in estimating the spatial distribution of bracken fern

4.3.4 Changes in bracken fern distribution

Figure 4.2 shows the spatial distribution of bracken fern during the green up phase in 2015 and 2020. The spatial distribution maps show that in 2015, bracken fern was mostly concentrated in the western parts of the study site, while the southern areas had a low infestation. The eastern parts of the site had the lowest concentration of the fern. In 2020 there was a general increase in bracken fern infestation in the entire study area. More small patches started emerging in the eastern section, signalling potential heavy infestation in the future. In 2015 the total area covered by bracken fern was estimated to be approximately 6,4km^2 and this constituted 9% of the entire study area. In 2020, the total area covered by the invasive fern increased to 12,2km^2 and this constituted 17% of the entire study site. The total percentage cover increased by more than 90% in five years. Corresponding to the changes in percentage cover statistics, the spatial distribution maps also show a significant increase in bracken fern cover from 2015 to 2020. The distribution maps show that bracken fern cover almost doubled during the five-year period.
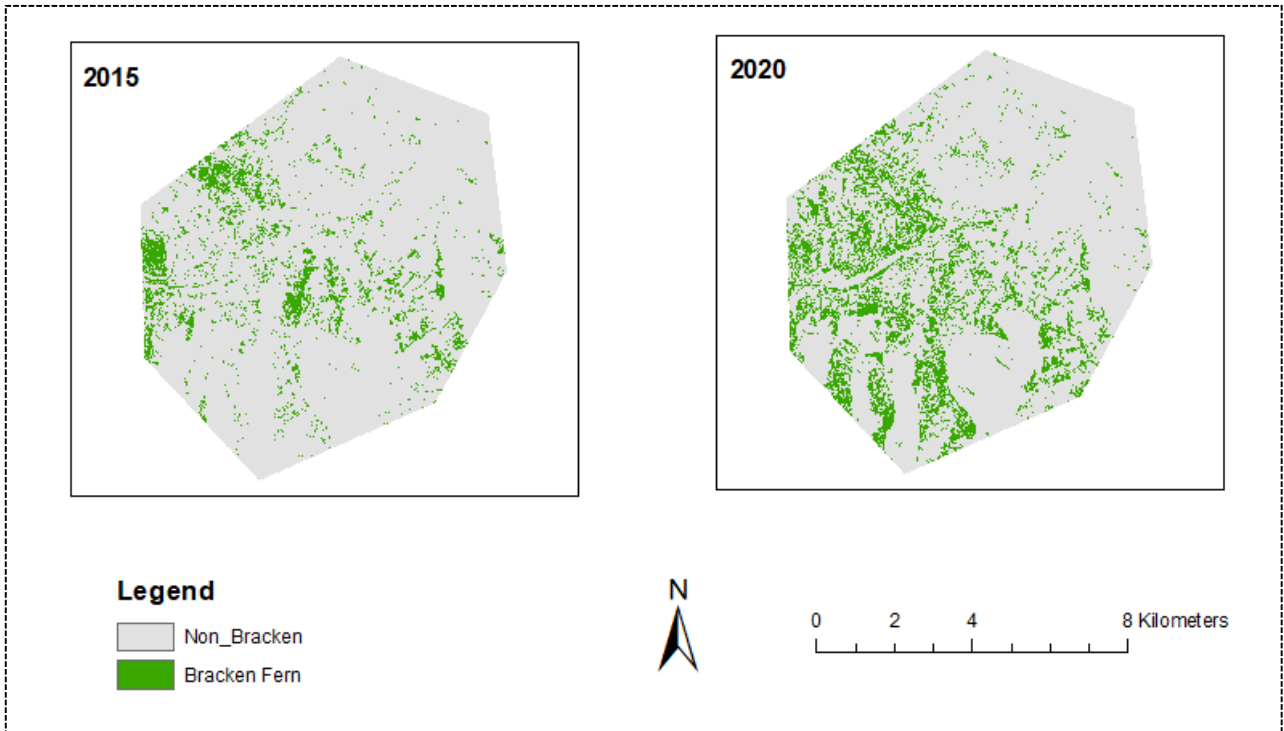
Figure 4.2: Spatial distribution of bracken fern in 2015 and 2020

4.4 Discussion

4.4.1 OCC algorithms and data set combinations performance

The current study applied BSVM and OCSVM algorithms to estimate the spatial distribution of bracken fern during the green up phase based on different variable combinations. The BSVM algorithm produced the best model for estimating the spatial extent of bracken fern during the green up phenological stage when compared to OCSVM. The combination of spectral bands, vegetation indices and topographic variables yielded high results compared to all other datasets. OCSVM had well defined negative samples that were used to train the model, whereas BSVM only relied on randomly generated unlabelled samples (Piiroinen et al., 2018). Eventually, this would have given OCSVM a predictive power advantage over BSVM. However, findings from the current study proved otherwise, as BSVM accuracies were higher than OCSVM. The better performance of BSVM over OCSVM has also been previously reported in the literature (Mũnoz-Marí et al., 2010, Li et al., 2010). The BSVM algorithm has the advantage of using unlabelled data to train the classifier and it only uses fewer positive data samples. One of the challenges of using OCSVM is its principle of including well defined negative samples in the OCC workflow. This will mean more cost and time for data collection, an obstacle that OCC methods initially target to minimize.

As indicated by the slightly lower recall but higher precision the OCSVM was good at predicting the positive class, but it only detected a small proportion of the total number of positive outcomes. In some cases, this could mean the model could be underpredicting. In models where OCSVM performed better than BSVM, there were no significant differences in the classification accuracies, hence the cost of including negative samples in the classification is not worthy. Another drawback of OCSVM is its high sensitivity in free parameter tuning (Manevitz and Yousef, 2001). To address this challenge, users may increase the number of iterations during model fitting in the process of trying to find the optimal model. However, in the process of training the model and continuously predicting over test data, OCSVM may result in overfitting. The Sentinel-2's ability to discriminate bracken fern from other land cover classes shows the optimal performance of the NIR and Red spectral bands. The relevance of NIR and Red edge portions of the electromagnetic spectrum as optimum variables in discriminating invasive species was also reported by previous studies in land cover classification (Dube et al., 2020).

Although there is no universal rule of thumb indicating that the accuracy of a machine learning algorithm is directly proportional to the number of features used to train it, findings from the current study shows that the addition of more variables improved classification accuracy. As more variables were included in the classification models, the accuracies also significantly increased by an average of 2.5% in both OCSVM and BSVM algorithms. Combining spectral bands with other variables such as vegetation indices and topographic variables improves the performance of classification algorithms as these additional variables (topographic and spectral indices) are reported to be sensitive to species occurrence (Makhaya et al., 2022, Kuebler et al., 2016, Morcillo-Pallarés et al., 2019), compared to spectral bands. The addition of variables provides the classification algorithm with more information about the physiological and chemical characteristics of the targeted land cover classes. The improved performance of classification algorithms that combine spectral bands and other variables such as topographic variables has also been previously reported in the literature (Matongera et al., 2017, Dube et al., 2020).

Consistent with findings reported by Odindi et al. (2014) our study established that the NIR and red edge portions of the electromagnetic spectrum were amongst the variables having the greatest influence on the estimation of bracken fern spatial distribution during the green up phase. NIR operates in the best spectral region to distinguish vegetation varieties and conditions (Hennessy et al., 2020). Amongst the topographic variables used in this study, elevation was the most significant variable which improved model performance. This result agrees with previous studies by Khare et al. (2019) who noted that elevation was the most important topographic variable in detecting the spatial distribution of invasive species. The occurrence of most of the invasive species is mainly influenced by elevation more than other topographic variables. Vegetation indices hold a particular promise in vegetation classification (Huete, 1988b). In this study, the use of vegetation indices developed from Sentinel-2 spectral bands improved bracken fern classification accuracy. Specifically, the TDVI was ranked as the best spectral index in mapping bracken fern. The performance of the TDVI could be attributed to its ability to reduce the effects of bare soil during land cover classification. Bannari et al. (2002) reported that the TDVI does not saturate like NDVI or SAVI and it revealed good linearity as a function of the rate of vegetation cover and shows the same sensitivity as the SAVI to the optical proprieties of bare soil.

4.4.2 Bracken fern spatial distribution

For the whole study area, there was a noticeable spatial consistency in the distribution of bracken fern from 2015 to 2020. Bracken fern is not distributed randomly across the Drakensberg landscape, rather it is distributed along different environmental gradients. The spatial distribution of bracken fern was closely related to edaphic and topographic factors such as elevation. Most of the large bracken fern patches were found in the higher altitude areas, which could be explained by its high invasiveness which enables the fern to quickly establish in high altitude areas where the management influence is low. Previous findings by (Marrs et al., 2000b) also reported that bracken fern in high altitude areas. In general, bracken fern abundance increased with elevation. Higher infestations of Bracken fern were mostly detected in western and northern sections of the study side while the southern and eastern parts had low levels of infestation especially in 2015. The western side is considered favorable for bracken fern invasion compared to the other parts. However, the temporal pattern of the fern shows that in 2020, the infestation had significantly increased in the southern and eastern parts as well.

4.4.3 Implications of findings in bracken fern management

The effective management of rangelands requires continuous data sources that track the changes in various vegetation species that are within a landscape (Al-Bukhari et al., 2018). The free availability of high spatial and temporal resolution data sets such as Sentinel-2 enables rangeland managers to continuously monitor the changes that occur within areas of their jurisdiction. Being a biodiversity hot spot (Matongera et al., 2017), Drakensberg needs to be protected from further encroachment of bracken fern. The current study provides crucial information about the locations of bracken fern in the Drakensberg. The current study sought to find a model that minimizes false negatives (pixels that are bracken fern but are classified as non-bracken) in the classification process. The bracken fern distribution maps help rangeland managers to visualize the overall spread of the invasive fern in a broader context. The occurrence patterns of bracken fern show the area that is mostly invaded by bracken fern; hence they are most severe to environmental threat.

4.5 Conclusions

Accurate and repeatable mapping of bracken fern invasion is essential to develop cost-effective management strategies for conserving and management of rangelands. The utility of two OCC algorithms in estimating the spatial distribution of bracken fern has been presented and evaluated in this study.

- The BSVM algorithm combined with spectral vegetation indices proved to be a reliable method for the estimation of bracken fern spatial distribution during green up phenological phase.
- The BSVM algorithm proved to be efficient in minimizing false negatives in the classification process. This would ensure that most bracken fern species are detected and potential countermeasures against further spreading can be efficiently implemented. The advantages of BSVM algorithm are that it enables the detection of target bracken fern in a heterogonous landscape, and it requires only a small set of positive data, thus saving time and resources.
- In 2020, the total area covered by the invasive fern increased to 12,2km^2 and this constituted 17% of the entire study site. The total percentage cover increased by more than 90% in five years.

The spatial distribution maps produced in this study are critical for improving the precision in the controlling of the spread of bracken fern as well as in implementing active protection strategies against the invasion of highly susceptible rangelands. However, the vegetation indices used in this study were not ranked as the most important variables in mapping bracken fern during green up phenological stage. Thus, in the following Chapter Five, an existing spectral vegetation index is optimized to improve the mapping and monitoring bracken fern phenology.

Chapter Five

Optimizing the Transformed Difference Vegetation Index to map and monitor bracken fern phenology

This chapter is based on a paper:

Abstract

Bracken fern is one of the well-known invasive alien plants threatening the existence of indigenous species as it causes genetic alteration, change in population density and disturbances of community structures in ecosystems. Mapping and monitoring the spatial and temporal distribution of the fern is an important aspect of the management of rangelands. The Transformed Difference Vegetation Index (TDVI) was developed for minimizing soil background effects during vegetation mapping. However, the TDVI is computed using the Near Infrared (NIR) and the red band which is not effective when distinguishing different land cover types especially during the peak of the vegetation seasons. Consequently, five Optimized Transformed Difference Vegetation Index (OTDVI) variants were developed based on the spectral bands ratios that showed maximum discrimination between bracken fern and other land cover classes. The $OTDVI_3$ which was developed using red edge (Band 7) and Near Infrared (NIR) was the most influential index in mapping bracken fern during green up and green peak stages. The $OTDVI_4$ developed using SWIR (Band 11) and NIR was ranked as the best feature for mapping bracken fern during dormancy phenological stage. Generally, the bracken fern classification results were good across all phenological stages with an average overall accuracy of 90%. The optimization and development of new spectral vegetation indices improve the understanding of the underlying processes and factors that influence the growth patterns of invasive alien plants such as bracken fern at both local and global scales.

Keywords: Spectral index, Bracken fern, Separability, Spectral confusion, Phenology, Sentinel-2

5.1 Introduction

The introduction of invasive alien plants has increased globally over the past decade due to the increased movement of people and goods (Vaz et al., 2017). The encroachment of invasive alien plants such as bracken fern (*Pteridium Aquilinum*) these invasive species causes ecosystem changes that have detrimental effects on rangelands productivity and health, raising many challenges for management authorities (Mouta et al., 2021, Royimani et al., 2019, Ndlovu et al., 2018). Many attempts to control the encroachment of the fern over large areas have not permanently solved the invasion problem (Levy-Tacher et al., 2015b, Schneider, 2006, Marrs et al., 2000b). In some cases, there has been re-emergence of the fern within of 3-5 years after the control approaches have been implemented, leading to huge economic losses (Levy-Tacher et al., 2015b). The accurate mapping of bracken fern at various phenological stages has the potential to improve the management of the infested landscapes. The ecology, biology and encroachment mechanisms of bracken fern have been widely studied in many regions around the world (Schneider and Fernando, 2010, Dolling, 1999, Pakeman and Marrs, 1992). However, the phenological developments of the fern from a remote sensing perspective have not been fully explored. The inclusion of phenological information has the potential to improve precision in the management of rangelands.

Remote sensing has been recognized as a valuable tool for mapping and monitoring the spatial and temporal distribution of vegetation at various phenological stages at local and global scales (Berra and Gaulton, 2021, Shuchman et al., 2013, Jenkins and Frazier, 2010, Treitz and Rogan, 2004). Through satellite images, remote sensing provides global data sets that are used to constantly monitor changes on the earth's terrestrial surface (Fu et al., 2020). The majority of the polar-orbiting multi-spectral satellite sensors collect information from the earth's surface in the visible, near-infrared (NIR) and short-wave infrared (SWIR) sections of the electromagnetic spectrum (Phiri et al., 2020, Avdan and Jovanovska, 2016, Jombo et al., 2020). However, spectral confusion between land cover classes is a very common problem in remote sensing studies. For instance, Lasaponara (2006) reported that there was high spectral confusion between burned and unburned pixels especially in the spectral bands that are within the visible section of the electromagnetic spectrum. Zhao et al. (2016) highlighted that it was challenging to obtain good classification maps based on Landsat Thematic Mapper (TM) data due to high spectral similarity between the vegetation types and the effects of topographic and atmospheric factors. Bracken fern is also confused with other land cover types because of its

spectral similarity with other co-existing land cover classes such as grassland and shrubs (Ngubane et al., 2014). Specifically, the spectral reflectance of bracken fern has been reported to be similar to C3 and C4 grasses such *Festuca costata* and *Themeda triandra* (Matongera et al., 2017). The separability crisis makes it challenging to accurately understand the spatial distribution and encroachment patterns of the bracken fern at different phenological stages. The sensor related errors such as sun view angle and atmospheric influences also play a significant role in distorting the spectral reflectance of objects on the earth's surface as well as the ability of users to accurately interpret data from satellite images (Xue and Su, 2017).

Spectral vegetation indices have been developed and widely used to resolve spectral confusion amongst land cover classes by minimizing the variability caused by soil background, atmospheric interferences, sensor related errors and topographic effects (Jiang et al., 2019, Prananda et al., 2020, Seong et al., 2020, Zhu et al., 2014). The first generation of spectral vegetation indices were simple ratios such as the Normalized Difference Vegetation Index (NDVI) (Rouse Jr, 1972), which were primarily developed to characterize the spectral properties of vegetation at various stages of growth. The NDVI is a well-known spectral index that is sensitive to changes in chlorophyll content and vigor of green vegetation and is often used in local, regional and global vegetation assessments (Xue and Su, 2017). Nevertheless, the NDVI is limited by its sensitivity to the effects of soil brightness, cloud shadow and atmospheric impurities. The second generation of indices such as the Transformed Difference Vegetation Index (TDVI) was designed to reduce soil background effects and atmospheric distortions when working with remotely sensed data (Bannari et al., 2002).

The TDVI was successfully used in various applications such as crop identification in agriculture (Mróz and Sobieraj, 2004), vegetation cover mapping (Bannari et al., 2002) and urban land use classification (Ozbakir and Bannari, 2008). Generally, the findings from the aforementioned studies show that the TDVI performs better than NDVI and the Soil-Adjusted Vegetation Index (SAVI), as it did not saturate in most cases. Additionally, vegetation mapping crop detection studies the TDVI demonstrate excellent linearity as a function of the rate of chlorophyll content and vegetation cover (Bannari et al., 2002). However, the TDVI is mathematically constructed using the spectral reflectance from the visible (Red band) and NIR portions of the electromagnetic spectrum, which may not yield the best results in all remote sensing applications. For instance, (Xue and Su, 2017) highlighted that using the vegetation indices computed from the spectral bands in the visible that are mostly affected by atmospheric

77

influences to extract phenological metrics may affect the accuracy of the phenological estimates. Furthermore, literature also show that the visible spectral bands have weak vegetation discriminatory ability especially during the peak for the vegetation season, when canopy cover is large (Fernandes et al., 2013, Xue and Su, 2017, Svinurai et al., 2018). Therefore, the optimization of the TDVI through computation using the spectral bands where targeted vegetation species show maximum separability with co-existing land cover classes has the potential to improve accuracy in mapping the spatial and temporal distribution of vegetation at various phenological stages.

The launching of new generation satellite sensors such as Sentinel-2 Multispectral Instrument (MSI) with improved spectral and spatial resolution provides a potential to develop new indices as well as optimize the existing indices for them to suit the various application (Matongera et al., 2021b). Sentinel-2 acquires data in 13 spectral settings, with three of them in the red-edge section while two of them cover the SWIR spectrum at 20m spatial resolution (Sibanda et al., 2019). A plethora of studies reported on the supremacy of red-edge and SWIR in detecting, mapping, and monitoring the encroachment of invasive alien plants (Sibanda et al., 2019, Malahlela et al., 2014, Masemola et al., 2020). The availability of the Sentinel-2's additional red-edge and SWIR bands with improved vegetation species detection capabilities provides the potential to develop new spectral indices that can improve accuracy in mapping the phenology of bracken fern (Matongera et al., 2021b). When new vegetation indices are developed or new optimized variants are proposed, there is a need to validate them using measurable vegetation biophysical variables related to plant canopy growth before claiming their superiority from the existing indices (Xue and Su, 2017). Leaf Area Index (LAI) is one of the most widely used biophysical variable that is used to validate spectral vegetation indices (Wang et al., 2007). Therefore, the objectives of this study were to i) determine the phenological stage at which bracken fern could be optimally discriminated from other existing species, ii) identify the spectral regions of the electromagnetic spectrum that result in maximum separability of bracken fern and other species. The study then sought to develop a bracken fern index for mapping bracken fern using the most separable spectral bands.

5.2 Materials and Methods

5.2.1 Field data collection

The ground-based location points for bracken fern, shrubs, bare soil and grassland classes were collected using the Trimble CB 460 Global Positioning System (GPS) during the summer period of October 2021. The grassland class was comprised of C_3 (*Festuca costata*) and C_4 (*Themeda triandra*) grasses that are abundant in the Cathedral Peak. A total of 85 GPS points were collected for each class, resulting in a total of 340 points. The differential correction was performed for the sampled points using the Hartebeesthoek trigonometrical beacon. The corrected points were exported in a table format into ArcGIS for extraction of spectral data from Sentinel-2 image for further analysis. The Bracken fern Leaf Area Index (LAI) was measured using a handheld Licor 2200 meter during clear-sky conditions. The Licor 2200-meter estimates LAI using the amount of light energy transmitted by a plant canopy. To facilitate comparison with optimized spectral vegetation indices, the LAI measurements were collected on bracken fern canopy portions that were previously sampled. Three LAI measurements were measured and averaged within the 100m^2 plot. The mean values were used for the correlation analysis with the optimized spectral indices. A total of 85 bracken fern LAI measurements were collected. The bracken fern location points and LAI measurements were randomly split into 70% training and 30% testing.

5.2.2 Satellite data acquisition and pre-processing

The Sentinel-2 Multi Spectral Instrument (MSI) data was obtained from the European Space Agency (ESA) online platform at processing level 2A. A total of four Sentinel-2 orthorectified, atmospherically and topographic corrected images representing the green up (October 2020), green peak (February 2021), senescence (April 2021) and dormancy (July 2021) phenological stages of bracken fern were acquired. The Sentinel-2 sensor collects data using 13 spectral channels at 10, 20 and 60m spatial resolutions (Matongera et al., 2021a). Only spectral bands at 10m and 20m spatial resolution were used, while band 1, 9 and 10 which collects spectral data at 60m spatial resolution were excluded since they were not relevant in this study. The sensor has a temporal resolution of 3-5 days at an orbital angular distance of 180km with a 290km swath width (Transon et al., 2018).

5.2.3 Separability analysis

The evaluation and quantification of the spectral separability of bracken fern and other land cover classes at four phenological stages were performed using the Transformed Divergence Spectral Index (TDSI) statistical test. The TDSI separability test determines how similar or different the distributions of two groups of pixels are using the class means and the distribution of the values. The TDSI statistical measure has values that range between 0 –2, with values close to 0 indicating non-separability and values close to 2 indicating high separability (Chemura and Mutanga, 2017). The TDSI was formulated as:

$$TDSI = \left[1 - \exp\left(-\frac{D}{8}\right)\right]$$

$$D = \frac{1}{2} tr\left[(C_1 - C_2)(C_2^{-1} - C_2^{-1})\right] + \frac{1}{2} tr\left[(C_1^{-1} - C_2^{-1})(\mu_1 - \mu_2)\,T\right]$$

Equation 5.1

Where C1 represents the covariance matrix of class1, μ_1 is regarded as the mean vector of class 1, tr is the matrix trace function and T is the matrix transposition function.

5.2.4 Optimized spectral vegetation indices

Spectral vegetation indices were chosen based on their utility in vegetation mapping and their ability to increase the dimensionality of remotely sensed data (Kiala et al., 2020). The original TDVI was developed by Bannari et al. (2002) for vegetation cover mapping. The TDVI was designed to reduce the effects of bare soil during land cover classification. Bannari et al. (2002) reported that the TDVI does not saturate like NDVI or SAVI and it revealed good linearity as a function of the rate of vegetation cover and shows the same sensitivity as the SAVI to the optical proprieties of bare soil. However, the TDVI remains limited in terms of differentiating vegetation covers that have similar spectral reflectance. To remedy this, the current study proposes the optimization of the TDVI based on the spectral separability tests for the land cover classes under investigation. In the process of optimizing the TDVI, the mathematical formulation of the TDVI was maintained (Equation 5.1), only spectral bands were changed based on their capability to separate bracken fern from other land cover classes at various phenological stages. The NDVI was chosen as a reference index to compare the accuracy and sensitivity of the optimized indices to the ground measured LAI. The computation of TDVI was performed as follows;

$$TDVI = 1.5 * \left[(NIR - Red)/\sqrt{NIR^2 + R + 0.5} \right]$$ Equation 5.2

5.2.5 Validation of the optimized indices

The validation of newly developed or optimized spectral vegetation indices includes the computation of statistical tests of correlations between the vegetation indices and in situ measurements of vegetation characteristics such as vegetation cover, biomass and LAI. A direct application of NDVI is to characterize canopy growth; therefore, many scientists have compared it with the LAI (Fan et al., 2009, Kang et al., 2016, Towers et al., 2019). Similarly, the TDVI also characterizes canopy growth while it minimizes the effects of soil background effects, hence this study adopted the use of LAI to validate OTDVI for bracken fern phenology mapping. The bracken fern sampled locations were used to extract values from the optimized vegetation indices maps for correlation analysis with bracken LAI. To quantify the statistical relationships between optimized vegetation indices and ground measured bracken fern LAI, the coefficient of determination was computed. The optimized indices were used as a dependent variable while LAI measurements were used as the independent variable.

5.2.6 Bracken fern phenology mapping

5.2.6.1 Random Forest

Random forest, an ensemble decision-based classification algorithm (Chan and Paelinckx, 2008) was used to test the effectiveness of the optimized spectral vegetation indices in mapping bracken fern at its four phenological stages. Random forest is designed as a machine learning algorithm governed by decision trees, where each learning contributes one vote for the most frequent class to classify an input vector (Kiala et al., 2020). However, RF heavily relies on the fine tuning of the input hyper-parameters, and if not adjusted sufficiently could negatively influence the classification accuracy. Consequently, the current study adopts the Improved Grid Search Optimization Random Forest (IGSO-RF) for mapping bracken fern at its four phenological stages. The detailed technical workflow process of the IGSO-RF algorithm can be found in (Xu et al., 2021). To test the performance of the optimized indices in mapping bracken fern phenology, three data sets were used in the first part of the analysis as detailed in Table 5.1. The first stage of the classification process was performed using the default IGSO-RF parameters. The data set which yielded the highest overall accuracy was used to select the best features for mapping bracken fern based on the sequential forward selection (SFS) method.

Table 5.1: Combination of variables tested in mapping bracken fern

Data set	Variable combinations	Total number of variables
i)	B2, B3, B4, B5, B6, B7, B8, B8A, B11, B12 + NDVI + TDVI	12
ii)	B2, B3, B4, B5, B6, B7, B8, B8A, B11, B12 + OTDVI$_{1-5}$	16
iii)	B2, B3, B4, B5, B6, B7, B8, B8A, B11, B12 + OTDVI$_{1-5}$ + NDVI + TDVI	18

5.2.6.2 Feature selection

Feature selection is a preprocessing method that is used for improving model performance and predictive accuracy (Li et al., 2017). The feature selection process reduces the effect of dimensionality which has a negative impact on the classification accuracy (Kiala et al., 2019). Furthermore, feature selection eliminates redundant or noisy variables by choosing one feature amongst the highly correlated features (Chandrashekar and Sahin, 2014). The sequential forward selection (SFS) was used to select the best features for mapping bracken fern. To assemble the best set of features, the SFS search begins on an empty set and features are added one by one until the required subset is reached (Pudil et al., 1994).

5.2.6.3 Accuracy assessment

To evaluate the mapping capability of the proposed optimized spectral indices in mapping bracken fern at four phenological stages, the overall, producer and user accuracy metrics were computed. The estimated land cover classes were cross-tabulated against the ground-sampled land cover classes for the corresponding pixels in a confusion matrix. Ten-fold cross validation model selection criterion was used to validate the IGSO-RF model at each phenological stage.

5.3 Results

5.3.1 Spectral separability of bracken fern and other classes

Figure 5.1 shows the Sentinel-2 spectral reflectance curves for bracken fern and other land cover classes during the four phenological stages of bracken fern. The spectral curves show that bracken fern was highly separable from other land cover types in the red edge bands (Band 7 and 8A) and the near infrared (Band 8) during green up (Figure 5.1 a) and green peak (Figure 5.1 b) phenological stages. There was less separability between bracken fern and other classes in the visible part of the electromagnetic spectrum during the green peak and senescence phenological stages.
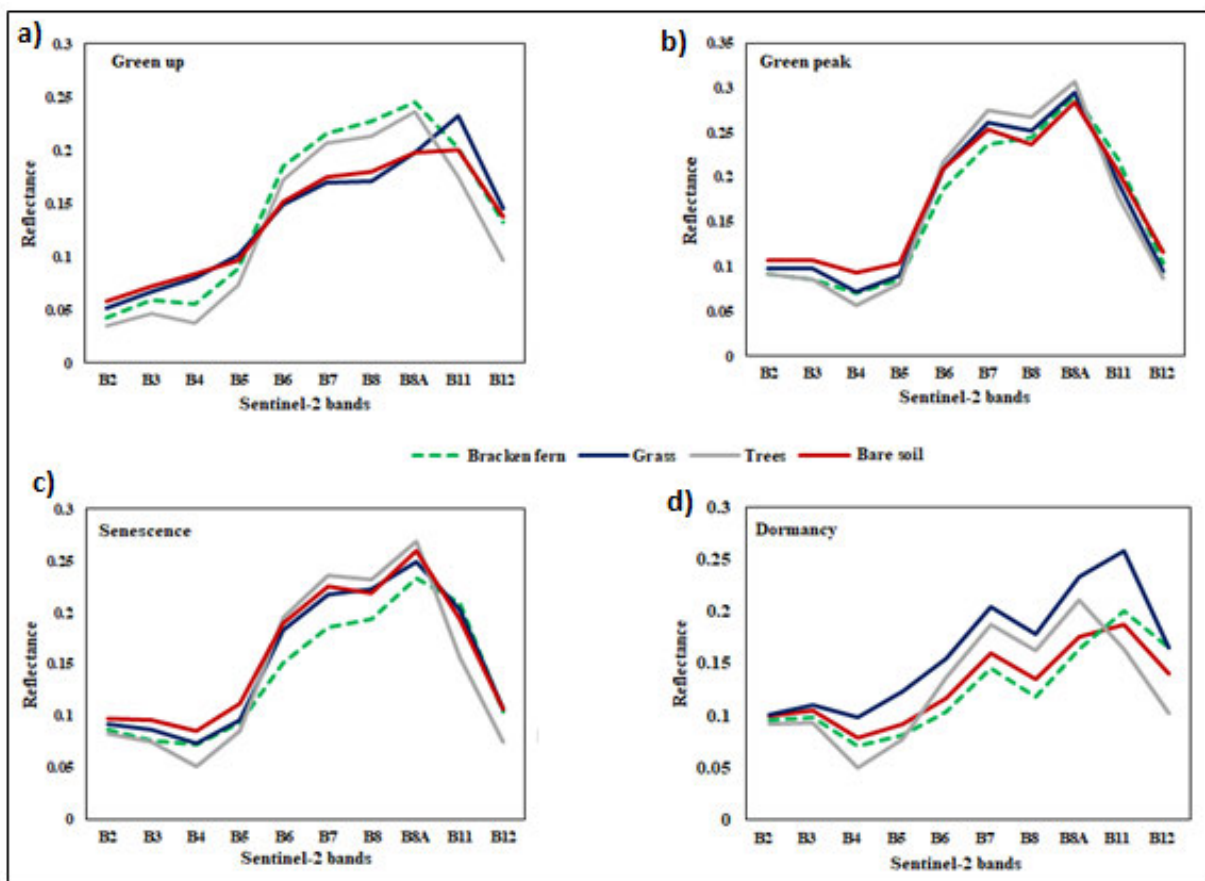
Figure 5.1: Spectral profile of bracken fern and other land cover classes during bracken fern growth cycle

Specifically, bracken fern showed the least separability with bare soil and grassland at all phenological stages in the blue and green bands while the red showed better separability. Spectral separability of bracken fern and other classes was also very low in the shortwave

region (Band 11 and 12) especially during the green peak and senescence (Figure 5.1 c) phenological stages while it was very high in the dormancy stage. A visual analysis of the spectral profiles shows that there was less overlap between bracken fern and other classes in the red edge and NIR region of the electromagnetic spectrum. Table 5.2 shows the TDSI statistical scores of bracken fern and other land cover classes during the four phenological stages of the fern. The spectral separability scores between other land cover classes were not included in this study because bracken fern was the class of interest. Overall, the TDSI statistical scores revealed that bracken fern was spectrally distinct (TDSI < 1.4) from other co-existing land cover classes at all phenological stages.

Table 5.2: Spectral separability of bracken fern and other classes based on the TDSI statistical test

Phenological Stages		Land cover classes			
		Bracken fern	Grassland	Shrubs	Bare soil
Green up	Bracken fern	-----	1.78	1.86	1.96
Green peak	Bracken fern	----	1.46	1.64	1.75
Senescence	Bracken fern	----	1.69	1.98	1.76
Dormancy	Bracken fern	----	1.88	1.98	1.97

Bracken fern was highly separable from other classes during the dormancy phenological stage as revealed by the pairwise TDSI statistical scores which were above 1.8. There was high spectral confusion between bracken fern and grassland during the green peak stage. Bracken fern and grass recorded the lowest TDSI score of 1.4 during the green peak phenological stage. However, despite high spectral confusion during this stage, it was still possible to separate bracken fern from other land cover classes such as shrubs (TDSI = 1.64) and bare soil (TDSI = 1.75). Based on these observations and statistical analysis, the study proposed a new spectral vegetation index for mapping bracken fern. Based on the spectral separability tests, current study proposed the optimized transformed vegetation index (OTDVI) to improve bracken fern mapping at different phenological stages. The NIR band was not replaced, since it showed good

separability between bracken fern and other land cover classes at all phenological stages. The near infrared was used to compute all the proposed indices, hence the NIR became the constant in the optimization process. The red band showed low separability between bracken fern and other land cover classes, hence it was replaced by three red edge and two SWIR bands when computing the optimized indices. Consequently, five OTDVI variants were developed based on these separability findings. The formulations of the optimized indices are detailed in Table 5.3.

Table 5.3: Formulation of the optimized spectral vegetation indices proposed

Spectral index	Expression	Reference
OTDVI$_1$	$1.5 * \left[(NIR - RE_1)/\sqrt{NIR^2 + RE_1 + 0.5} \right]$	Equation 5.5
OTDVI$_2$	$1.5 * \left[(NIR - RE_2)/\sqrt{NIR^2 + RE_2 + 0.5} \right]$	Equation 5.6
OTDVI$_3$	$1.5 * \left[(NIR - RE_3)/\sqrt{NIR^2 + RE_3 + 0.5} \right]$	Equation 5.7
OTDVI$_4$	$1.5 * \left[(NIR - SWIR_1)/\sqrt{NIR^2 + SWIR_1 + 0.5} \right]$	Equation 5.8
OTDVI$_5$	$1.5 * \left[(NIR - SWIR_2)/\sqrt{NIR^2 + SWIR_2 + 0.5} \right]$	Equation 5.9

Where: RE$_{1,2,3}$ represents spectral bands 5, 6 and 7 respectively SWIR$_{1,2}$ represents spectral bands 11 and 12 respectively

5.3.2 Correlation between LAI and optimized indices

The test data set was used to assess the correlation between LAI and optimized spectral indices. There was a positive correlation between all the tested spectral vegetation indices and ground measured LAI ($r < 0.51$; $p < 0.01$) at all four-bracken fern phenological stages. Table 5.4 shows the Pearson correlation between vegetation indices and LAI at four bracken fern phenological stages. The OTDVI$_3$, computed using the NIR and red edge (Band 7) produced the highest correlation score ($r = 0.86$) during the green peak stage. The NDVI showed the lowest sensitivity to the changes in bracken fern LAI, with the dormancy phenological stage recording the lowest correlation coefficient ($r = 0.51$).

Table 5.4: Pearson correlation (r values) matrix comparing vegetation indices and bracken fern LAI

Spectral vegetation index	Green up	Green peak	Senescence	Dormancy
NDVI	0.56	0.57	0.68	0.51
TDVI	0.72	0.76	0.74	0.63
$OTDVI_1$	0.75	0.80	0.76	0.76
$OTDVI_2$	0.76	0.82	0.75	0.77
$OTDVI_3$	0.85	0.86	0.85	0.79
$OTDVI_4$	0.78	0.72	0.73	0.75
$OTDVI_5$	0.75	0.74	0.70	0.68

The optimized indices computed using the red-edge spectral bands were more sensitive to LAI changes when compared to those computed using SWIR. The magnitude of difference between the red edge and SWIR optimized indices was approximately 8%. On average, the green peak stage recorded the highest correlations (r = 0.76) between spectral indices and LAI, while the dormancy stage scored the lowest correlations (r = 0.71) (Table 5.4). Figure 5.2 shows the temporal curve of the original and optimized spectral vegetation indices in relation to LAI from the green up to the dormancy phenological stage. Two optimized spectral indices were included in the visualization of the bracken fern temporal curve, one from the red edge and the other one from the SWIR group of indices. Therefore, the $OTDV1_3$ and $OTDVI_5$ were used as they had recorded the highest correlation with LAI in their respective groups. The original NDVI and TDVI were also included for reference.
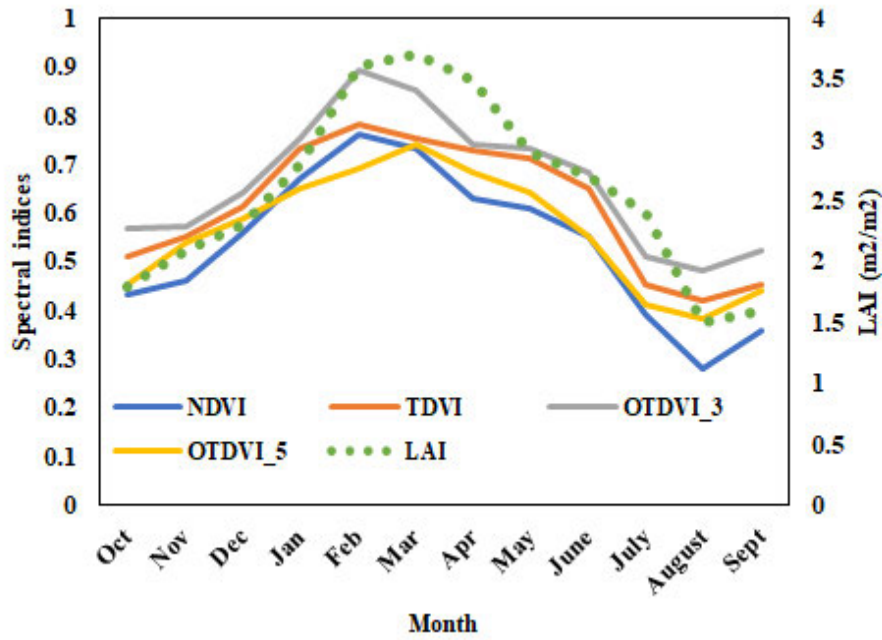
Figure 5.2: Temporal profile of the spectral vegetation indices and LAI during the bracken fern growth cycle

Generally, the variability of OTDVI indices and LAI were highly correlated as visually shown in Figure 5.2. At the beginning of the season, OTDVI indices trends show lower values around 0.45 while LAI values fluctuated around $1.6m^2/m^2$. The $OTDVI_3$ recorded a sharp spike towards the peak of the season in February while the $OTDVI_5$ experienced a steady increase, reaching its peak around March. The bracken fern LAI had a continuous steady increase towards its peak which was around March, with an all-time high record of $3.7m^2/m^2$. As depicted by the LAI curve, bracken fern had an elongated peak of the season from February to April, producing a bell-shaped curve. Both NDVI and TDVI reached the peak of the season towards the end of February which coincided with the bracken fern green peak phenological stage.

In April, most of the spectral indices started dropping significantly, signaling the beginning of the bracken fern senescence phenological stage. On the other hand, LAI started showing signs of dropping in May. There was a sharp decline in all spectral indices and LAI in July and August, a period which coincided with the bracken fern end of the growing season. Amongst all the vegetation indices, the $OTDVI_3$ recorded the highest values throughout the bracken fern growing season while NDVI had the lowest values during the green peak, senescence, and dormancy phenological stages.

5.3.3 Mapping bracken fern phenology

5.3.3.1 Comparison of data set accuracies

Figure 5.3 shows the overall classification accuracies of the three data set combinations tested at each bracken fern phenological stage. The overall accuracy results were based on the default IGSO-RF parameters. The full list of variables contained in the three data set combinations is described in detail in Table 5.1. Data set (iii) which had spectral bands, optimized indices and the original indices was the best performing combination with an average overall accuracy of 87% across bracken's four phenological stages. The data set with optimized indices outperformed the original indices in all phenological stages by an average of 11 % across all phenological stages. Data set (i) yielded the lowest overall accuracy results in all phenological stages when compared to the other two data sets. The best classification accuracies were obtained in the dormancy phenological stage for data set (i) and (ii) while data set (iii) recorded its highest accuracy during the green up phase. Based on its superior performance, data set (iii) was selected for feature selection analysis.
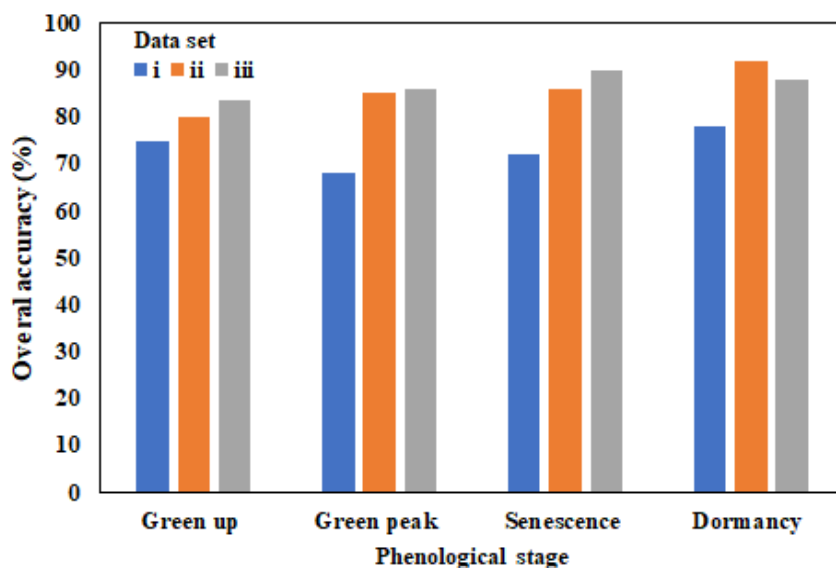
Figure 5.3: Overall accuracy for compared data set combinations

5.3.3.2 Feature importance

Based on the SFS analysis, the optimal variables used for model development in mapping bracken fern at its four phenological stages have been presented in Figure 5.4. Overall, the $OTDVI_3$ was the most significant spectral vegetation index in building models that accurately mapped bracken fern throughout its growth cycle. The $OTDVI_3$ was ranked as the most influential variable for the green peak and senescence phenological stages, while it was ranked second in the green up stage. The $OTDVI_3$ recorded feature importance scores above 0.17 at all phenological stages. The $OTDVI_4$ and $OTDV_5$ performed better during the senescence and dormancy phenological stages as they appeared in the top six influential variables in the two stages. The majority of the OTDVI variances outperformed the original TDVI and NDVI across the bracken fern growing season.

Using spectral bands, the SFS analysis revealed that the red edge and SWIR sections of the electromagnetic spectrum are the most important features in mapping bracken fern throughout its phenological cycle. The red edge spectral bands were most influential during the beginning and peak of the bracken fern season while SWIR spectral bands demonstrated their importance during the senescence and dormancy phenological stages. The visible (red, green and blue) wavebands were the least important features during the green peak stage while they showed improved performance in the dormancy stage. The NIR was also a very important feature in mapping bracken fern especially during the beginning and peak of the bracken fern season, as shown by its feature importance which was above 0.18.
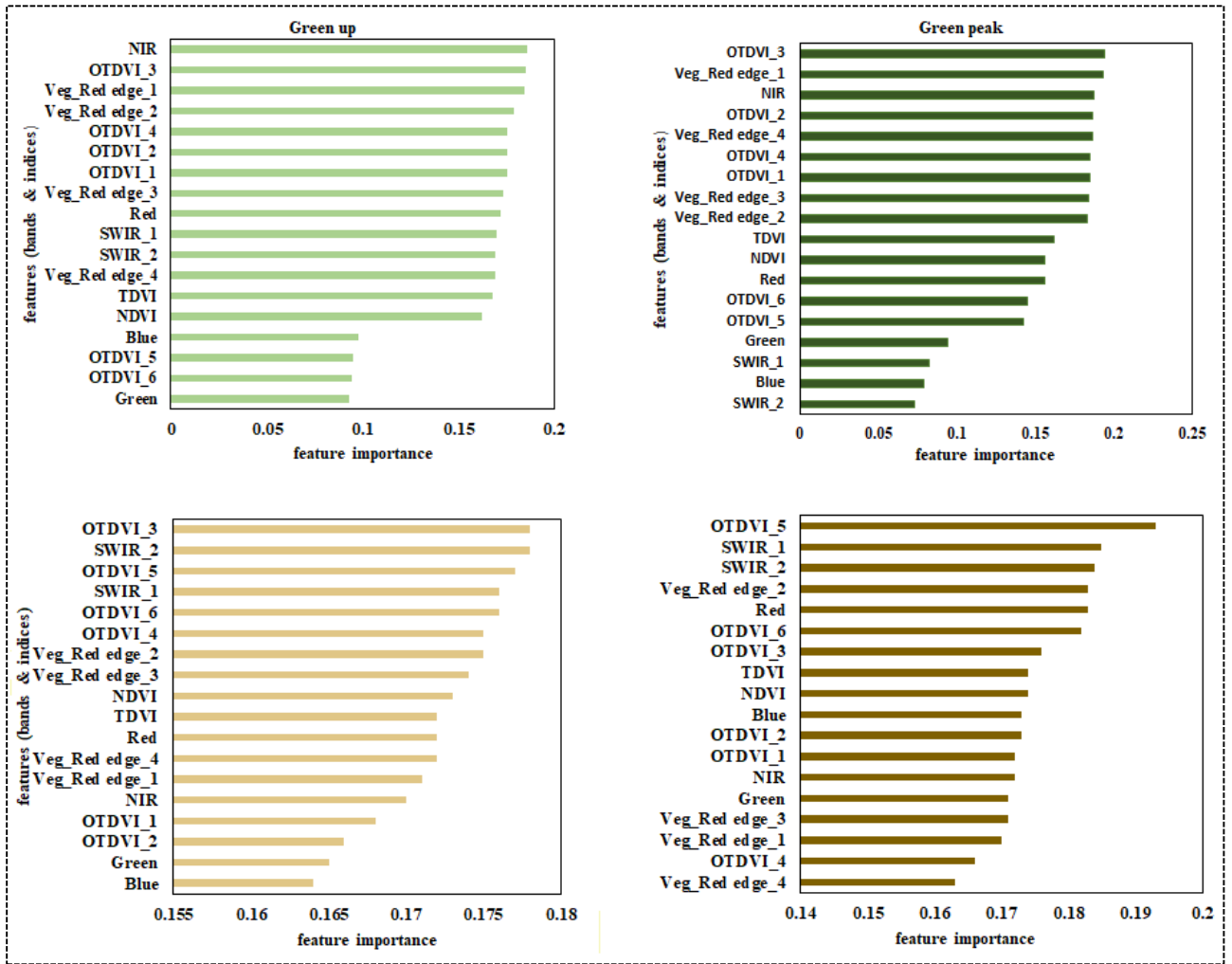
Figure 5.4: Importance of features in mapping bracken fern during its growth cycle

5.3.3.3 Accuracies based on the SFS best features

Table 5.5 shows the summary of classification accuracies based on the best SFS features that were selected at each phenological stage. Generally, there was an increase in the overall classification accuracy when the best features were used to map bracken fern at each stage. The classification accuracies improved by an average of 3.5% across all phenological stages. Of all the phenological stages, the dormancy produced the highest increase (6%) in overall accuracy, while green peak stage recorded the lowest change (1%).

Table 5.5: Error matrix of the classified maps at bracken fern's four phenological cycles

	Green up		Green peak		Senescence		Dormancy	
	PA	UA	PA	UA	PA	UA	PA	UA
Bracken fern	85	88	84	86	90	92	95	96
Grassland	78	77	85	87	93	93	94	95
Bare	90	94	89	85	92	90	92	90
Shrubs	96	97	92	80	98	96	96	97
Overall accuracy	**88**		**87**		**93**		**94**	

The shrubs were the most accurately modelled land cover class with producer and user accuracies above 90% across the four phenological stages. Bracken fern was more accurately classified in the dormancy phenological stage as shown by its user and producer accuracies (97% and 96% respectively) while the green peak recorded the lowest use and producer accuracies (84% and 86% respectively). The best feature subset with the most stable performance for the variables was used to produce the spatial distribution maps for bracken fern at each phenological stage. Since the focus of the study is bracken, only the bracken fern class was shown in Figure 5.5.
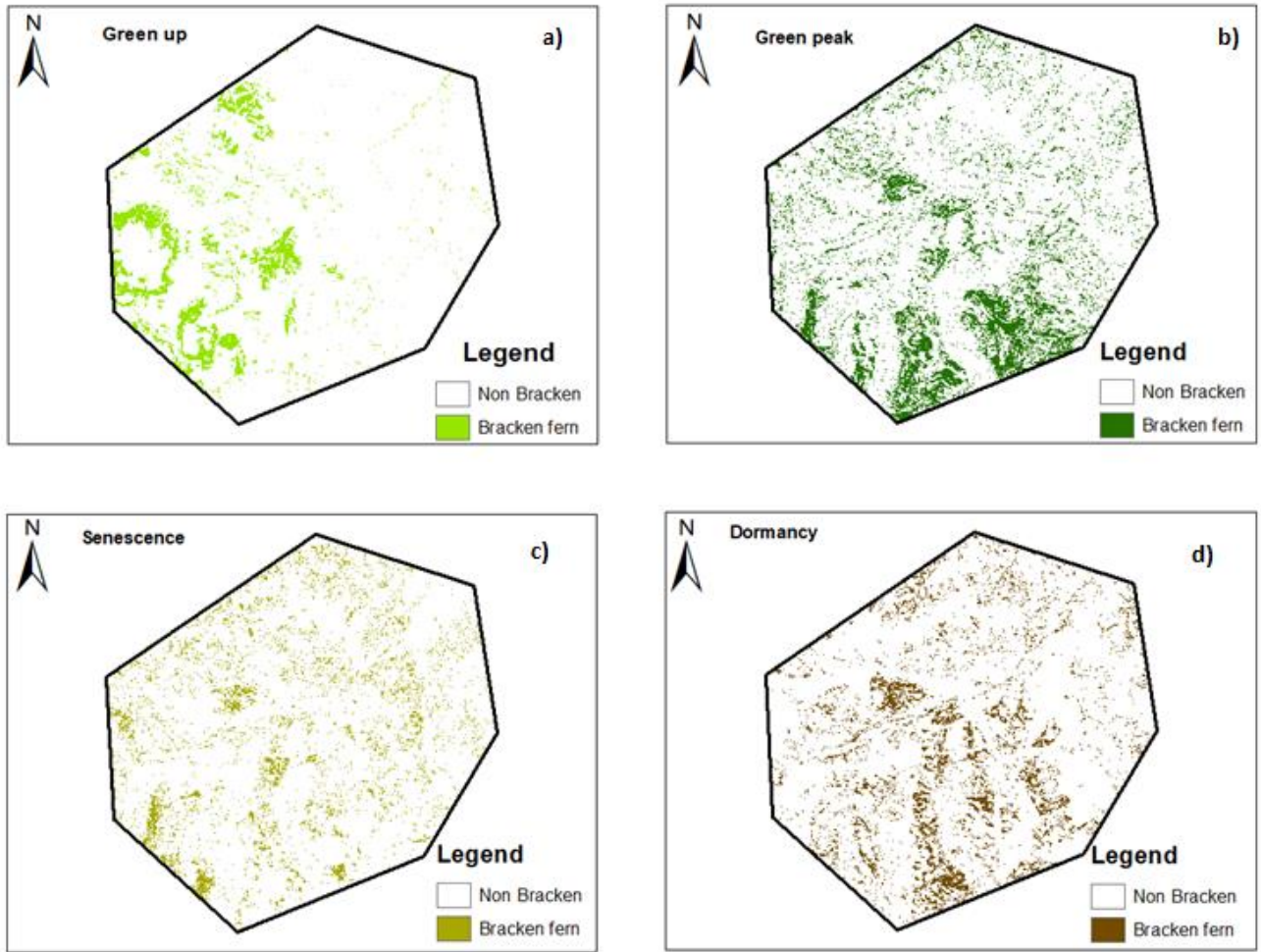
Figure 5.5: Bracken fern spatial distribution during the four phenological stages

5.4 Discussion

The focus of this study was to optimize the TDVI for mapping the spatial distribution of bracken fern at its four phenological cycles in the Drakensberg Mountains in South Africa. The study assessed the optimal spectral bands that separated bracken fern from other land cover classes and optimized the TDVI based on separability analysis findings.

5.4.1 Bracken fern spectral characteristics

During the green up and green peak phenological stages, bracken fern was more separable from other land cover classes in the red edge and NIR wavebands sections of the electromagnetic spectrum, while there was low separability in the visible and SWIR regions. The better performance of the red edge bands in distinguishing bracken from other species could be attributed to the sensitivity of the red edge spectral bands to the changes in the vegetation chlorophyll (Xie et al., 2018, Curran et al., 1990). During the green peak season, bracken fern is similar to other vegetation species, hence the increase in the spectral confusion between bracken fern and other species such as grassland especially in the visible part of the electromagnetic spectrum (Pitman, 2000). The low separability of the fern and other classes in the SWIR region during the green peak stage could be attributed to the fact that bracken fern exhibits a deep green hue similar to other vegetation during the peak of the season, which is less detected by SWIR (Marzialetti et al., 2020). As depicted in Figure 5.1 the spectral reflectance curve of bracken fern and grass were similar in the visible and SWIR sections of the electromagnetic spectrum during the peak of the bracken fern season. This is mainly due to the asymptotic nature of the relationship between spectral reflectance and LAI in the visible, particularly the red band and water absorption in the SWIR (Mutanga and Skidmore, 2004).

During the dormancy phenological stage, bracken fern was spectrally distinct from the co-existing species in most of the portions of the electromagnetic spectrum. The high separability of bracken fern during the dormancy could be attributed to the fact that there is a strong contrast between dead fern and other vegetation during the winter season (Holland and Aplin, 2013). Consequently, the low chlorophyll content in the fern fronds generally results in lower reflectance values when compared to other co-existing species. Findings from the current study are consistent with those of Odindi et al. (2014) who reported high accuracy in discriminating bracken fern from other vegetation species during the wither season since bracken fern dies

back and exhibits different spectral characteristics. The SWIR section recorded the least spectral overlap between bracken fern and other land cover classes.

5.4.2 Vegetation indices sensitivity to LAI changes

The seasonal changes in OTDVI variants exhibited a significant positive correlation with LAI patterns during the bracken fern phenological cycle as illustrated in Figure 5.2. There was a high correlation between $OTDVI_3$ and LAI during the green up and green peak phenological stages while $OTDVI_5$ had its highest correlation with ground measured LAI during the bracken fern dormancy stage. Towards the end of the season, bracken fern canopy cover is reduced (Matongera et al., 2021a), and the bare soil is exposed, hence the soil background effects are high. Similar to the original TDVI (Bannari et al., 2002) and Enhanced Vegetation Index (EVI) (Huete et al., 2002), the optimized indices showed a significant reduction in the effect of soil background reflectance, saturation and atmospheric errors. The NDVI-LAI relationship was weak especially during the peak of the bracken fern season. This could be attributed to the high saturation of NDVI when leaf area index and biomass accumulation are at maximum. This exposes the major challenge associated with using NDVI as an indicator of canopy structure or chemical content for well-developed canopies during the peak of the season (Potithep et al., 2010). Although the correlation between NDVI and LAI was lower than the optimized indices, NDVI did not saturate as it normally does in the deciduous forest (Birky, 2001) when LAI values are very high.

5.4.3 Bracken fern mapping

Generally, the classification of bracken fern at its four phenological cycles yielded good results using the dataset which combined spectral bands, original vegetation indices and optimized indices. The best feature selection analysis revealed that amongst the optimized vegetation indices, the $OTDVI_3$ was ranked as one of the most important variables in the classification of bracken fern. Specifically, the $OTDVI_3$ was more influential in classifying the fern during green up and green peak phenological stages. The performance of $OTDVI_3$ could be attributed to its formulation which includes the red edge portion of the electromagnetic spectrum has been reported to be more sensitive to vegetation characteristics (Sun et al., 2019, Xie et al., 2018, Cui and Kerekes, 2018). The red edge wavebands are also well known for their sensitivity to subtle changes in the canopy structure, gap fraction and senescence (Potter et al., 2012). Findings from the current study also correspond with previous works that also reported the superiority of vegetation indices calculated from the red edge region in classifying various

invasive alien plants (Iqbal et al., 2021a, Masemola et al., 2020, Rajah et al., 2019). Mapping bracken fern during summer is also constrained by atmospheric influences such as cloud cover.

The OTDVI$_4$ and OTDVI$_5$ performed well in the classification of bracken fern during the senescence and dormancy phenological stages. The two optimized indices were formulated using the NIR and SWIR spectral bands. The significance of SWIR in mapping bracken fern could be attributed to the fact that SWIR bands are valuable in discriminating bracken fern from other land cover types, especially in winter when the fern is characterized by a thick mass of dead matter (Holland and Aplin, 2013). Overall, producer and user accuracies further improved when the classification was performed using the best features based on the SFS. However, the use of only the most important features in mapping invasive alien plants does not always result in the improvement of classification accuracies. For instance, Kiala et al. (2019) concluded that feature selection did not improve the classification model for mapping Parthenium alien invasive weed in KwaZulu-Natal, South Africa.

5.5 Conclusion

The current study assessed the utility of the optimized transformed difference vegetation index in mapping bracken fern phenology. Five OTDVI variants were developed based on the spectral regions that depicted maximum separation of bracken fern from other land cover classes. The performance of the optimized indices was tested in mapping bracken fern at each phenological stage. Based on the results established at bracken fern's four phenological stages, the following conclusions were drawn;

- Bracken fern was optimally discriminated from other co-existing species during the dormancy phenological stage
- The red edge and NIR spectral bands were able to discriminate bracken fern from other land cover classes during the green up and green peak phenological stages, while the SWIR section was best during the dormancy stage.
- The optimized indices exhibited bracken fern growth patterns that were significantly correlated to the ground measured LAI throughout the fern's growth cycle.
- The OTDVI$_3$ and OTDVI$_5$ outperformed the traditional NDVI and TDVI indices in mapping bracken fern during its four growth stages. The optimized indices proved to be more sensitive to changes in vegetation than NDVI and TDVI, but less sensitive to the soil background.

Although bracken fern was successfully mapped at its four phenological stages, evidence from the field assessments shows that at the end of the bracken fern season, there are remnant green patches of bracken fern across the landscape. The mapping approach used in this study did not account for the spatial variability of bracken fern during the dormancy phenological stage. Thus, in the following Chapter Six, an object-based image analysis approach is developed to assess the spatial variability of bracken fern during the dormancy phenological stage.

Chapter Six

Assessing the spatial variability of bracken fern during dormancy phenological stage using object-based image analysis

This chapter is based on a paper:

Abstract

The spread of invasive alien plants such as bracken fern is now internationally recognized as one of the most serious threat to biodiversity after habitat destruction. Spatially explicit maps of bracken fern are critical to understand its spatiotemporal distribution patterns. The study aimed at assessing the spatial variability of bracken fern during dormancy phenological stage using object based image analysis. Through image analysis, remote sensing provides an efficient tool to map the spatial distribution and variability of bracken fern at different phenological stages. Pixel-based classification approaches have been widely used in the remote sensing of bracken fern. However, pixel-based image analysis approaches are associated with the "salt and pepper effect", which is normally caused by sharp and sudden disturbances in the image signal. The study used the Simple Non-Iterative Clustering (SNIC) to identify the spatial clusters while the Gray-Level Co-occurrence Matrix (GLCM) was employed to compute textural indices on a cluster basis. The spatial variability patterns of bracken fern across the landscape and its relationship to topographic variables during the dormancy was also examined. The findings from the current study showed that the object-based classification approach which included bracken fern texture information yielded the highest overall accuracy (89%). The major topographic variables influencing the spatial variability of bracken fern during the dormancy phenological stage were elevation, Topographic Wetness Index (TWI), valley depth and positive openness. The green bracken patches were found in areas characterized by low elevation, high TWI, high valley depth and low positive openness.

Keywords: Spatial variability, Object based, Google Earth Engine, Phenology, Sentinel-2, Dormancy

6.1 Introduction

Globally, the land surface is at risk of being invaded by invasive species that have devastating consequences on local ecosystems and human livelihoods (Pepin et al., 2019). Bracken fern is amongst the highly invasive and destructive plants that cause economic and environmental problems to farmers, conservationists and ecologists in many parts of the world (Francesco et al., 2011, Schneider and Initiative, 2004, Morgan-Davies et al., 2005). The hydrological impacts of bracken fern on catchments have also been reported by Clauson-Kaas et al. (2016). Specifically, in areas with dense patches, bracken fern intercepts precipitation and prevents it from reaching the ground surface (McGlone et al., 2005). The subtropical bracken fern which is commonly found in South Africa has an exceptionally dynamic phenological cycle (Matongera et al., 2021a). The fern produces new green shoots during the beginning of the summer season around October, followed by a swift growth to green peak around February(Matongera et al., 2021a). The end of the phenological cycle is estimated to be around July, which coincides with the winter season (Matongera et al., 2021a). The dormancy phenological stage signals the gradual decrease of photosynthetic activity leading to drying of bracken fern fronds. Evidence from field observations shows that when bracken fern has reached dormancy, some of the plants do not dry and die as expected. Instead, there are remnant green patches that have the potential to sprout further and occupy virgin areas as well as those areas previously occupied by the dead fern. Therefore, it is necessary to map the distribution of both the dead and live bracken fern material to understand factors that influence their resilience.

The large-scale control of invasive species has been less effective because of the spatial variability in the expansion of many invasive species (Pepin et al., 2019). The existing management control plans of the majority of the invasive species show that there is a general assumption that a certain invasive species would reach a peak or fall in a well-defined phenological cycle (Marrs et al., 2000b). On the other hand, evidence from literature reveals that some of the invasive plants reach peak or dormancy at a different rate (Pyšek and Richardson, 2010, García-Díaz et al., 2019). Consequently, the exclusion of these fluctuating variability in invasive management frameworks reduces the effectiveness of the management efforts (Dew et al., 2017). Therefore, applying the same control methods at a certain phenological stage throughout the study site will not be effective. Hence there is a need to assess the spatial variability of the fern to determine the suitable interventions in different

sections of the targeted areas. Furthermore, the invasion vulnerability maps which show the spatial variability of alien and indigenous vegetation are crucial in the management of rangelands infested by invasive plants (Turbelin et al., 2017, Dai et al., 2020).

Remote sensing provides the data sets, tools and technical environment for biological invasion monitoring and prediction, and it also allows for the coverage of large areas (Skowronek et al., 2017, Rocchini et al., 2015). Through the availability of freely accessible satellite sensors such as Sentinel-2 Multi-Spectral Instrument (MSI), it is possible to assess and quantify the spatial variability of bracken fern across landscapes (Matongera et al., 2021a). The Sentinel-2 sensor which acquires its data at 10 – 60m spatial resolution with a 3-5-day revisit (Gatti and Bertolini, 2013)time presents an opportunity for successful assessment of the spatial variability of bracken fern at various scales. The Sentinel-2 sensor samples 13 spectral bands in the visible-near infrared (NIR) and short wave infrared (SWIR) (Traganos and Reinartz, 2018). Amongst these spectral bands, the sensor measures three strategically located spectral bands in the red edge region of the electromagnetic spectrum, which is very critical in estimating and monitoring the phenological developments of vegetation (Shoko and Mutanga, 2017). Various software packages and data processing algorithms have been developed for vegetation analysis using remotely sensed data over the last four decades (Ormsby et al., 2010, Eklundh and Jönsson, 2015, Wang and Zhao, 2005). However, the effective management of invasive alien plants in rangelands requires continuous monitoring of infested landscapes. The constant monitoring of the earth's surface requires big data, which is often attributed to large volumes of datasets that require huge storage space and advanced processing techniques (Tamiminia et al., 2020).

Google Earth Engine (GEE), an open-source cloud-based computing platform has emerged as an invaluable platform that facilitates the access, processing and analysis of huge amounts of remotely sensed data in a single environment (Mutanga and Kumar, 2019, Xiong et al., 2017, Shelestov et al., 2017a). The platform enables the users to easily access, pre-process and analyze remote sensing data without downloading it to a local machine, hence reducing the computing power and time required to perform the task (Amani et al., 2020b). GEE is suitable for tracking and monitoring the encroachment of bracken fern as it provides access to a wide range of remotely sensed data sets as well as built in data processing algorithms such as classification models. The Support Vector Machine (SVM) is a machine learning algorithm that was designed to solve sophisticated problems in classification, regression, and novelty

detection ([Shelestov et al., 2017a](#), [Awad and Khanna, 2015](#), [Pal and Mather, 2005](#)). One of the outstanding attributes of the SVM is that the determination of the model parameters matches with a convex optimization problem, hence, any local parameter settings can also be used at a global scale ([Jain and Kar, 2017](#)). The mapping of invasive alien plants has been undertaken using traditional pixel-based SVM classification models at various scales ([Pouteau et al., 2012](#), [Gavier-Pizarro et al., 2012](#), [Sabat-Tomala et al., 2020](#)). Nevertheless, most pixel-based classifications have several challenges that limit their applications in heterogeneous landscapes. For instance, in a pixel-based classification, the spectral heterogeneity within a particular land cover class can lead to misclassification of pixels appearing within classes causing what is known as a 'salt and pepper' effect ([Whiteside et al., 2011](#)). Object based classification methods have gained traction due to their ability to delineate and classify objects using useful features such as shape, texture and context relations with other objects, an aspect that pixel-based approaches lack ([Hay and Castilla, 2006](#)). In that regard, the object analysis approach has the potential to provide better spatial detail and more accurate detection of the bracken boundary.

To further understand the spatial variability of bracken fern, it is crucial to uncover the unprecedented process of invasion which is deeply influenced by the traits of receiving rangelands. Environmental variables are well known site conditions that influence species occurrence and variability at micro and macro scales ([Hofer et al., 2008](#), [Dubuis et al., 2013](#), [Syphard and Franklin, 2010](#)). Topography is one of the most common environmental factors that influence species distribution locally. For instance, topography influences climatic conditions ([Grzyl et al., 2014](#)), runoff and erosion ([Jiao et al., 2009](#)) as well as soil formation ([Ridolfi et al., 2008](#)). Identifying the most influential topographic factors controlling the variability of bracken fern under different spatial scales is thus crucial for the sustainable management of rangelands. Therefore, study aimed to assess the spatial variability of bracken fern across the Cathedral Peak Nature Reserve landscape using the object-based image analysis. The study also examined the key topographic factors influencing the spatial variability of bracken fern during the dormancy phenological stage.

6.2 Materials and methods

6.2.1 Field data collection

The ancillary data collection was conducted during the bracken fern dormancy phenological stage, which was in July 2021. The locations of dry bracken fern and remnant green bracken fern patches were collected using the Leica GS20 Global Positioning System (GPS). A total of 65 plots with bracken fern green patches were recorded while 110 dry bracken patches were also documented. Purposive sampling was used to identify green and dry fern patches, based on the preliminary encroachment information that was supplied by Ezemvelo KwaZulu-Natal Wildlife. The sampled plots were located at least 100m away from each other to avoid autocorrelation. The bracken fern sampled locations were documented in a table format and later converted into a point map in ArcGIS 10.6. Photographs of green and dry bracken fern were captured during the field visit to provide better visualization of the spatial variability at a landscape scale. Figure 6.1 shows the phenological discrepancies in the bracken fern's appearance during the dormancy stage.
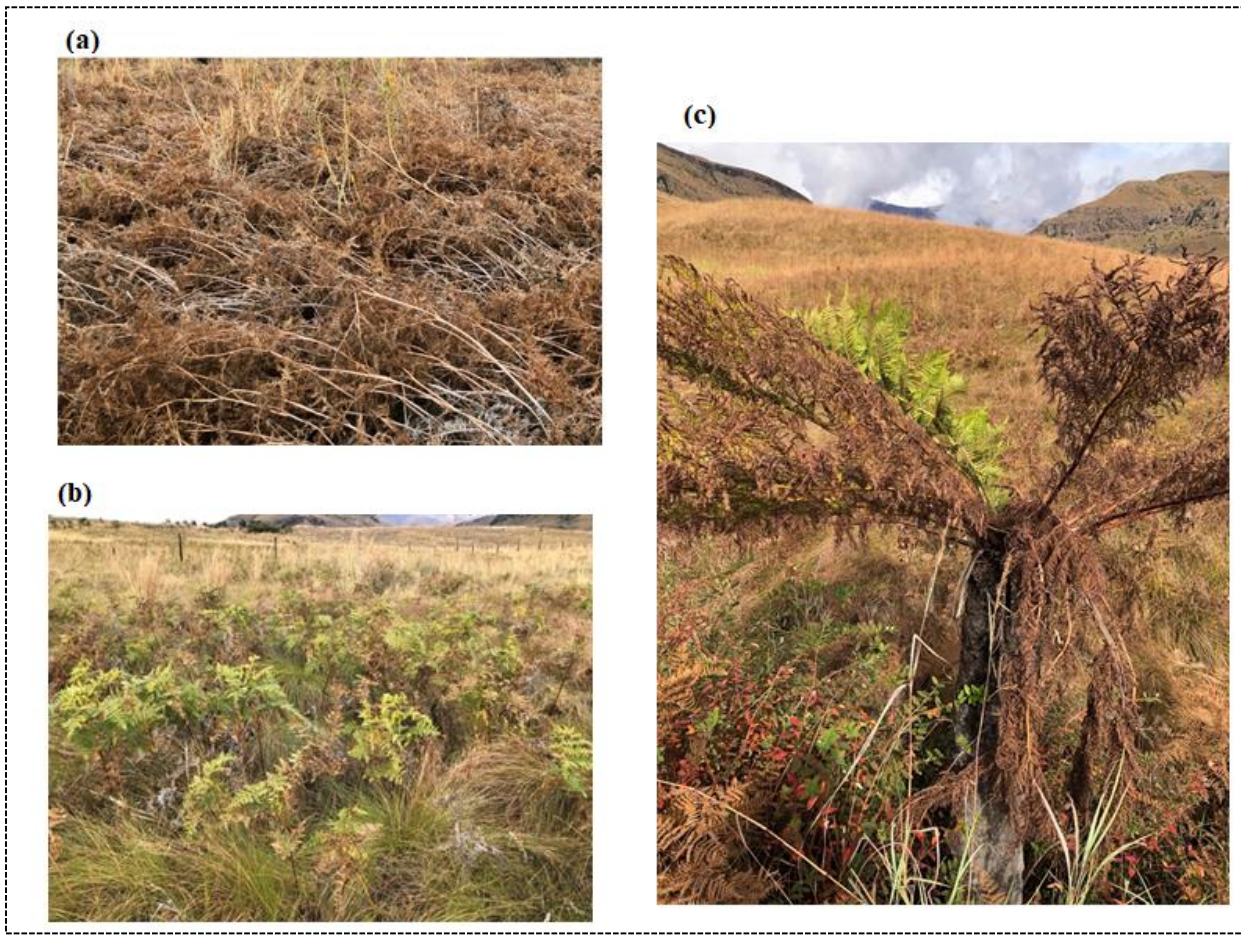
Figure 6.1: Bracken fern field photographs showing a) dry bracken fern; b) green remnant patches and c) rare huge bracken fern plant

6.2.2 Remotely sensed data acquisition

The Copernicus Sentinel-2 satellite data was accessed through the Google Earth Engine platform (https://earthengine.google.com/). The data was based on the median values of the Sentinel-2B images acquired from 14 June to 1 August 2021 obtained at processing level 2A. The images were resampled in the GEE platform and the composites were merged into a single date image in preparation for the classification process. The Sentinel-2 sensor acquires 13 spectral bands at 10, 20 and 60m spatial resolution. These spectral bands cover the visible, Near Infrared (NIR), red edge and shortwave (SWIR) portions of the electromagnetic spectrum, making the sensor invaluable for a wide range of applications (Ndlovu et al., 2018). The Sentinel-2 sensor has a temporal resolution of 3-5 days at an orbital angular distance of 180km with a 290km swath width (Kiala et al., 2019). The coastal aerosol and circus bands were excluded from the analysis as they do not contain relevant information useful for assessing the spatial variability of bracken fern.

6.2.3 Bracken fern classification

The object-based classification and accuracy assessment of bracken fern was implemented in the GEE script editor. For evaluation of the effectiveness of the object-based approach in detecting the spatial variability of bracken fern, the pixel-based method was also executed using the same training and test data sets in the GEE platform. The object-based classification process was performed in three stages as follows;

- **Spatial clustering**: Involved the grouping of similar pixels together into clusters using the Simple Non-Iterative Clustering (SNIC) (Achanta and Susstrunk, 2017) algorithm available within the GEE platform. SNIC generates a regular grid of seeds and iteratively selects pixels and assigns them to a super-pixel. The clusters were developed into objects using the "Image.reduceConnectedComponents" function. The SINC algorithm relies on a seed pixel that is the center of the cluster (Yuan et al., 2018). SNIC requires the setting of parameters such as "compactness" which determines the cluster shape, "connectivity" which influences contiguity based on the merge of adjacent clusters and "neighborhoodSize" to minimize boundary artifacts (Tassi and Vizzari, 2020). In our study, the parameters were set as follows; "compactness" = 0, "connectivity" = 4 and "neighborhoodSize' = 128.

- **Object textural analysis**: The Gray-Level Co-occurrence Matrix (GLCM) was used to compute textural indices on a cluster basis. The GLCM algorithm calculates second-order statistics of texture features using the statistical distribution of observed combinations of intensities at specified positions relative to each other in the satellite image (Mohanaiah et al., 2013). GLCM requires a grey-level 8-bit image as input. The study selected the most relevant seven textural indices according to what was suggested. The grayscale conversion was performed using the weighted linear combination (Equation 1) (Ge and Liu, 2020) which is normally used for red green blue (RGB) image to grayscale conversions. The GLCM was computed as follows;

$$\text{Gray} = (0.3 \times \text{B4}) + (0.59 \times \text{B3}) + (0.11 \times \text{B2}). \qquad \text{Equation 6.1}$$

A Principal Component Analysis (PCA) of the most relevant 7 GLCM metric (Table 6.1), selected according to Hall-Beyer (2017), is applied to derive a single representative band (the first PC) which generally contains the majority of the textural information. The average of PC1 is then calculated in a separate band for each object included in the SNIC "clusters" band (Tassi

and Vizzari, 2020). The PC1 object-averaged band is finally added to those extracted from the SNIC segmentation process.

- **Classification algorithm**: The Support Vector Machine (SVM) classifier was applied for both object and pixel-based classification approaches. The SVMs find a hyperplane splitting the samples of the target class from the origin with the best possible separation (Noble, 2006). The SVM radial basis function kernel (RBF) was applied (with gamma = 1 and cost = 10).

Table 6.1: Description of the selected the Gray-Level Co-occurrence Matrix (GLCM) metrics

GLCM metric	Description
Angular Second Moment	Measures the uniformity or energy of the gray level distribution of the image
Contrast	Measures the contrast based on the local gray level variation
Correlation	Measures the linear dependency of gray levels of neighbouring pixels
Entropy	Measures the degree of the disorder among pixels in the image
Variance	Measures the dispersion of the gray level distribution to emphasize the visual edges of land-cover patches
Inverse Difference Moment	Measures the smoothness (homogeneity) of the gray level distribution
Sum Average	Measures the mean of the gray level sum distribution of the image

6.2.4 Accuracy assessment

The validation data set was used to compute the accuracy metrics to statistically evaluate the quality of the bracken fern spatial variability classification output. The confusion matrix enabled the computation of overall accuracy (OA), user (error of omission) and producer (error of commission) accuracies. For comparison, the confusion matrices were produced for the object and pixel-based classifications.

6.2.5 Topographic variables

The topographic variables were extracted using the digital elevation model (DEM) derived from NASA's 30m Shuttle Radar Topography Mission (SRTM) which is available within the GEE platform. Table 6.2 provides a list, brief description, and relevance of all the topographic variables used to explain the spatial variability of bracken fern during the dormancy

phenological stage. These variables have been documented in literature as the essential driving factors for invasive species occurrence and distribution (Ndlovu et al., 2018, Makori et al., 2017).

6.2.6 Statistical analysis

Logistic regression was used to explain the main topographic drivers influencing the existence of green bracken fern at the end of the season when all the fern was expected to be dry as documented in the literature (Matongera et al., 2021a, Odindi et al., 2014, Holland and Aplin, 2013). Logistic regression is a statistical tool that relates a binary dependent variable to several continuous or discreet independent variables (Suslick, 2001). This logistic regression model was built using 65 presence records for green bracken fern and 250 absence records selected randomly from the classified map. Therefore, green bracken fern was regarded as present while the dry bracken fern was regarded as an absence.

After fitting the logistic regression to the dataset, the list of topographic variables which were correlated to the occurrence of green bracken fern was obtained. Dominancy analysis was used to explore the importance of each topographic variable to predict the occurrence of green bracken fern patches during the dormancy phenological stage. The dominancy analysis is used to determine the relative importance of predictors in a regression analysis (Azen and Budescu, 2003). The dominancy analysis assumes that the influence of variables are not equal, some predictors may dominate others. The McFadden index (R^2M) was used to quantify the dominancy of each variable. The relationship between bracken fern spatial variability and topographic variables was visually presented by taking random samples of pixels classified as green and dry fern and extracting all the values for the variables that are listed in Table 6.2. Box plots were plotted to show the patterns of green and dry fern occurrence in relation to topographic variables.

Table 6.2: List of topographic variables that influence bracken fern spatial variability

Variable	Description	Relevance
Elevation	The height above the sea level	Influences the altitudinal zonality of soils across the landscape
Aspect	Compass direction	Determines the total incoming solar radiation received by a location
Slope	Slope gradient	Controls microclimate attributes such as evapotranspiration, air and soil temperature

Topographic wetness index	Steady state wetness index	Represents relative local soil moisture availability
Valley depth	Difference between the elevation and an interpolated ridge level	Controls the total amount of direct solar radiation received by a location, regardless of the compass direction
Terrain ruggedness	Topographic heterogeneity based on the amount of elevation difference between the cells.	Calculates the variability of elevation in each geographical location
Positive openness	angular measure of the relation between surface relief and horizontal distance. Expressing openness above the surface	Directly influences drainage features such as soil water content
Negative openness	angular measure of the relation between surface relief and horizontal distance. Expresses openness below the surface	Directly influences drainage features such as soil water content
Direct insolation	Potential incoming insolation	Affects the photosynthetic activity of vegetation

6.3 Results

6.3.1 Classification accuracies

Table 6.3 shows the summary of classification accuracies of bracken fern spatial variability during the dormancy phenological stage based on the object based and pixel-based approaches. The best OA (89%) results were obtained using the OB classification approach which included the GLCM textural information. The OB method without GLCM textural information outperformed the PB approach by an average OA of 9%. In that regard, the PB yielded the lowest results (OA = 74%). The incorporation of bracken fern textural information significantly improved the OA by 6%. As expected, the UA and PA metrics also increased by an average rate of 4.7% when the textural data was included in the classification process. On average, the dry fern class recorded the highest UA (85%) and PA (84%) metrics across the three classification approaches. The lower UA and PA recorded by the green fern class across the three approaches shows that there was a high error of omission and commission between green fern and other co-existing land cover classes.

Table 6.3: Error matrix of the classified bracken fern maps at four phenological cycles

	Object based		Object based_Texture		Pixel based	
	PA	UA	PA	UA	PA	UA
Dry bracken	88	85	91	93	75	77
Green bracken	74	84	85	87	69	72
OA	**83**		**89**		**74**	

Figure 6.3 shows classification maps depicting the spatial variability of bracken fern during the dormancy phenological stage based on the OB_GLCM and PB approaches. There is a difference between the outputs of the two classification approaches as evidenced by the maps. The visual interpretation based on the OB reveals a high density of both green and dry fern across the study site, while the OB_GLCM shows a lower density of both green and dry ferns. Therefore, the OB_GLCM suggests a smaller area coverage of bracken fern during the dormancy stage. In terms of variability, the visuals in Figure 6.3 show that in the Southern part of the study area, the separation between green and dry fern pixels was not crystal clear. There is evidence of spectral overlap and possible confusion between the green fern and other land

cover classes. On the other hand, the OB_GLCM shows superiority in detecting the spatial variability of the fern. However, comparing the two land cover maps, the bracken fern variability is generally consistent, the hot spot areas with remnant green patches of bracken fern seem to be in the same geographical locations detected by the two classifiers.

In terms of the computation time, the PB approach was the fastest (21 seconds) and easiest to execute while the OB_GLCM took a bit more time (73 seconds) to complete the classification, probably due to the complexity of its processing parameters. The execution time reported excludes the importation of training data and the exportation of the final land cover maps.
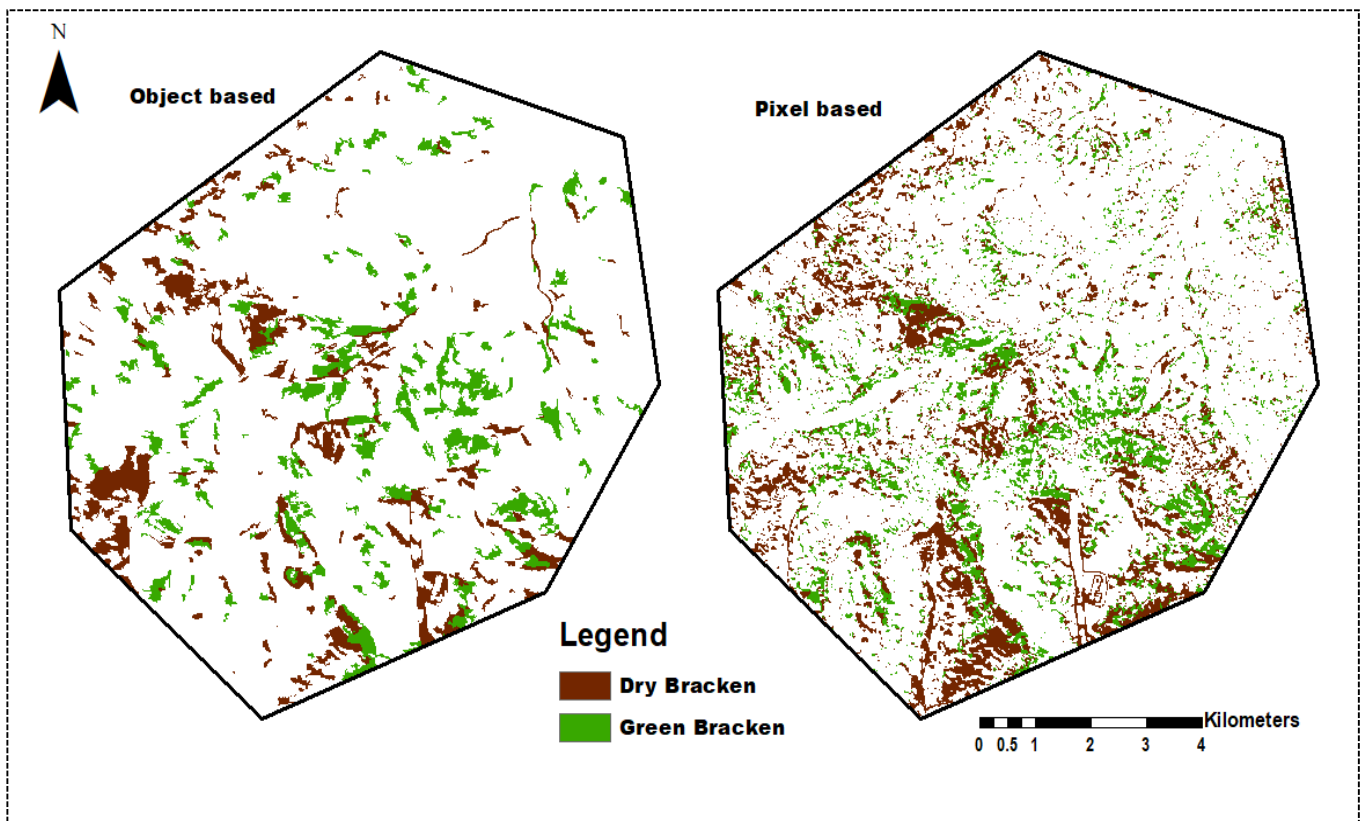
Figure 6.3: Bracken fern spatial variability classification maps produced using object based and pixel-based approaches

6.3.2 Bracken variability and topographic variables

The results showed that the presence of remnant green bracken fern during the dormancy phenological stage was related to topographic factors Findings from the logistic regression analysis shows that elevation, TWI, valley depth, terrain ruggedness, positive openness and aspect had positive coefficients, which indicated that the occurrence of green bracken fern was associated with these topographic variables. Elevation, TWI, valley depth, terrain ruggedness, positive openness and aspect were statistically significant predictors ($p < 0.05$) of bracken fern spatial variability. Figure 6.4 shows the dominancy ranking of topographic variables in the occurrence of green bracken fern during the dormancy phenological stage. Elevation and TWI recorded the highest R^2 M values (0.128 and 0.125 respectively) suggesting that these two predictors had a strong association with the occurrence of remnant green bracken fern patches during the dormancy phenological stage. On the other hand, direct insolation, negative openness and slope had the lowest R^2 M values lower than 0.05, suggesting that these predictors had less influence on the occurrence of green bracken fern across the landscape.
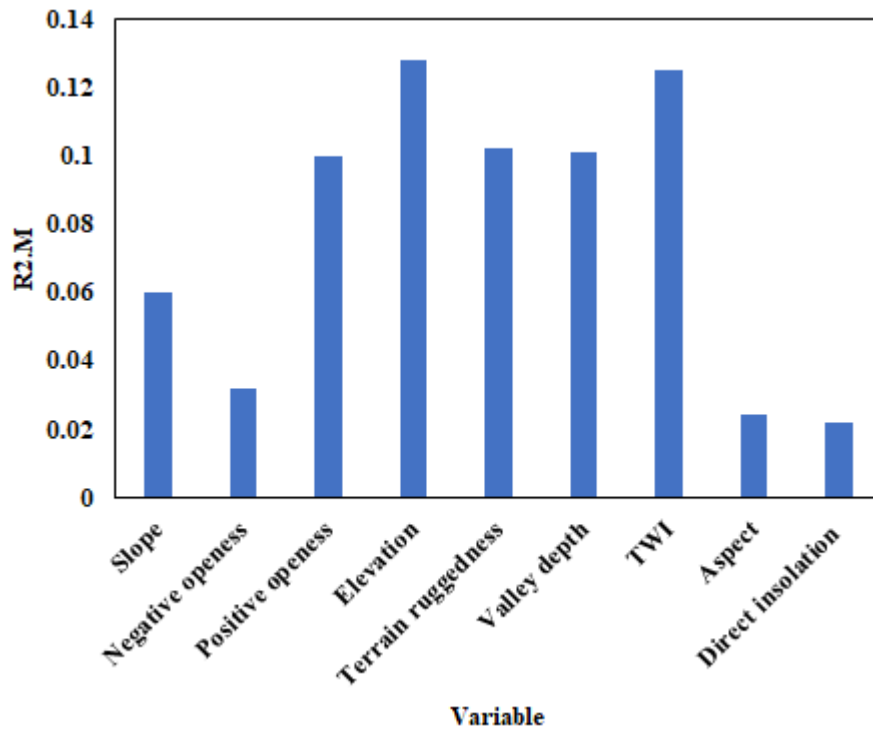
Figure 6.4: The dominance of topographic variables in the occurrence of green bracken fern

Figure 6.5 shows the box plots depicting the distribution of mean values of dry and green to fern topographic values. The three topographic variables which had R^2 M values lower than 0.05 were excluded from the visual analysis. The plots illustrate the spatial variability of bracken fern spatial distribution as a function of each topographic variable during the dormancy phenological stage. The variability of bracken fern shows a pattern that has a relationship with topographic variables. For instance, the green patches of bracken fern are mostly found in lower lying areas that have an elevation below 1400m above sea level. On the other hand, the dry bracken fern patches are mostly found in higher elevation areas that are more than 1410m above sea level. The valley depth also influences the spatial variability of bracken fern. Evidence shows that the remnant green patches of bracken fern are highly concentrated in valleys that range from 60 to 100m. There is a very low concentration of dry bracken fern in valleys that are deeper than 60m. As expected, the topographic wetness index shows a clear distinction in the spatial distribution of dry and green bracken fern during the dormancy phenological stage. Landscapes with high TWI favoured the existence of remnant green patches when most of the fern was expected to be dry during the end of the season. The TWI values which favoured the proliferation of green fern ranged from 12 to 18. The terrain ruggedness and aspect show an increased overlap between areas with green and dry fern. Unlike other topographic variables,

110

aspect and terrain ruggedness do not show a clear distinction between portions with green and dry fern. There is evidence of the existence of both dry and green bracken fern within the 1 – 1.5 range of terrain ruggedness. Similarly, green and dry fern existed within the 1.8 – 2.2 range of aspect.
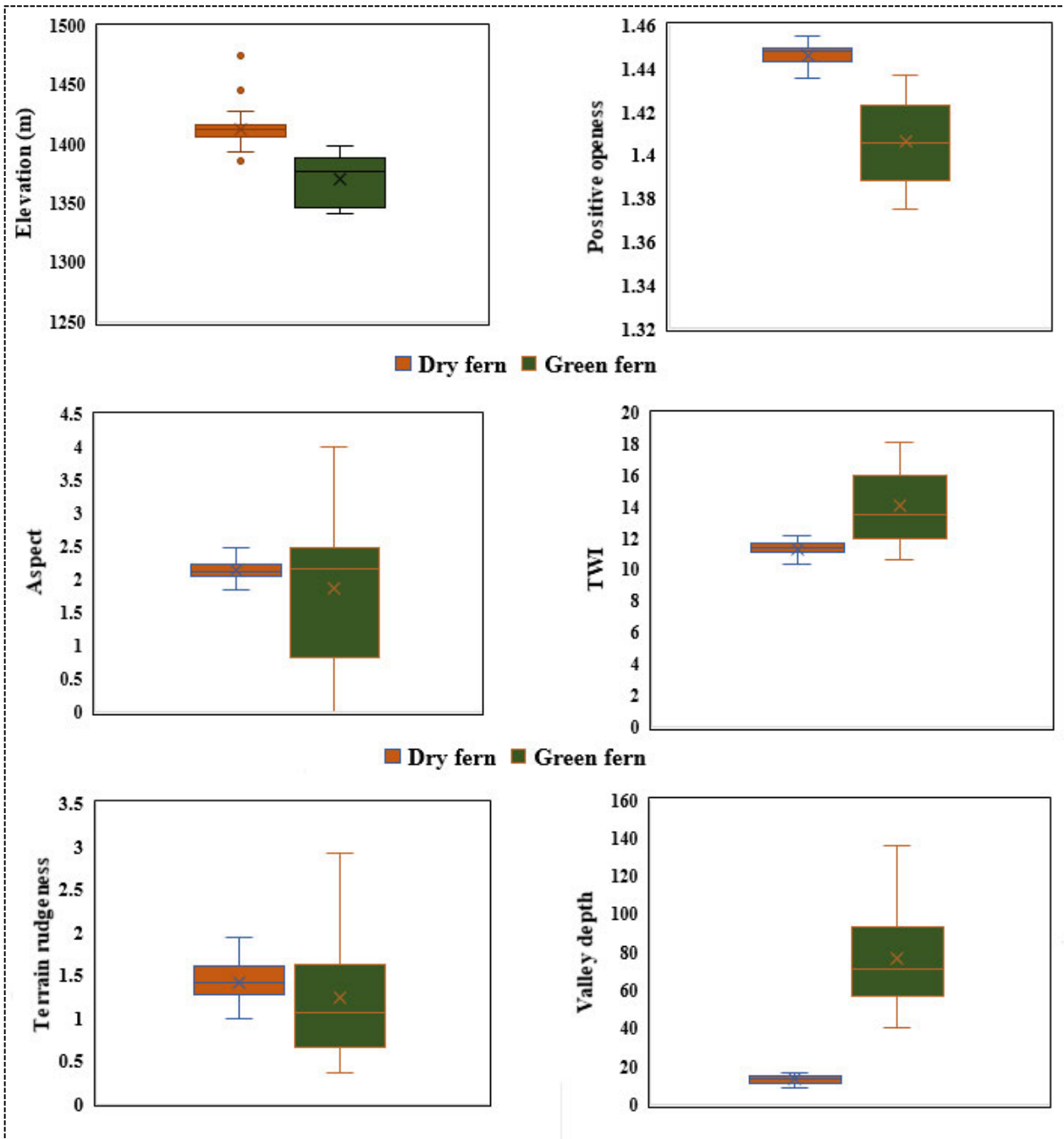
Figure 6.5: Box plots illustrating the variability of bracken fern as a function of topographic variables

6.4 Discussion

The focus of this study was to assess the spatial variability of bracken fern during the dormancy phenological stage. The study tested the effectiveness of the object-based classification method in detecting the variability of the fern at the end of its growing season. The topographic variables that influence the variability of bracken fern were also examined.

6.4.1 Performance of classifiers

The OB_GLCM classification approach yielded the highest overall accuracy in assessing the spatial variability of bracken fern during the dormancy phenological stage. The OB_GLCM achieved higher accuracy in the classification due to the combined use of Sentinel-2 spectral, spatial and textural data. The inclusion of bracken fern textural information significantly enhanced the classification results. The addition of spatial attributes such as texture improves the image segmentation process computed by the OB_GLCM approach (Ryherd and Woodcock, 1996). In object-based image analysis, texture enables the derivation of spatial characteristics that can be expressed in terms of spatial autocorrelation, a measure of the relationship between an image pixel and its neighbours (Tassi and Vizzari, 2020). Based on the regularly spaced seed, the SNIC algorithm was effective in identifying and delineating bracken fern clusters, resulting in the reduction of the 'salt and pepper effect' a problem that is more evident in the pixel–based land cover map. Corresponding to findings reported in this study, the combination of the GLCM and SNIC algorithms in the classification of remotely sensed data has yielded very good results in the literature (Tassi et al., 2021, Iqbal et al., 2021b).

There was high misclassification of green fern and other land cover types as shown by the lower user and producer accuracies. However, the OB_GLC approach minimized these errors of omission and commission since it recorded slightly higher user and accuracies for the green fern class. The misclassification of the remnant green bracken fern could be attributed to the similarity between the fern and other land cover classes such as shrubs and grasses that are usually still green in winter. The spectral confusion between bracken fern and grass species was also previously reported in the literature (Odindi et al., 2014, Pakeman et al., 1996, Birnie and Miller, 1985). Generally, the assertion emphasized in these studies is that bracken fern exhibits similar spectral reflectance with other vegetation species, hence, causing poor delineation of invaded landscapes. However, Holland and Aplin (2013) was able to accurately delineate green fern from other co-existing species using the super resolution analysis, an

object-based classification approach. Their conclusions correspond with findings from the current study which noted the importance of object-based image classification techniques in discriminating green bracken fern from other land cover classes which exhibits similar spectral reflectance with the fern at any phenological stage.

6.4.2 Factors influencing bracken fern spatial variability

The main driving forces causing bracken fern spatial variability during the dormancy phenological stage are elevation, TWI, valley depth, terrain ruggedness, aspect, and positive openness. As depicted in Figure 6.5, there was a distinct elevation gradient between areas with dry and green bracken fern. The remnant bracken green patches are mostly found in low lying areas while the dry patches are found in high elevation areas. The variability could be attributed to the fact that at the lower elevation of Savanna regions, there is slow thermal accumulation which leads to delayed bracken fern canopy development and generally leads to longer growing seasons than those at high elevation. Findings from our study correspond with Olsson et al. (2013) who confirmed that variation of vegetation phenology is generally related to average air temperature and that this is partly controlled by the local elevation. Similarly, (Birhanu et al., 2021) elevation also influences the atmospheric pressure, moisture, and temperature which have a direct effect on the growth and development of vegetation over time. Portions of the study site characterized by deeper valley depth were also the hotspots for remnant green bracken fern. Deep valleys in mountainous regions receive less direct solar radiation (Matzinger et al., 2003). Consequently, areas receiving less solar radiation have slow photosynthetic activities, hence tend to have an extended growing season. The bracken fern patches along perennial rivers remained green even during the end of the bracken phenological cycle.

The green bracken fern patches were abundant in regions with high TWI while the dry fern was mostly concentrated in low TWI regions. The variability of bracken fern in relation to TWI was attributed to the fact that soil moisture is one of the most crucial drivers of vegetation composition and variability in rangelands (Chaturvedi and Raghubanshi, 2018, Yang et al., 2018). Terrain ruggedness relates to the topographic heterogeneity based on the amount of elevation difference between the cells. There was low bracken fern variability in relation to terrain ruggedness across the Drakensberg landscape. Both dry and green bracken fern was abundant in areas that ranged above 1.5m of terrain ruggedness. Our findings correspond with Nellemann and Fry (1995) who highlighted that high terrain ruggedness causes high diversity

of vegetation types and ecotones at a local scale. Therefore, terrain ruggedness did not significantly influence the variability of bracken fern during the dormancy phenological cycle.

Aspect refers to the direction the slope is facing and has been reported as a factor that influences the total incoming solar radiation that is received by a specific location within a landscape (Yetemen et al., 2015). However, this study aspect did not seem to show a clear distinction between dry and green bracken fern at a landscape. On the other hand, dry fern patches were concentrated in aspect values around 2. There was evidence of sporadic distribution of green bracken fern patches in the areas with low positive openness, while dry bracken patches were mostly found in areas with high positive openness. The variability could be explained by the fact that landscapes with high positive openness receive more direct solar radiation and high wind speed which subsequently amounts to a high level of evapotranspiration (Yokoyama et al., 2002). Consequently, bracken fern patches exposed to more evapotranspiration and low moisture content due to positive openness will dry quicker than those which are less exposed.

6.5 Conclusions

The current study assessed the spatial variability of bracken fern during the dormancy phenological stage. Specifically, this study tested the utility of the objected based classification approach in detecting the spatial variability of the fern. The study also evaluated the influence of topographic variables on the phenological occurrence of bracken fern during the dormancy stage. Based on the results, the study concluded that:

- The object-based classification approach (OB_GLCM) which combined Sentinel-2 spectral bands and bracken fern textural features outperformed the traditional pixel-based approach.

- They key topographic variables which mostly influence the spatial variability of bracken fern are elevation, TWI, valley depth and positive openness. Specifically, the green bracken patches were found in areas characterized by low elevation, high TWI, high valley depth and low positive openness.

The findings of this work are significant in the formulation of management plans in rangelands. Specifically, the use of bracken fern spatial distribution maps which considers spatial variability has the potential to improve the efficiency of mechanical, biological, and chemical control methods at various scales.

Chapter Seven

Estimating and monitoring the phenological cycle of bracken fern using remote sensing: A Synthesis

7.1 Synthesis

The encroachment of invasive alien plants such as bracken fern has been a challenge in many rangelands environments. The management and control of bracken fern has been an issue of concern in infected areas. However, evidence from the literature shows that very little work has been done in understanding the phenological cycles of bracken fern using remotely sensed data sets. Previous efforts to monitor and manage the encroachment of bracken fern did not incorporate phenological data obtained from remote sensing platforms. Bracken fern's phenological information will assist conservationists and farmers in determining the most effective methods and appropriate time for controlling the fern across its life cycle stage, to ensure the complete eradication of the fern with minimum costs and inputs. The collection of bracken phenological information has been relying on traditional field surveys and phenological networks that have teams of professionals who record recurring biological events of specific plants. However, field surveys are labour intensive, time consuming and expensive for large scale studies. The launching of new generation satellite sensors such as Sentinel-2 with improved spectral and spatial resolution provides a potential to estimate and track the phenology of bracken fern at various scales free of charge.

Long term satellite data archives present an opportunity to retrospectively extract phenological characteristics of vegetation regularly. The continuous monitoring of invasive alien plants such as bracken fern requires effective data processing packages and algorithms that can process large amounts of data with limited resources. GEE provides users with a wide range of machine learning algorithms such as Random Forest (RF) and Support Vector Machines (SVM) that can be used for mapping and monitoring the phenological cycle of bracken fern. Therefore, this study provided a foundation to advance knowledge on the role of remote sensing in understanding the phenological cycle of bracken fern and how the phenological data can be used in the effective management of bracken fern invasions in rangelands around the world.

7.2 Conclusions

The thesis aimed at estimating and monitoring the phenological cycle of bracken fern using remotely sensed data from Sentinel-2 satellite sensor. The findings reported in this study revealed that the freely available Sentinel-2 sensor with its 10m spatial resolution and high revisit time is a reliable data source that can effectively estimate and monitor the phenological cycle of bracken fern invasive species. The main conclusions were as follows;

a) Evidence from literature revealed that remote sensing is an invaluable tool that enables the generation of the phenological profiles of vegetation at local, regional and global scales, a mammoth task that was previously difficult to achieve using traditional ground based phenological observations. Although milestones have been achieved in developing vegetation indices that can be used for retrieving LSP metrics, the modelling of vegetation phenology remains a challenge as it is difficult to develop vegetation indices models that can be used effectively in all environments. Therefore, the choice of vegetation indices used depends on the type of environment as well as the objective of that application.

b) The Sentinel-2 based phenological metrics showed a good correlation with bracken fern ground observed phenological events, making remote sensing technology a potential tool for effective bracken fern management at various phenological stages. The EVI2 outperformed NDVI in retrieving phenological metrics that were comparable to bracken fern phenological developments.

c) The BSVM algorithm presents a cost-effective framework that efficiently quantifies the spatial distribution of bracken fern with limited field data without losing predictive accuracy. The data sets which combined spectral bands, vegetation indices and topographic variables yielded the highest accuracies in mapping bracken fern during green up phenological stage compared to all other datasets.

d) The optimized indices exhibited bracken fern growth patterns that were significantly correlated to the ground measured LAI throughout the fern's growth cycle. The $OTDVI_3$ and $OTDVI_4$ outperformed the traditional NDVI and TDVI indices in mapping bracken fern during its four growth stages. The optimized indices proved to be more sensitive to changes in vegetation than NDVI and TDVI, but less sensitive to the soil background.

e) The object-based classification approach (OB_GLCM) which combined Sentinel-2 spectral bands and bracken fern textural features outperformed the traditional pixel-based approach. The key topographic variables which mostly influence the spatial variability of bracken fern are elevation, TWI, valley depth and positive openness. Specifically, the green bracken patches were found in areas characterized by low elevation, high TWI, high valley depth and low positive openness.

7.3 Recommendations for the future

The findings of this study underscore the relevance of the freely available sensors such as Sentinel-2 in effectively monitoring and management of bracken fern in rangelands across various regions around the world. The effective management of rangelands infected by bracken fern relies in the ability of rangeland managers in understanding its phenological cycle, spatial and temporal distribution, in relation to the surrounding environment. In this regard, the following recommendations should be considered for future research:

- The validation of LSP metrics remains a challenge in many biomes covering the African continent. The current study suggests that international phenology research networks in collaboration with African governments should fund and facilitate the launching of standardized ground phenology networks that collect plant phenological data using UAVs.

- The availability of remotely sensed data and the algorithms that efficiently process the data play a critical role in the effective management of the environment at various special scales. Future research should probably invest more in deep learning to further develop robust software packages with the abundance of data processing tools and techniques that can be used to better characterize the phenological cycles of vegetation in rangelands.

- Findings reported in this study show that the current rangeland management plans assume a normal bracken phenological cycle, where all bracken fern patches reach a certain phenological stage uniformly. However, our results show that bracken fern patches do not reach the dormancy phenological stage at the same time. Future research studies can further investigate the spatial variability of bracken fern at another phenological stage which is not covered in this research. Additionally, it will be valuable if rangeland managers consider using bracken fern spatial distribution maps that consider the fern's spatial variability when formulating management plans. The

inclusion of phenology data in formulating invasive management plans promises to improve the efforts to control the sporadic encroachment of invasive species such as bracken fern.

- Although the TIMESAT algorithm performed well in extracting bracken fern phenology metrics at a local scale, there were challenges associated the compatibility of data types from TerrSet to TIMESAT. In some cases, the conversion of data types led to the alteration of pixel information. To solve some of these challenges, the current study recommends future research to focus on developing phenology specific packages in an all-in-one high-performance cloud-based environment such as Google Earth Engine (GEE).

- Vegetation indices have played a significant role in estimating and monitoring the phenology of vegetation for various applications. However, from the reviewed literature, most of the studies recycle the well-known traditional vegetation indices that are mostly calculated from the visible and near-infrared sections of the electromagnetic spectrum. To unpack the full potential of the utility of vegetation indices in phenology applications, the current study recommends the continuous development of spectral vegetation indices that suit various phenology scenarios.

References

ACHANTA, R. & SUSSTRUNK, S. Superpixels and polygons using simple non-iterative clustering. Proceedings of the IEEE Conference on Computer Vision and Pattern Recognition, 2017. 4651-4660.

ADJORLOLO, C., MUTANGA, O. & CHO, M. A. 2014. Estimation of canopy nitrogen concentration across C3 and C4 grasslands using WorldView-2 multispectral data. *IEEE Journal of Selected Topics in Applied Earth Observations and Remote Sensing,* 7**,** 4385-4392.

ADOLE, T., DASH, J. & ATKINSON, P. M. 2018. Characterising the land surface phenology of Africa using 500 m MODIS EVI. *Applied geography,* 90**,** 187-199.

AGHA, S. B., ALVAREZ, M., BECKER, M., FÈVRE, E. M., JUNGLEN, S. & BORGEMEISTER, C. 2021. Invasive Alien Plants in Africa and the Potential Emergence of Mosquito-Borne Arboviral Diseases—A Review and Research Outlook. *Viruses,* 13**,** 32.

AL-BUKHARI, A., HALLETT, S. & BREWER, T. 2018. A review of potential methods for monitoring rangeland degradation in Libya. *Pastoralism,* 8**,** 1-14.

ALBERTON, B., TORRES, R. D. S., CANCIAN, L. F., BORGES, B. D., ALMEIDA, J., MARIANO, G. C., DOS SANTOS, J. & MORELLATO, L. P. C. 2017. Introducing digital cameras to monitor plant phenology in the tropics: applications for conservation. *Perspectives in Ecology and Conservation,* 15**,** 82-90.

AMANI, M., BRISCO, B., MAHDAVI, S., GHORBANIAN, A., MOGHIMI, A., DELANCEY, E., MERCHANT, M. A., JAHNCKE, R., FEDORCHUK, L. & MUI, A. 2020a. Evaluation of the Landsat-based Canadian Wetland Inventory Map using Multiple Sources: Challenges of Large-scale Wetland Classification using Remote Sensing. *IEEE Journal of Selected Topics in Applied Earth Observations and Remote Sensing*.

AMANI, M., GHORBANIAN, A., AHMADI, S. A., KAKOOEI, M., MOGHIMI, A., MIRMAZLOUMI, S. M., MOGHADDAM, S. H. A., MAHDAVI, S., GHAHREMANLOO, M. & PARSIAN, S. 2020b. Google earth engine cloud computing platform for remote sensing big data applications: A comprehensive review. *IEEE Journal of Selected Topics in Applied Earth Observations and Remote Sensing,* 13**,** 5326-5350.

ANDREW, M. E. & USTIN, S. L. 2008. The role of environmental context in mapping invasive plants with hyperspectral image data. *Remote Sensing of Environment,* 112**,** 4301-4317.

ARAYA, S., OSTENDORF, B., LYLE, G. & LEWIS, M. 2018. CropPhenology: An R package for extracting crop phenology from time series remotely sensed vegetation index imagery. *Ecological informatics,* 46**,** 45-56.

ASMAL, O. E. 1995. *Land degradation in the Cathedral Peak area of the Natal Drakensburg: 1945 to 1992.* University of Cape Town.

ASSMANN, J. J., MYERS-SMITH, I. H., KERBY, J. T., CUNLIFFE, A. M. & DASKALOVA, G. N. 2020. Drone data reveal heterogeneity in tundra greenness and phenology not captured by satellites. *Environmental Research Letters,* 15**,** 125002.

AVDAN, U. & JOVANOVSKA, G. 2016. Algorithm for automated mapping of land surface temperature using LANDSAT 8 satellite data. *Journal of sensors,* 2016.

AWAD, M. & KHANNA, R. 2015. Support vector machines for classification. *Efficient learning machines.* Springer.

AYALA-IZURIETA, J. E., MÁRQUEZ, C. O., GARCÍA, V. J., RECALDE-MORENO, C. G., RODRÍGUEZ-LLERENA, M. V. & DAMIÁN-CARRIÓN, D. A. 2017. Land cover classification in an ecuadorian mountain geosystem using a random forest classifier, spectral vegetation indices, and ancillary geographic data. *Geosciences,* 7**,** 34.

AZEN, R. & BUDESCU, D. V. 2003. The dominance analysis approach for comparing predictors in multiple regression. *Psychological methods,* 8**,** 129.

BAKER, C. M. & BODE, M. 2016. Placing invasive species management in a spatiotemporal context. *Ecological Applications,* 26**,** 712-725.

120

BALDECK, C. A. & ASNER, G. P. 2014. Single-species detection with airborne imaging spectroscopy data: A comparison of support vector techniques. *IEEE Journal of Selected Topics in Applied Earth Observations and Remote Sensing,* 8**,** 2501-2512.

BALZAROLO, M., VICCA, S., NGUY-ROBERTSON, A., BONAL, D., ELBERS, J., FU, Y., GRÜNWALD, T., HOREMANS, J., PAPALE, D. & PEÑUELAS, J. 2016. Matching the phenology of Net Ecosystem Exchange and vegetation indices estimated with MODIS and FLUXNET in-situ observations. *Remote Sensing of Environment,* 174**,** 290-300.

BANNARI, A., ASALHI, H. & TEILLET, P. M. Transformed difference vegetation index (TDVI) for vegetation cover mapping. IEEE International geoscience and remote sensing symposium, 2002. IEEE, 3053-3055.

BARBOSA, J. M., ASNER, G. P., MARTIN, R. E., BALDECK, C. A., HUGHES, F. & JOHNSON, T. 2016. Determining subcanopy Psidium cattleianum invasion in Hawaiian forests using imaging spectroscopy. *Remote Sensing,* 8**,** 33.

BARTALEV, S. & BELWARD, A. Land cover and phenological monitoring in boreal ecosystems using the SPOT-VEGETATION instrument: new observations for climate studies. proceedings of the Use of Earth Observation data for phenological monitoring workshop held in Joint Research Centre, Ispra (VA) Italy 12th, 2002. Citeseer, 41-48.

BEAUBIEN, E. G. & HALL-BEYER, M. 2003. Plant phenology in western Canada: trends and links to the view from space. *Environmental Monitoring and Assessment,* 88**,** 419-429.

BELNAP, J., LUDWIG, J. A., WILCOX, B. P., BETANCOURT, J. L., DEAN, W. R. J., HOFFMANN, B. D. & MILTON, S. J. 2012. Introduced and invasive species in novel rangeland ecosystems: friends or foes? *Rangeland Ecology & Management,* 65**,** 569-578.

BERGET, C., DURAN, E. & BRAY, D. B. 2015. Participatory restoration of degraded agricultural areas invaded by bracken fern (Pteridium aquilinum) and conservation in the Chinantla Region, Oaxaca, Mexico. *Human ecology,* 43**,** 547-558.

BERMAN, E. E., GRAVES, T. A., MIKLE, N. L., MERKLE, J. A., JOHNSTON, A. N. & CHONG, G. W. 2020. Comparative Quality and Trend of Remotely Sensed Phenology and Productivity Metrics across the Western United States. *Remote Sensing,* 12**,** 2538.

BERRA, E. F. & GAULTON, R. 2021. Remote sensing of temperate and boreal forest phenology: A review of progress, challenges and opportunities in the intercomparison of in-situ and satellite phenological metrics. *Forest Ecology and Management,* 480**,** 118663.

BERRA, E. F., GAULTON, R. & BARR, S. Use of a digital camera onboard a UAV to monitor spring phenology at individual tree level. 2016 IEEE International Geoscience and Remote Sensing Symposium (IGARSS), 2016. IEEE, 3496-3499.

BIRHANIE, M., ZEGEYE, W., ASAYE, G. & ANDUALEM, M. 2020. Abundance and Geographical Distribution of Invasive Weed Species in the Western Amhara Region, Ethiopia. *Abyssinia Journal of Science and Technology,* 5**,** 18-25.

BIRHANU, L., BEKELE, T., TESFAW, B. & DEMISSEW, S. 2021. Relationships between topographic factors, soil and plant communities in a dry Afromontane forest patches of Northwestern Ethiopia. *PloS one,* 16**,** e0247966.

BIRKY, A. K. 2001. NDVI and a simple model of deciduous forest seasonal dynamics. *Ecological Modelling,* 143**,** 43-58.

BIRNIE, R. & MILLER, D. 1985. *The bracken problem in Scotland: a new assessment using remotely sensed data*, Parthenon.

BIRTH, G. S. & MCVEY, G. R. 1968. Measuring the color of growing turf with a reflectance spectrophotometer 1. *Agronomy Journal,* 60**,** 640-643.

BOLMGREN, K. & LÖNNBERG, K. 2005. Herbarium data reveal an association between fleshy fruit type and earlier flowering time. *International Journal of Plant Sciences,* 166**,** 663-670.

BOLTON, D. K., GRAY, J. M., MELAAS, E. K., MOON, M., EKLUNDH, L. & FRIEDL, M. A. 2020. Continental-scale land surface phenology from harmonized Landsat 8 and Sentinel-2 imagery. *Remote Sensing of Environment,* 240**,** 111685.

BORCHERT, R. 1980. Phenology and ecophysiology of tropical trees: Erythrina poeppigiana OF Cook. *Ecology,* 61**,** 1065-1074.

BORNEZ, K., DESCALS, A., VERGER, A. & PEÑUELAS, J. 2020. Land surface phenology from VEGETATION and PROBA-V data. Assessment over deciduous forests. *International Journal of Applied Earth Observation and Geoinformation,* 84**,** 101974.

BÓRNEZ, K., VERGER, A., FILELLA, I. & PENUELAS, J. Land surface phenology from Copernicus Global Land time series. 2017 9th International Workshop on the Analysis of Multitemporal Remote Sensing Images (MultiTemp), 2017. IEEE, 1-4.

BOSCHETTI, M., STROPPIANA, D., BRIVIO, P. & BOCCHI, S. 2009. Multi-year monitoring of rice crop phenology through time series analysis of MODIS images. *International journal of remote sensing,* 30**,** 4643-4662.

BOYD, D. S., ALMOND, S., DASH, J., CURRAN, P. J. & HILL, R. A. 2011. Phenology of vegetation in Southern England from Envisat MERIS terrestrial chlorophyll index (MTCI) data. *International Journal of Remote Sensing,* 32**,** 8421-8447.

BRADLEY, B. A. & MUSTARD, J. F. 2006. Characterizing the landscape dynamics of an invasive plant and risk of invasion using remote sensing. *Ecological Applications,* 16**,** 1132-1147.

BROWNING, D., LALIBERTE, A., RANGO, A. & HERRICK, J. Prospects for phenological monitoring in an arid southwestern US rangeland using field observations with hyperspatial and moderate resolution imagery. AGU Fall Meeting Abstracts, 2009. B43C-0392.

BROWNING, D. M., KARL, J. W., MORIN, D., RICHARDSON, A. D. & TWEEDIE, C. E. 2017. Phenocams bridge the gap between field and satellite observations in an arid grassland ecosystem. *Remote Sensing,* 9**,** 1071.

BROWNING, D. M., SNYDER, K. A. & HERRICK, J. E. 2019. Plant phenology: taking the pulse of rangelands. *Rangelands,* 41**,** 129-134.

BUSETTO, L., MERONI, M. & COLOMBO, R. 2008. Combining medium and coarse spatial resolution satellite data to improve the estimation of sub-pixel NDVI time series. *Remote Sensing of Environment,* 112**,** 118-131.

CAI, Z., JÖNSSON, P., JIN, H. & EKLUNDH, L. 2017. Performance of smoothing methods for reconstructing NDVI time-series and estimating vegetation phenology from MODIS data. *Remote Sensing,* 9**,** 1271.

CAO, R., CHEN, J., SHEN, M. & TANG, Y. 2015. An improved logistic method for detecting spring vegetation phenology in grasslands from MODIS EVI time-series data. *Agricultural and Forest Meteorology,* 200**,** 9-20.

CAPARROS-SANTIAGO, J. A., RODRIGUEZ-GALIANO, V. & DASH, J. 2021. Land surface phenology as indicator of global terrestrial ecosystem dynamics: A systematic review. *ISPRS Journal of Photogrammetry and Remote Sensing,* 171**,** 330-347.

CATUNEANU, O., WOPFNER, H., ERIKSSON, P., CAIRNCROSS, B., RUBIDGE, B., SMITH, R. & HANCOX, P. 2005. The Karoo basins of south-central Africa. *Journal of African Earth Sciences,* 43**,** 211-253.

CHAN, J. C.-W. & PAELINCKX, D. 2008. Evaluation of Random Forest and Adaboost tree-based ensemble classification and spectral band selection for ecotope mapping using airborne hyperspectral imagery. *Remote Sensing of Environment,* 112**,** 2999-3011.

CHANDRASHEKAR, G. & SAHIN, F. 2014. A survey on feature selection methods. *Computers & Electrical Engineering,* 40**,** 16-28.

CHATURVEDI, R. & RAGHUBANSHI, A. 2018. Effect of soil moisture on composition and diversity of trees in tropical dry forest. *MOJ Ecology and Environmental Sciences,* 3**,** 0059.

CHEMURA, A. & MUTANGA, O. 2017. Developing detailed age-specific thematic maps for coffee (Coffea arabica L.) in heterogeneous agricultural landscapes using random forests applied on Landsat 8 multispectral sensor. *Geocarto International,* 32**,** 759-776.

CHEN, C.-F., HUANG, S.-W., SON, N.-T. & CHANG, L.-Y. 2011. Mapping double-cropped irrigated rice fields in Taiwan using time-series Satellite Pour I'Observation de la Terre data. *Journal of Applied Remote Sensing,* 5**,** 053528.

CHEN, J. M., PAVLIC, G., BROWN, L., CIHLAR, J., LEBLANC, S., WHITE, H., HALL, R., PEDDLE, D., KING, D. & TROFYMOW, J. 2002. Derivation and validation of Canada-wide coarse-resolution leaf area index maps using high-resolution satellite imagery and ground measurements. *Remote sensing of environment,* 80**,** 165-184.

CHEN, X., WANG, D., CHEN, J., WANG, C. & SHEN, M. 2018. The mixed pixel effect in land surface phenology: A simulation study. *Remote Sensing of Environment,* 211**,** 338-344.

CHENG, Y., VRIELING, A., FAVA, F., MERONI, M., MARSHALL, M. & GACHOKI, S. 2020. Phenology of short vegetation cycles in a Kenyan rangeland from PlanetScope and Sentinel-2. *Remote sensing of environment,* 248**,** 112004.

CHMIELEWSKI, F.-M. & RÖTZER, T. 2001. Response of tree phenology to climate change across Europe. *Agricultural and Forest Meteorology,* 108**,** 101-112.

CHO, M. A., RAMOELO, A. & DZIBA, L. 2017. Response of land surface phenology to variation in tree cover during green-up and senescence periods in the semi-arid savanna of Southern Africa. *Remote Sensing,* 9**,** 689.

CHOI, C.-H. & JUNG, S.-G. 2014. Analysis of the MODIS-based vegetation phenology using the HANTS algorithm. *Journal of the Korean Association of Geographic Information Studies,* 17**,** 20-38.

CHURKINA, G., SCHIMEL, D., BRASWELL, B. H. & XIAO, X. 2005. Spatial analysis of growing season length control over net ecosystem exchange. *Global Change Biology,* 11**,** 1777-1787.

CLAUSON-KAAS, F., RAMWELL, C., HANSEN, H. C. B. & STROBEL, B. W. 2016. Ptaquiloside from bracken in stream water at base flow and during storm events. *Water research,* 106**,** 155-162.

CLELAND, E. E., CHUINE, I., MENZEL, A., MOONEY, H. A. & SCHWARTZ, M. D. 2007. Shifting plant phenology in response to global change. *Trends in ecology & evolution,* 22**,** 357-365.

CLINTON, N. E., POTTER, C., CRABTREE, B., GENOVESE, V., GROSS, P. & GONG, P. 2010. Remote Sensing–Based Time-Series Analysis of Cheatgrass (Bromus tectorum L.) Phenology. *Journal of Environmental Quality,* 39**,** 955-963.

CONWAY, E. 1957. Spore production in bracken (Pteridium aquilinum (L.) Kuhn). *The Journal of Ecology***,** 273-284.

COOPS, N. C., HILKER, T., BATER, C. W., WULDER, M. A., NIELSEN, S. E., MCDERMID, G. & STENHOUSE, G. 2012. Linking ground-based to satellite-derived phenological metrics in support of habitat assessment. *Remote Sensing Letters,* 3**,** 191-200.

COPPOCK, D. L., FERNÁNDEZ-GIMÉNEZ, M., HIERNAUX, P., HUBER-SANNWALD, E., SCHLOEDER, C., VALDIVIA, C., ARREDONDO, J. T., JACOBS, M., TURIN, C. & TURNER, M. 2017. Rangeland systems in developing nations: conceptual advances and societal implications. *Rangeland systems***,** 569.

COURTOIS, P., FIGUIERES, C., MULIER, C. & WEILL, J. 2018. A cost–benefit approach for prioritizing invasive species. *Ecological Economics,* 146**,** 607-620.

CUI, Z. & KEREKES, J. P. 2018. Potential of red edge spectral bands in future landsat satellites on agroecosystem canopy green leaf area index retrieval. *Remote Sensing,* 10**,** 1458.

CURRAN, P. J., DUNGAN, J. L. & GHOLZ, H. L. 1990. Exploring the relationship between reflectance red edge and chlorophyll content in slash pine. *Tree physiology,* 7**,** 33-48.

D'ALLESTRO, P. & PARENTE, C. 2015. GIS application for NDVI calculation using Landsat 8 OLI images. *International Journal of Applied Engineering Research,* 10**,** 42099-42102.

D'ODORICO, P., GONSAMO, A., GOUGH, C. M., BOHRER, G., MORISON, J., WILKINSON, M., HANSON, P. J., GIANELLE, D., FUENTES, J. D. & BUCHMANN, N. 2015. The match and mismatch between photosynthesis and land surface phenology of deciduous forests. *Agricultural and Forest Meteorology,* 214**,** 25-38.

DAI, J., ROBERTS, D. A., STOW, D. A., AN, L., HALL, S. J., YABIKU, S. T. & KYRIAKIDIS, P. C. 2020. Mapping understory invasive plant species with field and remotely sensed data in Chitwan, Nepal. *Remote Sensing of Environment,* 250**,** 112037.

DAMBREVILLE, A., LAURI, P.-E., NORMAND, F. & GUÉDON, Y. 2015. Analysing growth and development of plants jointly using developmental growth stages. *Annals of Botany,* 115**,** 93-105.

DANNENBERG, M., WANG, X., YAN, D. & SMITH, W. 2020. Phenological characteristics of global ecosystems based on optical, fluorescence, and microwave remote sensing. *Remote Sensing,* 12**,** 671.

DASH, J. & CURRAN, P. 2004a. The MERIS terrestrial chlorophyll index.

DASH, J. & CURRAN, P. J. Evaluation of the MERIS terrestrial chlorophyll index. IGARSS 2004. 2004 IEEE International Geoscience and Remote Sensing Symposium, 2004b. IEEE.

DAVI, H., SOUDANI, K., DECKX, T., DUFRENE, E., LE DANTEC, V. & FRANCOIS, C. 2006. Estimation of forest leaf area index from SPOT imagery using NDVI distribution over forest stands. *International Journal of Remote Sensing,* 27**,** 885-902.

DAVID, O. A., AKOMOLAFE, G. F., ONWUSIRI, K. C. & FABOLUDE, G. O. 2021. Predicting the distribution of the invasive species Hyptis suaveolens in Nigeria. *European Journal of Environmental Sciences,* 10**,** 98-106.

DAVIS, C., HOFFMAN, M. & ROBERTS, W. 2017. Long-term trends in vegetation phenology and productivity over Namaqualand using the GIMMS AVHRR NDVI3g data from 1982 to 2011. *South African Journal of Botany,* 111**,** 76-85.

DAVIS, C. C., WILLIS, C. G., CONNOLLY, B., KELLY, C. & ELLISON, A. M. 2015. Herbarium records are reliable sources of phenological change driven by climate and provide novel insights into species' phenological cueing mechanisms. *American Journal of Botany,* 102**,** 1599-1609.

DAWSON, T. P., JACKSON, S. T., HOUSE, J. I., PRENTICE, I. C. & MACE, G. M. 2011. Beyond predictions: biodiversity conservation in a changing climate. *science,* 332**,** 53-58.

DE BEURS, K. M. & HENEBRY, G. M. 2010. Spatio-temporal statistical methods for modelling land surface phenology. *Phenological research***,** 177-208.

DE WIT, A. & SU, B. Deriving phenological indicators from SPOT-VGT data using the HANTS algorithm. 2nd international SPOT-VEGETATION user conference, 2005. Antwerp Belgium, 195-201.

DELBART, N., BEAUBIEN, E., KERGOAT, L. & LE TOAN, T. 2015. Comparing land surface phenology with leafing and flowering observations from the PlantWatch citizen network. *Remote Sensing of Environment,* 160**,** 273-280.

DELBART, N., KERGOAT, L., LE TOAN, T., LHERMITTE, J. & PICARD, G. 2005. Determination of phenological dates in boreal regions using normalized difference water index. *Remote Sensing of Environment,* 97**,** 26-38.

DEN OUDEN, J. 2000. *The role of bracken (Pteridium aquilinum) in forest dynamics=[De rol van adelaarsvaren (Pteridium aquilinum) in de bosdynamiek]*.

DENG, X., LI, W., LIU, X., GUO, Q. & NEWSAM, S. 2018. One-class remote sensing classification: one-class vs. binary classifiers. *International Journal of Remote Sensing,* 39**,** 1890-1910.

DESCALS, A., VERGER, A., YIN, G. & PEÑUELAS, J. 2020. Improved estimates of arctic land surface phenology using Sentinel-2 time series. *Remote Sensing,* 12**,** 3738.

DEW, L. A., ROZEN-RECHELS, D., LE ROUX, E., CROMSIGT, J. & TE BEEST, M. 2017. Evaluating the efficacy of invasive plant control in response to ecological factors. *South African Journal of Botany,* 109**,** 203-213.

DING, C., LIU, X. & HUANG, F. 2017. Temporal interpolation of satellite-derived leaf area index time series by introducing spatial-temporal constraints for heterogeneous grasslands. *Remote Sensing,* 9**,** 968.

DOLLING, A. 1999. The vegetative spread of Pteridium aquilinum in a hemiboreal forest–invasion or revegetation? *Forest Ecology and Management,* 124**,** 177-184.

DONLON, C., BERRUTI, B., BUONGIORNO, A., FERREIRA, M.-H., FÉMÉNIAS, P., FRERICK, J., GORYL, P., KLEIN, U., LAUR, H. & MAVROCORDATOS, C. 2012. The global monitoring for environment and security (GMES) sentinel-3 mission. *Remote Sensing of Environment,* 120**,** 37-57.

DORIGO, W. A., ZURITA-MILLA, R., DE WIT, A. J., BRAZILE, J., SINGH, R. & SCHAEPMAN, M. E. 2007. A review on reflective remote sensing and data assimilation techniques for enhanced agroecosystem modeling. *International journal of applied earth observation and geoinformation,* 9**,** 165-193.

DOUTERLUNGNE, D., LEVY-TACHER, S. I., GOLICHER, D. J. & DAÑOBEYTIA, F. R. 2010. Applying indigenous knowledge to the restoration of degraded tropical rain forest clearings dominated by bracken fern. *Restoration Ecology,* 18**,** 322-329.

DRAGONI, D. & RAHMAN, A. F. 2012. Trends in fall phenology across the deciduous forests of the Eastern USA. *Agricultural and Forest Meteorology,* 157**,** 96-105.

DUARTE, L., TEODORO, A. C., MONTEIRO, A. T., CUNHA, M. & GONÇALVES, H. 2018. QPhenoMetrics: An open source software application to assess vegetation phenology metrics. *Computers and Electronics in Agriculture,* 148**,** 82-94.

DUBE, T., SHOKO, C., SIBANDA, M., MADILENG, P., MALULEKE, X. G., MOKWATEDI, V. R., TIBANE, L. & TSHEBESEBE, T. 2020. Remote sensing of invasive lantana camara (verbenaceae) in semiarid savanna rangeland ecosystems of south africa. *Rangeland Ecology & Management,* 73**,** 411-419.

DUBUIS, A., GIOVANETTINA, S., PELLISSIER, L., POTTIER, J., VITTOZ, P. & GUISAN, A. 2013. Improving the prediction of plant species distribution and community composition by adding edaphic to topo-climatic variables. *Journal of Vegetation Science,* 24**,** 593-606.

DUCHEMIN, B., HADRIA, R., ERRAKI, S., BOULET, G., MAISONGRANDE, P., CHEHBOUNI, A., ESCADAFAL, R., EZZAHAR, J., HOEDJES, J. & KHARROU, M. 2006. Monitoring wheat phenology and irrigation in Central Morocco: On the use of relationships between evapotranspiration, crops coefficients, leaf area index and remotely-sensed vegetation indices. *Agricultural Water Management,* 79**,** 1-27.

DUNN, A. H. & DE BEURS, K. M. 2011. Land surface phenology of North American mountain environments using moderate resolution imaging spectroradiometer data. *Remote Sensing of Environment,* 115**,** 1220-1233.

EASTMAN, J. A. 2003. *The book of field and roadside: open-country weeds, trees, and wildflowers of eastern North America*, Stackpole Books.

EKLUNDH, L. & JÖNSSON, P. 2012. TIMESAT 3.1 software manual. *Lund University, Sweden***,** 1-82.

EKLUNDH, L. & JÖNSSON, P. 2015. TIMESAT: A software package for time-series processing and assessment of vegetation dynamics. *Remote sensing time series.* Springer.

EKLUNDHA, L. & JÖNSSON, P. 2017. TIMESAT 3.3 with seasonal trend decomposition and parallel processing Software Manual. Lund University.

ESTRELLA, N., SPARKS, T. H. & MENZEL, A. 2007. Trends and temperature response in the phenology of crops in Germany. *Global Change Biology,* 13**,** 1737-1747.

EYIBIO OLAIFA, F. 2018. Response of Clarias gariepinus juveniles to varying concentrations of copper in water containing Pteridium aquilinium (Bracken Fern) and Poultry manure. *International Journal of Aquatic Science,* 9**,** 99-105.

FACCIN, T. C., CARGNELUTTI, J. F., DE SOUZA RODRIGUES, F., DE MENEZES, F. R., PIAZER, J. V. M., DE MELO, S. M. P., LAUTERT, B. F., FLORES, E. F. & KOMMERS, G. D. 2018. Bovine upper alimentary squamous cell carcinoma associated with bracken fern poisoning: Clinical-pathological aspects and etiopathogenesis of 100 cases. *PloS one,* 13**,** e0204656.

FADÓN, E., HERRERO, M. & RODRIGO, J. 2015. Flower development in sweet cherry framed in the BBCH scale. *Scientia Horticulturae,* 192**,** 141-147.

FAN, L.-Y., GAO, Y.-Z., BRÜCK, H. & BERNHOFER, C. 2009. Investigating the relationship between NDVI and LAI in semi-arid grassland in Inner Mongolia using in-situ measurements. *Theoretical and applied climatology,* 95**,** 151-156.

FASSNACHT, K. S., GOWER, S. T., NORMAN, J. M. & MCMURTRIC, R. E. 1994. A comparison of optical and direct methods for estimating foliage surface area index in forests. *Agricultural and Forest Meteorology,* 71**,** 183-207.

FAUZAN, M. A., KUMARA, I. S., YOGYANTORO, R., SUWARDANA, S., FADHILAH, N., NURMALASARI, I., APRIYANI, S. & WICAKSONO, P. 2017. Assessing the capability of Sentinel-2A data for mapping seagrass percent cover in Jerowaru, East Lombok. *The Indonesian Journal of Geography,* 49**,** 195-203.

FENSHOLT, R. & SANDHOLT, I. 2003. Derivation of a shortwave infrared water stress index from MODIS near-and shortwave infrared data in a semiarid environment. *Remote Sensing of Environment,* 87**,** 111-121.

FERNANDES, M. R., AGUIAR, F. C., FERREIRA, M. T. & PEREIRA, J. M. C. 2013. Spectral separability of riparian forests from small and medium-sized rivers across a latitudinal gradient using multispectral imagery. *International journal of remote sensing,* 34**,** 2375-2401.

FERNÁNDEZ-MANSO, A., FERNÁNDEZ-MANSO, O. & QUINTANO, C. 2016. SENTINEL-2A red-edge spectral indices suitability for discriminating burn severity. *International journal of applied earth observation and geoinformation,* 50**,** 170-175.

FINCH, J. M., HILL, T. R., MEADOWS, M. E., LODDER, J. & BODMANN, L. 2021. Fire and montane vegetation dynamics through successive phases of human occupation in the northern Drakensberg, South Africa. *Quaternary International*.

FISHER, J. I. & MUSTARD, J. F. 2007. Cross-scalar satellite phenology from ground, Landsat, and MODIS data. *Remote Sensing of Environment,* 109**,** 261-273.

FISHER, J. I., MUSTARD, J. F. & VADEBONCOEUR, M. A. 2006. Green leaf phenology at Landsat resolution: Scaling from the field to the satellite. *Remote sensing of environment,* 100**,** 265-279.

FLETCHER, D., GILLINGHAM, P., BRITTON, J., BLANCHET, S. & GOZLAN, R. E. 2016. Predicting global invasion risks: a management tool to prevent future introductions. *Scientific reports,* 6**,** 1-8.

FONTANA, F., RIXEN, C., JONAS, T., ABEREGG, G. & WUNDERLE, S. 2008. Alpine grassland phenology as seen in AVHRR, VEGETATION, and MODIS NDVI time series-a comparison with in situ measurements. *Sensors,* 8**,** 2833-2853.

FOODY, G. M. 2002. Status of land cover classification accuracy assessment. *Remote sensing of environment,* 80**,** 185-201.

FOODY, G. M., MATHUR, A., SANCHEZ-HERNANDEZ, C. & BOYD, D. S. 2006. Training set size requirements for the classification of a specific class. *Remote Sensing of Environment,* 104**,** 1-14.

FOURNIER, A., PENONE, C., PENNINO, M. G. & COURCHAMP, F. 2019. Predicting future invaders and future invasions. *Proceedings of the National Academy of Sciences,* 116**,** 7905-7910.

FRANCESCO, B., GIORGIO, B., ROSARIO, N., SAVERIO, R. F., ROMANO, M., ADRIANO, S., CINZIA, R., ANTONIO, T., FRANCO, R. & VALERIA, R. 2011. A new, very sensitive method of assessment of ptaquiloside, the major bracken carcinogen in the milk of farm animals. *Food chemistry,* 124**,** 660-665.

FRANKIE, G. W., BAKER, H. G. & OPLER, P. A. 1974. Comparative phenological studies of trees in tropical wet and dry forests in the lowlands of Costa Rica. *The Journal of Ecology***,** 881-919.

FU, W., MA, J., CHEN, P. & CHEN, F. 2020. Remote sensing satellites for digital earth. *Manual of digital earth.* Springer, Singapore.

GAO, B.-C. 1996. NDWI—A normalized difference water index for remote sensing of vegetation liquid water from space. *Remote sensing of environment,* 58**,** 257-266.

GAO, F., MORISETTE, J. T., WOLFE, R. E., EDERER, G., PEDELTY, J., MASUOKA, E., MYNENI, R., TAN, B. & NIGHTINGALE, J. 2008. An algorithm to produce temporally and spatially continuous MODIS-LAI time series. *IEEE Geoscience and Remote Sensing Letters,* 5**,** 60-64.

GARCÍA-DÍAZ, P., ANDERSON, D. P. & LURGI, M. 2019. Evaluating the effects of landscape structure on the recovery of an invasive vertebrate after population control. *Landscape ecology,* 34**,** 615-626.

GARCÍA-JORGENSEN, D. B., DIAMANTOPOULOS, E., KISIELIUS, V., ROSENFJELD, M., RASMUSSEN, L. H., STROBEL, B. W. & HANSEN, H. C. B. 2021. Bracken growth, toxin production and transfer from plant to soil: a 2-year monitoring study. *Environmental Sciences Europe,* 33**,** 1-14.

GAŠPAROVIĆ, M., MEDAK, D., PILAŠ, I., JURJEVIĆ, L. & BALENOVIĆ, I. Fusion of Sentinel-2 and PlanetScope Imagery for Vegetation Detection and Monitorin. Volumes ISPRS TC I Mid-term Symposium Innovative Sensing-From Sensors to Methods and Applications, 2018.

GATTI, A. & BERTOLINI, A. 2013. Sentinel-2 products specification document. *Available online (accessed February 23, 2015)* https://earth*. esa. int/documents/247904/685211/Sentinel-2+ Products+ Specification+ Document*.

GAVIER-PIZARRO, G. I., KUEMMERLE, T., HOYOS, L. E., STEWART, S. I., HUEBNER, C. D., KEULER, N. S. & RADELOFF, V. C. 2012. Monitoring the invasion of an exotic tree (Ligustrum lucidum) from 1983 to 2006 with Landsat TM/ETM+ satellite data and Support Vector Machines in Córdoba, Argentina. *Remote Sensing of Environment,* 122**,** 134-145.

GE, J. & LIU, H. Investigation of image classification using hog, glcm features, and svm classifier. International Conference on Man-Machine-Environment System Engineering, 2020. Springer, 411-417.

GHARARI, R., KAZEMINEJAD, H., KOJOURI, N. M. & HEDAYAT, A. 2018. A review on hydrogen generation, explosion, and mitigation during severe accidents in light water nuclear reactors. *International Journal of Hydrogen Energy,* 43**,** 1939-1965.

GILL, A. M. & CATLING, P. C. 2002. Fire regimes and biodiversity of forested landscapes of southern Australia. *Flammable Australia: the fire regimes and biodiversity of a continent***,** 35-372.

GILLANDERS, S. N., COOPS, N. C., WULDER, M. A., GERGEL, S. E. & NELSON, T. 2008. Multitemporal remote sensing of landscape dynamics and pattern change: describing natural and anthropogenic trends. *Progress in physical geography,* 32**,** 503-528.

GITELSON, A. A. 2004. Wide dynamic range vegetation index for remote quantification of biophysical characteristics of vegetation. *Journal of plant physiology,* 161**,** 165-173.

GONG, Z., KAWAMURA, K., ISHIKAWA, N., GOTO, M., WULAN, T., ALATENG, D., YIN, T. & ITO, Y. 2015. MODIS normalized difference vegetation index (NDVI) and vegetation phenology dynamics in the Inner Mongolia grassland. *Solid Earth,* 6**,** 1185-1194.

GONSAMO, A., CHEN, J. M., PRICE, D. T., KURZ, W. A. & WU, C. 2012a. Land surface phenology from optical satellite measurement and CO2 eddy covariance technique. *Journal of Geophysical Research: Biogeosciences,* 117.

GONSAMO, A., CHEN, J. M. & WU, C. 2013. Citizen Science: linking the recent rapid advances of plant flowering in Canada with climate variability. *Scientific reports,* 3**,** 2239.

GONSAMO, A., CHEN, J. M., WU, C. & DRAGONI, D. 2012b. Predicting deciduous forest carbon uptake phenology by upscaling FLUXNET measurements using remote sensing data. *Agricultural and forest meteorology,* 165**,** 127-135.

GONZALEZ-DUGO, M., NEALE, C., MATEOS, L., KUSTAS, W., PRUEGER, J., ANDERSON, M. & LI, F. 2009. A comparison of operational remote sensing-based models for estimating crop evapotranspiration. *Agricultural and Forest Meteorology,* 149**,** 1843-1853.

GOPAL, S. & WOODCOCK, C. 1996. Remote sensing of forest change using artificial neural networks. *IEEE Transactions on Geoscience and Remote Sensing,* 34**,** 398-404.

GOUGHERTY, A. V. & GOUGHERTY, S. W. 2018. Sequence of flower and leaf emergence in deciduous trees is linked to ecological traits, phylogenetics, and climate. *New Phytologist,* 220**,** 121-131.

GOWARD, S. N., MARKHAM, B., DYE, D. G., DULANEY, W. & YANG, J. 1991. Normalized difference vegetation index measurements from the Advanced Very High Resolution Radiometer. *Remote sensing of environment,* 35**,** 257-277.

GRANADOS, J. A., GRAHAM, E. A., BONNET, P., YUEN, E. M. & HAMILTON, M. 2013. EcoIP: An open source image analysis toolkit to identify different stages of plant phenology for multiple species with pan–tilt–zoom cameras. *Ecological informatics,* 15**,** 58-65.

GRZYL, A., KIEDRZYŃSKI, M., ZIELIŃSKA, K. M. & REWICZ, A. 2014. The relationship between climatic conditions and generative reproduction of a lowland population of Pulsatilla vernalis: the last breath of a relict plant or a fluctuating cycle of regeneration? *Plant ecology,* 215**,** 457-466.

GUYON, D., GUILLOT, M., VITASSE, Y., CARDOT, H., HAGOLLE, O., DELZON, S. & WIGNERON, J.-P. 2011. Monitoring elevation variations in leaf phenology of deciduous broadleaf forests from SPOT/VEGETATION time-series. *Remote Sensing of Environment,* 115**,** 615-627.

HAGHVERDI, A., WASHINGTON-ALLEN, R. A. & LEIB, B. G. 2018. Prediction of cotton lint yield from phenology of crop indices using artificial neural networks. *Computers and Electronics in Agriculture,* 152**,** 186-197.

HALL-BEYER, M. 2017. Practical guidelines for choosing GLCM textures to use in landscape classification tasks over a range of moderate spatial scales. *International Journal of Remote Sensing,* 38**,** 1312-1338.

HAMER, U., POTTHAST, K., BURNEO, J. I. & MAKESCHIN, F. 2013. Nutrient stocks and phosphorus fractions in mountain soils of Southern Ecuador after conversion of forest to pasture. *Biogeochemistry,* 112**,** 495-510.

HAQUE, M. I. & BASAK, R. 2017. Land cover change detection using GIS and remote sensing techniques: A spatio-temporal study on Tanguar Haor, Sunamganj, Bangladesh. *The Egyptian Journal of Remote Sensing and Space Science,* 20**,** 251-263.

HARALICK, R. M., HLAVKA, C. A., YOKOYAMA, R. & CARLYLE, S. 1980. Spectral-temporal classification using vegetation phenology. *IEEE Transactions on Geoscience and Remote Sensing***,** 167-174.

HAY, G. & CASTILLA, G. Object-based image analysis: strengths, weaknesses, opportunities and threats (SWOT). Proc. 1st Int. Conf. OBIA, 2006. 4-5.

HELMAN, D. 2018. Land surface phenology: What do we really 'see' from space? *Science of the Total Environment,* 618**,** 665-673.

HENNESSY, A., CLARKE, K. & LEWIS, M. 2020. Hyperspectral classification of plants: a review of waveband selection generalisability. *Remote Sensing,* 12**,** 113.

HENZI, S., BYRNE, R. & WHITEN, A. 1992. Patterns of movement by baboons in the Drakensberg mountains: primary responses to the environment. *International Journal of Primatology,* 13**,** 601-629.

HIRD, J. N. & MCDERMID, G. J. 2009. Noise reduction of NDVI time series: An empirical comparison of selected techniques. *Remote Sensing of Environment,* 113**,** 248-258.

HMIMINA, G., DUFRÊNE, E., PONTAILLER, J.-Y., DELPIERRE, N., AUBINET, M., CAQUET, B., DE GRANDCOURT, A., BURBAN, B., FLECHARD, C. & GRANIER, A. 2013. Evaluation of the potential of MODIS satellite data to predict vegetation phenology in different biomes: An investigation using ground-based NDVI measurements. *Remote Sensing of Environment,* 132**,** 145-158.

HOFER, G., WAGNER, H. H., HERZOG, F. & EDWARDS, P. J. 2008. Effects of topographic variability on the scaling of plant species richness in gradient dominated landscapes. *Ecography,* 31**,** 131-139.

HOLLAND, J. & APLIN, P. 2013. Super-resolution image analysis as a means of monitoring bracken (Pteridium aquilinum) distributions. *ISPRS Journal of Photogrammetry and Remote sensing,* 75**,** 48-63.

HUETE, A. 1988a. A Soil-Adjusted Vegetation Index (SAVI). Remote Ssensing of Environment, 25, 295-309.

HUETE, A., DIDAN, K., MIURA, T., RODRIGUEZ, E. P., GAO, X. & FERREIRA, L. G. 2002. Overview of the radiometric and biophysical performance of the MODIS vegetation indices. *Remote sensing of environment,* 83**,** 195-213.

HUETE, A., LIU, H., BATCHILY, K. & VAN LEEUWEN, W. 1997. A comparison of vegetation indices over a global set of TM images for EOS-MODIS. *Remote sensing of environment,* 59**,** 440-451.

HUETE, A. R. 1988b. A soil-adjusted vegetation index (SAVI). *Remote sensing of environment,* 25**,** 295-309.

HUNT JR, E. R. & ROCK, B. N. 1989. Detection of changes in leaf water content using near-and middle-infrared reflectances. *Remote sensing of environment,* 30**,** 43-54.

IMMITZER, M., VUOLO, F. & ATZBERGER, C. 2016. First experience with Sentinel-2 data for crop and tree species classifications in central Europe. *Remote Sensing,* 8**,** 166.

IQBAL, I. M., BALZTER, H. & SHABBIR, A. 2021a. Identifying the Spectral Signatures of Invasive and Native Plant Species in Two Protected Areas of Pakistan through Field Spectroscopy. *Remote Sensing,* 13**,** 4009.

IQBAL, N., MUMTAZ, R., SHAFI, U. & ZAIDI, S. M. H. 2021b. Gray level co-occurrence matrix (GLCM) texture based crop classification using low altitude remote sensing platforms. *PeerJ Computer Science,* 7**,** e536.

IRWIN, D. & IRWIN, P. 1992. A field guide to the Natal Drakensberg. Rev. Grahamstown: Rhodes University (335p.)-illus., col. illus.. ISBN.

JAIN, P. & KAR, P. 2017. Non-convex optimization for machine learning. *arXiv preprint arXiv:1712.07897*.

JAYAWARDHANA, W. & CHATHURANGE, V. 2016. Extraction of agricultural phenological parameters of Sri Lanka using MODIS, NDVI time series data. *Procedia Food Science,* 6**,** 235-241.

JAZWA, M., JEDRZEJCZAK, E., KLICHOWSKA, E. & PLISZKO, A. 2018. Predicting the potential distribution area of Solidago xniederederi (Asteraceae). *Turkish Journal of Botany,* 42**,** 51-56.

JEGANATHAN, C., GANGULY, S., DASH, J., FRIEDL, M. & ATKINSON, P. M. Terrestrial vegetation phenology from MODIS and MERIS. 2010 IEEE International Geoscience and Remote Sensing Symposium, 2010. IEEE, 2699-2702.

JENKINS, R. B. & FRAZIER, P. S. 2010. High-resolution remote sensing of upland swamp boundaries and vegetation for baseline mapping and monitoring. *Wetlands,* 30**,** 531-540.

JIANG, H., WANG, S., CAO, X., YANG, C., ZHANG, Z. & WANG, X. 2019. A shadow-eliminated vegetation index (SEVI) for removal of self and cast shadow effects on vegetation in rugged terrains. *International Journal of Digital Earth,* 12**,** 1013-1029.

JIANG, Z., HUETE, A. R., DIDAN, K. & MIURA, T. 2008. Development of a two-band enhanced vegetation index without a blue band. *Remote sensing of Environment,* 112**,** 3833-3845.

JIANG, Z., HUETE, A. R., KIM, Y. & DIDAN, K. 2-band enhanced vegetation index without a blue band and its application to AVHRR data. Remote Sensing and Modeling of Ecosystems for Sustainability IV, 2007a. SPIE, 45-53.

JIANG, Z., HUETE, A. R., KIM, Y. & DIDAN, K. 2-band enhanced vegetation index without a blue band and its application to AVHRR data. Remote Sensing and Modeling of Ecosystems for Sustainability IV, 2007b. International Society for Optics and Photonics, 667905.

JIAO, J., ZOU, H., JIA, Y. & WANG, N. 2009. Research progress on the effects of soil erosion on vegetation. *Acta Ecologica Sinica,* 29**,** 85-91.

JIN, H., JÖNSSON, A. M., BOLMGREN, K., LANGVALL, O. & EKLUNDH, L. 2017. Disentangling remotely-sensed plant phenology and snow seasonality at northern Europe using MODIS and the plant phenology index. *Remote Sensing of Environment,* 198**,** 203-212.

JIN, J., JIANG, H., ZHANG, X. & WANG, Y. 2012. Characterizing Spatial-Temporal Variations in Vegetation Phenology over the North-South Transect of Northeast Asia Based upon the MERIS Terrestrial Chlorophyll Index. *Terrestrial, Atmospheric & Oceanic Sciences,* 23.

JOMBO, S., ADAM, E., BYRNE, M. J. & NEWETE, S. W. 2020. Evaluating the capability of Worldview-2 imagery for mapping alien tree species in a heterogeneous urban environment. *Cogent Social Sciences,* 6**,** 1754146.

JONSSON, P. & EKLUNDH, L. 2002. Seasonality extraction by function fitting to time-series of satellite sensor data. *IEEE transactions on Geoscience and Remote Sensing,* 40**,** 1824-1832.

JÖNSSON, P. & EKLUNDH, L. 2004. TIMESAT—a program for analyzing time-series of satellite sensor data. *Computers & geosciences,* 30**,** 833-845.

JUSTICE, C., HOLBEN, B. & GWYNNE, M. 1986. Monitoring East African vegetation using AVHRR data. *International Journal of Remote Sensing,* 7**,** 1453-1474.

JUSTICE, C., TOWNSHEND, J., VERMOTE, E., MASUOKA, E., WOLFE, R., SALEOUS, N., ROY, D. & MORISETTE, J. 2002. An overview of MODIS Land data processing and product status. *Remote sensing of Environment,* 83**,** 3-15.

JUSTICE, C. O., TOWNSHEND, J., HOLBEN, B. & TUCKER, E. C. 1985. Analysis of the phenology of global vegetation using meteorological satellite data. *International Journal of Remote Sensing,* 6**,** 1271-1318.

KANG, Y., ÖZDOĞAN, M., ZIPPER, S. C., ROMÁN, M. O., WALKER, J., HONG, S. Y., MARSHALL, M., MAGLIULO, V., MORENO, J. & ALONSO, L. 2016. How universal is the relationship between remotely sensed vegetation indices and crop leaf area index? A global assessment. *Remote sensing,* 8**,** 597.

KASUYA, E. 2019. On the use of r and r squared in correlation and regression. Wiley Online Library.

KAWAMURA, K., AKIYAMA, T., YOKOTA, H. O., TSUTSUMI, M., YASUDA, T., WATANABE, O. & WANG, S. 2005. Comparing MODIS vegetation indices with AVHRR NDVI for monitoring the forage quantity and quality in Inner Mongolia grassland, China. *Grassland Science,* 51**,** 33-40.

KAZMI, J., HAASE, D., SHAHZAD, A., SHAIKH, S., ZAIDI, S. & QURESHI, S. 2022. Mapping spatial distribution of invasive alien species through satellite remote sensing in Karachi, Pakistan: An urban ecological perspective. *International Journal of Environmental Science and Technology,* 19**,** 3637-3654.

KHAN, S. S. & MADDEN, M. G. 2014. One-class classification: taxonomy of study and review of techniques. *The Knowledge Engineering Review,* 29**,** 345-374.

KHARE, S., LATIFI, H., ROSSI, S. & GHOSH, S. K. 2019. Fractional cover mapping of invasive plant species by combining very high-resolution stereo and multi-sensor multispectral imageries. *Forests,* 10**,** 540.

KHOBKHUN, B., PRAYOTE, A., RAKWATIN, P. & DEJDUMRONG, N. Rice phenology monitoring using PIA time series MODIS imagery. 2013 10th International Conference Computer Graphics, Imaging and Visualization, 2013. IEEE, 84-87.

KIALA, Z., MUTANGA, O., ODINDI, J. & PEERBHAY, K. 2019. Feature selection on sentinel-2 multispectral imagery for mapping a landscape infested by parthenium weed. *Remote Sensing,* 11**,** 1892.

KIALA, Z., MUTANGA, O., ODINDI, J., PEERBHAY, K. Y. & SLOTOW, R. 2020. Automated classification of a tropical landscape infested by Parthenium weed (Parthenium hyterophorus). *International Journal of Remote Sensing,* 41**,** 8497-8519.

KROSS, A. S., ROULET, N. T., MOORE, T. R., LAFLEUR, P. M., HUMPHREYS, E. R., SEAQUIST, J. W., FLANAGAN, L. B. & AURELA, M. 2014. Phenology and its role in carbon dioxide exchange processes in northern peatlands. *Journal of Geophysical Research: Biogeosciences,* 119**,** 1370-1384.

KUEBLER, D., HILDEBRANDT, P., GUENTER, S., STIMM, B., WEBER, M., MOSANDL, R., MUNOZ, J., CABRERA, O., AGUIRRE, N. & ZEILINGER, J. 2016. Assessing the importance of topographic variables for the spatial distribution of tree species in a tropical mountain forest. *Erdkunde***,** 19-47.

KULYUKIN, V. & BLAY, C. 2015. An algorithm for mobile vision-based localization of skewed nutrition labels that maximizes specificity. *Emerging Trends in Image Processing, Computer Vision and Pattern Recognition.* Elsevier.

KUMARI, N., SRIVASTAVA, A. & DUMKA, U. C. 2021. A Long-Term Spatiotemporal Analysis of Vegetation Greenness over the Himalayan Region Using Google Earth Engine. *Climate,* 9**,** 109.

LARA, B. & GANDINI, M. 2016. Assessing the performance of smoothing functions to estimate land surface phenology on temperate grassland. *International Journal of Remote Sensing,* 37**,** 1801-1813.

LASAPONARA, R. 2006. Estimating spectral separability of satellite derived parameters for burned areas mapping in the Calabria region by using SPOT-Vegetation data. *Ecological Modelling,* 196**,** 265-270.

LAWTON, J. H. 1988. Biological control of bracken in Britain: constraints and opportunities. *Philosophical Transactions of the Royal Society of London. B, Biological Sciences,* 318**,** 335-355.

LAWTON, J. H. 1990. *Developments in the UK biological control programme for bracken*.

LEINENKUGEL, P., KUENZER, C., OPPELT, N. & DECH, S. 2013. Characterisation of land surface phenology and land cover based on moderate resolution satellite data in cloud prone areas—A novel product for the Mekong Basin. *Remote sensing of environment,* 136**,** 180-198.

LEVY-TACHER, S., VLEUT, I., ROMÁN-DAÑOBEYTIA, F. & ARONSON, J. 2015a. Natural regeneration after long-term bracken fern control with balsa (Ochroma pyramidale) in the Neotropics. *Forests,* 6**,** 2163-2177.

LEVY-TACHER, S. I., VLEUT, I., ROMÁN-DAÑOBEYTIA, F. & ARONSON, J. 2015b. Natural regeneration after long-term bracken fern control with balsa (Ochroma pyramidale) in the Neotropics. *Forests,* 6**,** 2163-2177.

LI, H., JIA, M., ZHANG, R., REN, Y. & WEN, X. 2019. Incorporating the Plant Phenological Trajectory into Mangrove Species Mapping with Dense Time Series Sentinel-2 Imagery and the Google Earth Engine Platform. *Remote Sensing,* 11**,** 2479.

LI, J. & ROY, D. P. 2017. A global analysis of Sentinel-2A, Sentinel-2B and Landsat-8 data revisit intervals and implications for terrestrial monitoring. *Remote Sensing,* 9**,** 902.

LI, J., TANG, J. & LIU, H. Reconstruction-based Unsupervised Feature Selection: An Embedded Approach. IJCAI, 2017. 2159-2165.

LI, M. & LIU, J. Reconstructing vegetation temperature condition index based on the Savitzky–Golay filter. International Conference on Computer and Computing Technologies in Agriculture, 2010. Springer, 629-637.

LI, P. & XU, H. 2010. Land-cover change detection using one-class support vector machine. *Photogrammetric Engineering & Remote Sensing,* 76**,** 255-263.

LI, W. & GUO, Q. 2013. A new accuracy assessment method for one-class remote sensing classification. *IEEE transactions on geoscience and remote sensing,* 52**,** 4621-4632.

LI, W., GUO, Q. & ELKAN, C. 2010. A positive and unlabeled learning algorithm for one-class classification of remote-sensing data. *IEEE transactions on geoscience and remote sensing,* 49**,** 717-725.

LIANG, L., SCHWARTZ, M. D. & FEI, S. 2011. Validating satellite phenology through intensive ground observation and landscape scaling in a mixed seasonal forest. *Remote Sensing of Environment,* 115**,** 143-157.

LIAO, C., CLARK, P. E. & DEGLORIA, S. D. 2018. Bush encroachment dynamics and rangeland management implications in southern Ethiopia. *Ecology and evolution,* 8**,** 11694-11703.

LINDERS, T. E. W., SCHAFFNER, U., ESCHEN, R., ABEBE, A., CHOGE, S. K., NIGATU, L., MBAABU, P. R., SHIFERAW, H. & ALLAN, E. 2019. Direct and indirect effects of invasive species: Biodiversity loss is a major mechanism by which an invasive tree affects ecosystem functioning. *Journal of Ecology,* 107**,** 2660-2672.

LIU, B., DAI, Y., LI, X., LEE, W. S. & YU, P. S. Building text classifiers using positive and unlabeled examples. Third IEEE International Conference on Data Mining, 2003. IEEE, 179-186.

LIU, X., HU, G., CHEN, Y., LI, X., XU, X., LI, S., PEI, F. & WANG, S. 2018. High-resolution multi-temporal mapping of global urban land using Landsat images based on the Google Earth Engine Platform. *Remote sensing of environment,* 209**,** 227-239.

LIU, X., LIU, H., DATTA, P., FREY, J. & KOCH, B. 2020. Mapping an Invasive Plant Spartina alterniflora by Combining an Ensemble One-Class Classification Algorithm with a Phenological NDVI Time-Series Analysis Approach in Middle Coast of Jiangsu, China. *Remote Sensing,* 12**,** 4010.

LIU, Y., WU, C., PENG, D., XU, S., GONSAMO, A., JASSAL, R. S., ARAIN, M. A., LU, L., FANG, B. & CHEN, J. M. 2016. Improved modeling of land surface phenology using MODIS land surface reflectance and temperature at evergreen needleleaf forests of central North America. *Remote Sensing of Environment,* 176**,** 152-162.

LU, L., KUENZER, C., WANG, C., GUO, H. & LI, Q. 2015. Evaluation of three MODIS-derived vegetation index time series for dryland vegetation dynamics monitoring. *Remote Sensing,* 7**,** 7597-7614.

LUKEY, P. & HALL, J. 2020. Biological invasion policy and legislation development and implementation in South Africa. *Biological Invasions in South Africa***,** 515-552.

LUMBIERRES, M., MÉNDEZ, P. F., BUSTAMANTE, J., SORIGUER, R. & SANTAMARÍA, L. 2017. Modeling biomass production in seasonal wetlands using MODIS NDVI land surface phenology. *Remote Sensing,* 9**,** 392.

131

MA, X., HUETE, A., TRAN, N. N., BI, J., GAO, S. & ZENG, Y. 2020. Sun-angle effects on remote-sensing phenology observed and modelled using himawari-8. *Remote Sensing,* 12**,** 1339.

MACK, B. & WASKE, B. 2017. In-depth comparisons of MaxEnt, biased SVM and one-class SVM for one-class classification of remote sensing data. *Remote sensing letters,* 8**,** 290-299.

MAKHAYA, Z., ODINDI, J. & MUTANGA, O. 2022. The influence of bioclimatic and topographic variables on grassland fire occurrence within an urbanized landscape. *Scientific African,* 15**,** e01127.

MAKORI, D. M., FOMBONG, A. T., ABDEL-RAHMAN, E. M., NKOBA, K., ONGUS, J., IRUNGU, J., MOSOMTAI, G., MAKAU, S., MUTANGA, O. & ODINDI, J. 2017. Predicting spatial distribution of key honeybee pests in Kenya using remotely sensed and bioclimatic variables: Key honeybee pests distribution models. *ISPRS International Journal of Geo-Information,* 6**,** 66.

MALAHLELA, O., CHO, M. A. & MUTANGA, O. 2014. Mapping canopy gaps in an indigenous subtropical coastal forest using high-resolution WorldView-2 data. *International Journal of Remote Sensing,* 35**,** 6397-6417.

MANEVITZ, L. M. & YOUSEF, M. 2001. One-class SVMs for document classification. *Journal of machine Learning research,* 2**,** 139-154.

MARRERO, E., BULNES, C., SANCHEZ, L., PALENZUELA, I., STUART, R., JACOBS, F. & ROMERO, J. 2001. Pteridium aquilinum (bracken fern) toxicity in cattle in the humid Chaco of Tarija, Bolivia. *Veterinary and human toxicology,* 43**,** 156-158.

MARRS, R., LE DUC, M., MITCHELL, R., GODDARD, D., PATERSON, S. & PAKEMAN, R. 2000a. The ecology of bracken: its role in succession and implications for control. *Annals of Botany,* 85**,** 3-15.

MARRS, R. H., LE DUC, M., MITCHELL, R., GODDARD, D., PATERSON, S. & PAKEMAN, R. 2000b. The ecology of bracken: its role in succession and implications for control. *Annals of Botany,* 85**,** 3-15.

MARZIALETTI, P., FUSILLI, L., LANEVE, G. & CADAU, E. EO Satellite Based system for monitoring Bracken Fern in Scotland. EGU General Assembly Conference Abstracts, 2020. 18442.

MASEMOLA, C., CHO, M. A. & RAMOELO, A. 2020. Sentinel-2 time series based optimal features and time window for mapping invasive Australian native Acacia species in KwaZulu Natal, South Africa. *International Journal of Applied Earth Observation and Geoinformation,* 93**,** 102207.

MATONGERA, T. N., MUTANGA, O., DUBE, T. & LOTTERING, R. T. 2018. Detection and mapping of bracken fern weeds using multispectral remotely sensed data: a review of progress and challenges. *Geocarto international,* 33**,** 209-224.

MATONGERA, T. N., MUTANGA, O., DUBE, T. & SIBANDA, M. 2017. Detection and mapping the spatial distribution of bracken fern weeds using the Landsat 8 OLI new generation sensor. *International journal of applied earth observation and geoinformation,* 57**,** 93-103.

MATONGERA, T. N., MUTANGA, O. & SIBANDA, M. 2021a. Characterizing bracken fern phenological cycle using time series data derived from Sentinel-2 satellite sensor. *Plos one,* 16**,** e0257196.

MATONGERA, T. N., MUTANGA, O., SIBANDA, M. & ODINDI, J. 2021b. Estimating and Monitoring Land Surface Phenology in Rangelands: A Review of Progress and Challenges. *Remote Sensing,* 13**,** 2060.

MATZINGER, N., ANDRETTA, M., GORSEL, E. V., VOGT, R., OHMURA, A. & ROTACH, M. 2003. Surface radiation budget in an Alpine valley. *Quarterly Journal of the Royal Meteorological Society: A journal of the atmospheric sciences, applied meteorology and physical oceanography,* 129**,** 877-895.

MAYA-ELIZARRARÁS, E. & SCHONDUBE, J. E. 2015. Birds, cattle, and bracken ferns: bird community responses to a Neotropical landscape shaped by cattle grazing activities. *Biotropica,* 47**,** 236-245.

MCDONALD, P. M., ABBOTT, C. S. & FIDDLER, G. O. 2003. Density and development of Bracken Fern (Pteridium aquilinum) in forest plantations as affected by manual and chemical application. *Native Plants Journal,* 4**,** 52-60.

MCGLONE, M. S., WILMSHURST, J. M. & LEACH, H. M. 2005. An ecological and historical review of bracken (Pteridium esculentum) in New Zealand, and its cultural significance. *New Zealand Journal of Ecology*, 165-184.

MELAAS, E. K., FRIEDL, M. A. & ZHU, Z. 2013a. Detecting interannual variation in deciduous broadleaf forest phenology using Landsat TM/ETM+ data. *Remote Sensing of Environment,* 132, 176-185.

MELAAS, E. K., RICHARDSON, A. D., FRIEDL, M. A., DRAGONI, D., GOUGH, C. M., HERBST, M., MONTAGNANI, L. & MOORS, E. 2013b. Using FLUXNET data to improve models of springtime vegetation activity onset in forest ecosystems. *Agricultural and Forest Meteorology,* 171, 46-56.

MGANGA, K. Z., MUSIMBA, N., NYARIKI, D., NYANGITO, M. & MWANG'OMBE, A. W. 2015. The choice of grass species to combat desertification in semi-arid Kenyan rangelands is greatly influenced by their forage value for livestock. *Grass and Forage Science,* 70, 161-167.

MHANGARA, P., MAPURISA, W. & MUDAU, N. 2020. Comparison of image fusion techniques using satellite pour l'Observation de la Terre (SPOT) 6 satellite imagery. *Applied Sciences,* 10, 1881.

MICHELE, V., ROSHANAK, M., TIEJUN, S., RAUL, W., KEES, Z.-M. & BRIAN, O. 2018. Vegetation phenology from Sentinel-2 and field cameras for a Dutch barrier island. *Remote sensing of environment*.

MIGLIAVACCA, M., REICHSTEIN, M., RICHARDSON, A. D., MAHECHA, M. D., CREMONESE, E., DELPIERRE, N., GALVAGNO, M., LAW, B. E., WOHLFAHRT, G. & ANDREW BLACK, T. 2015. Influence of physiological phenology on the seasonal pattern of ecosystem respiration in deciduous forests. *Global Change Biology,* 21, 363-376.

MISRA, G., CAWKWELL, F. & WINGLER, A. 2020. Status of phenological research using Sentinel-2 data: A review. *Remote Sensing,* 12, 2760.

MIURA, T., NAGAI, S., TAKEUCHI, M., ICHII, K. & YOSHIOKA, H. 2019. Improved characterisation of vegetation and land surface seasonal dynamics in central Japan with Himawari-8 hypertemporal data. *Scientific reports,* 9, 1-12.

MNGADI, M., ODINDI, J., SIBANDA, M., PEERBHAY, K. & MUTANGA, O. 2020. Testing the value of freely available Landsat 8 Operational Land Imager (OLI) and OLI pan-sharpened imagery in discriminating commercial forest species. *South African Geographical Journal*, 1-18.

MOHANAIAH, P., SATHYANARAYANA, P. & GURUKUMAR, L. 2013. Image texture feature extraction using GLCM approach. *International journal of scientific and research publications,* 3, 1-5.

MOON, M., ZHANG, X., HENEBRY, G. M., LIU, L., GRAY, J. M., MELAAS, E. K. & FRIEDL, M. A. 2019. Long-term continuity in land surface phenology measurements: a comparative assessment of the MODIS land cover dynamics and VIIRS land surface phenology products. *Remote Sensing of Environment,* 226, 74-92.

MORCILLO-PALLARÉS, P., RIVERA-CAICEDO, J. P., BELDA, S., DE GRAVE, C., BURRIEL, H., MORENO, J. & VERRELST, J. 2019. Quantifying the robustness of vegetation indices through global sensitivity analysis of homogeneous and forest leaf-canopy radiative transfer models. *Remote Sensing,* 11, 2418.

MORGAN-DAVIES, C., WATERHOUSE, T., SMYTH, K. & POLLOCK, M. L. 2005. Local area farming Plans—a common reality for farmers and conservationists in the Scottish Highlands? *Scottish Geographical Journal,* 121, 385-400.

MOTOHKA, T., NASAHARA, K., MIYATA, A., MANO, M. & TSUCHIDA, S. 2009. Evaluation of optical satellite remote sensing for rice paddy phenology in monsoon Asia using a continuous in situ dataset. *International Journal of Remote Sensing,* 30, 4343-4357.

MOTOHKA, T., NASAHARA, K. N., OGUMA, H. & TSUCHIDA, S. 2010. Applicability of green-red vegetation index for remote sensing of vegetation phenology. *Remote Sensing,* 2, 2369-2387.

MOULIN, S., KERGOAT, L., VIOVY, N. & DEDIEU, G. 1997. Global-scale assessment of vegetation phenology using NOAA/AVHRR satellite measurements. *Journal of Climate,* 10, 1154-1170.

MOURAD, R., JAAFAR, H., ANDERSON, M. & GAO, F. 2020. Assessment of Leaf Area Index Models Using Harmonized Landsat and Sentinel-2 Surface Reflectance Data over a Semi-Arid Irrigated Landscape. *Remote Sensing,* 12**,** 3121.

MOUTA, N., SILVA, R., PAIS, S., ALONSO, J. M., GONÇALVES, J. F., HONRADO, J. & VICENTE, J. R. 2021. 'The Best of Two Worlds'—Combining Classifier Fusion and Ecological Models to Map and Explain Landscape Invasion by an Alien Shrub. *Remote Sensing,* 13**,** 3287.

MOYA, M. M. & HUSH, D. R. 1996. Network constraints and multi-objective optimization for one-class classification. *Neural networks,* 9**,** 463-474.

MRÓZ, M. & SOBIERAJ, A. 2004. Comparison of several vegetation indices calculated on the basis of a seasonal SPOT XS time series, and their suitability for land cover and agricultural crop identification. *Technical sciences,* 7**,** 39-66.

MUCINA, L. & RUTHERFORD, M. C. 2006. *The vegetation of South Africa, Lesotho and Swaziland*, South African National Biodiversity Institute.

MULLER, R. N. 1978. The phenology, growth and ecosystem dynamics of Erythronium americanum in the northern hardwood forest. *Ecological Monographs,* 48**,** 1-20.

MŨNOZ-MARÍ, J., BOVOLO, F., GÓMEZ-CHOVA, L., BRUZZONE, L. & CAMP-VALLS, G. 2010. Semisupervised one-class support vector machines for classification of remote sensing data. *IEEE transactions on geoscience and remote sensing,* 48**,** 3188-3197.

MUÑOZ-MARÍ, J., BRUZZONE, L. & CAMPS-VALLS, G. 2007. A support vector domain description approach to supervised classification of remote sensing images. *IEEE Transactions on Geoscience and Remote Sensing,* 45**,** 2683-2692.

MUTANGA, O. & KUMAR, L. 2019. Google earth engine applications. Multidisciplinary Digital Publishing Institute.

MUTANGA, O. & SKIDMORE, A. K. 2004. Narrow band vegetation indices overcome the saturation problem in biomass estimation. *International journal of remote sensing,* 25**,** 3999-4014.

MYERS, E., KEREKES, J., DAUGHTRY, C. & RUSS, A. 2019. Assessing the Impact of Satellite Revisit Rate on Estimation of Corn Phenological Transition Timing through Shape Model Fitting. *Remote Sensing,* 11**,** 2558.

NAGAI, S., SAITOH, T. M., KOBAYASHI, H., ISHIHARA, M., SUZUKI, R., MOTOHKA, T., NASAHARA, K. N. & MURAOKA, H. 2012. In situ examination of the relationship between various vegetation indices and canopy phenology in an evergreen coniferous forest, Japan. *International journal of remote sensing,* 33**,** 6202-6214.

NALEPA, J. & KAWULOK, M. 2019. Selecting training sets for support vector machines: a review. *Artificial Intelligence Review,* 52**,** 857-900.

NDLOVU, P., MUTANGA, O., SIBANDA, M., ODINDI, J. & RUSHWORTH, I. 2018. Modelling potential distribution of bramble (rubus cuneifolius) using topographic, bioclimatic and remotely sensed data in the KwaZulu-Natal Drakensberg, South Africa. *Applied Geography,* 99**,** 54-62.

NEL, W. 2007. *On the climate of the Drakensberg: rainfall and surface-temperature attributes, and associated geomorphic effects.* University of Pretoria.

NELLEMANN, C. & FRY, G. 1995. Quantitative analysis of terrain ruggedness in reindeer winter grounds. *Arctic***,** 172-176.

NGUBANE, Z., ODINDI, J., MUTANGA, O. & SLOTOW, R. 2014. Assessment of the contribution of WorldView-2 strategically positioned bands in Bracken fern (Pteridium aquilinum (L.) Kuhn) mapping. *South African Journal of Geomatics,* 3**,** 210-223.

NGUYEN, H. C., JUNG, J., LEE, J., CHOI, S.-U., HONG, S.-Y. & HEO, J. 2015. Optimal atmospheric correction for above-ground forest biomass estimation with the ETM+ remote sensor. *Sensors,* 15**,** 18865-18886.

NGUYEN, L. H., JOSHI, D. R., CLAY, D. E. & HENEBRY, G. M. 2020. Characterizing land cover/land use from multiple years of Landsat and MODIS time series: A novel approach using land surface phenology modeling and random forest classifier. *Remote sensing of environment,* 238**,** 111017.

NIC LUGHADHA, E., WALKER, B. E., CANTEIRO, C., CHADBURN, H., DAVIS, A. P., HARGREAVES, S., LUCAS, E. J., SCHUITEMAN, A., WILLIAMS, E. & BACHMAN, S. P. 2019. The use and misuse of herbarium specimens in evaluating plant extinction risks. *Philosophical transactions of the Royal Society B,* 374**,** 20170402.

NOBLE, W. S. 2006. What is a support vector machine? *Nature biotechnology,* 24**,** 1565-1567.

NORWINE, J. & GREEGOR, D. 1983. Vegetation classification based on advanced very high resolution radiometer (AVHRR) satellite imagery. *Remote Sensing of Environment,* 13**,** 69-87.

O'CONNOR, T. G. & VAN WILGEN, B. W. 2020. The impact of invasive alien plants on rangelands in South Africa. *Biological Invasions in South Africa***,** 459.

ODINDI, J. O., ADAM, E. E., NGUBANE, Z., MUTANGA, O. & SLOTOW, R. 2014. Comparison between WorldView-2 and SPOT-5 images in mapping the bracken fern using the random forest algorithm. *Journal of Applied Remote Sensing,* 8**,** 083527.

OLSSON, C., BOLMGREN, K., LINDSTRÖM, J. & JÖNSSON, A. M. 2013. Performance of tree phenology models along a bioclimatic gradient in Sweden. *Ecological Modelling,* 266**,** 103-117.

ORMSBY, T., NAPOLEON, E., BURKE, R., GROESSL, C. & BOWDEN, L. 2010. *Getting to know ArcGIS desktop*, Citeseer.

OZBAKIR, A. & BANNARI, A. 2008. Performance of TDVI in Urban Land Use/Cover Classification for Quality of Place Measurement. *Proceedings of The International Archives of the Photogrammetry, Remote Sensing and Spatial Information Sciences***,** 691-694.

PAKEMAN, R. & MARRS, R. 1992. The conservation value of bracken Pteridium aquilinum (L.) Kuhn-dominated communities in the UK, and an assessment of the ecological impact of bracken expansion or its removal. *Biological Conservation,* 62**,** 101-114.

PAKEMAN, R., MARRS, R., HOWARD, D., BARR, C. & FULLER, R. 1996. The bracken problem in Great Britain: its present extent and future changes. *Applied Geography,* 16**,** 65-86.

PAKEMAN, R., MARRS, R. & JACOB, P. 1994. A model of bracken (Pteridium aquilinum) growth and the effects of control strategies and changing climate. *Journal of applied ecology***,** 145-154.

PAL, M. 2005. Random forest classifier for remote sensing classification. *International journal of remote sensing,* 26**,** 217-222.

PAL, M. & MATHER, P. 2005. Support vector machines for classification in remote sensing. *International journal of remote sensing,* 26**,** 1007-1011.

PALMER, A. R. & FORTESCUE, A. 2004. Remote sensing and change detection in rangelands. *African Journal of Range and Forage Science,* 21**,** 123-128.

PAN, Z., HUANG, J., ZHOU, Q., WANG, L., CHENG, Y., ZHANG, H., BLACKBURN, G. A., YAN, J. & LIU, J. 2015. Mapping crop phenology using NDVI time-series derived from HJ-1 A/B data. *International Journal of Applied Earth Observation and Geoinformation,* 34**,** 188-197.

PANCHEN, Z. A., PRIMACK, R. B., ANIŚKO, T. & LYONS, R. E. 2012. Herbarium specimens, photographs, and field observations show Philadelphia area plants are responding to climate change. *American Journal of Botany,* 99**,** 751-756.

PASTICK, N. J., DAHAL, D., WYLIE, B. K., PARAJULI, S., BOYTE, S. P. & WU, Z. 2020. Characterizing land surface phenology and exotic annual grasses in dryland ecosystems using Landsat and Sentinel-2 data in harmony. *Remote Sensing,* 12**,** 725.

PEARSON, K. D. 2019. A new method and insights for estimating phenological events from herbarium specimens. *Applications in Plant Sciences,* 7**,** e01224.

PEARSON, K. D., NELSON, G., ARONSON, M. F., BONNET, P., BRENSKELLE, L., DAVIS, C. C., DENNY, E. G., ELLWOOD, E. R., GOËAU, H. & HEBERLING, J. M. 2020. Machine learning using digitized herbarium specimens to advance phenological research. *BioScience,* 70**,** 610-620.

PEARSON, R. L. & MILLER, L. D. 1972. Remote mapping of standing crop biomass for estimation of the productivity of the shortgrass prairie. *Remote sensing of environment, VIII***,** 1355.

PENG, D., WANG, Y., XIAN, G., HUETE, A. R., HUANG, W., SHEN, M., WANG, F., YU, L., LIU, L. & XIE, Q. 2021. Investigation of land surface phenology detections in shrublands using multiple scale satellite data. *Remote Sensing of Environment,* 252**,** 112133.

PENG, D., WU, C., LI, C., ZHANG, X., LIU, Z., YE, H., LUO, S., LIU, X., HU, Y. & FANG, B. 2017. Spring green-up phenology products derived from MODIS NDVI and EVI: Intercomparison, interpretation and validation using National Phenology Network and AmeriFlux observations. *Ecological Indicators,* 77**,** 323-336.

PEPIN, K. M., WOLFSON, D. W., MILLER, R. S., TABAK, M. A., SNOW, N. P., VERCAUTEREN, K. C. & DAVIS, A. J. 2019. Accounting for heterogeneous invasion rates reveals management impacts on the spatial expansion of an invasive species. *Ecosphere,* 10**,** e02657.

PHIRI, D., SIMWANDA, M., SALEKIN, S., NYIRENDA, V. R., MURAYAMA, Y. & RANAGALAGE, M. 2020. Sentinel-2 data for land cover/use mapping: A review. *Remote Sensing,* 12**,** 2291.

PIIROINEN, R., FASSNACHT, F. E., HEISKANEN, J., MAEDA, E., MACK, B. & PELLIKKA, P. 2018. Invasive tree species detection in the Eastern Arc Mountains biodiversity hotspot using one class classification. *Remote Sensing of Environment,* 218**,** 119-131.

PITMAN, J. I. 2000. Absorption of photosynthetically active radiation, radiation use efficiency and spectral reflectance of bracken [Pteridium aquilinum (L.) Kuhn] canopies. *Annals of Botany,* 85**,** 101-111.

PÔÇAS, I., CALERA, A., CAMPOS, I. & CUNHA, M. 2020. Remote sensing for estimating and mapping single and basal crop coefficientes: A review on spectral vegetation indices approaches. *Agricultural Water Management,* 233**,** 106081.

POSSELT, R., MUELLER, R., STÖCKLI, R. & TRENTMANN, J. 2012. Remote sensing of solar surface radiation for climate monitoring—The CM-SAF retrieval in international comparison. *Remote Sensing of Environment,* 118**,** 186-198.

POTITHEP, S., NASAHARA, N., MURAOKA, H., NAGAI, S. & SUZUKI, R. 2010. What is the actual relationship between LAI and VI in a deciduous broadleaf forest. *International Archives of the Photogrammetry, Remote Sensing and Spatial Information Science,* 38.

POTTER, C., LI, S., HUANG, S. & CRABTREE, R. L. 2012. Analysis of sapling density regeneration in Yellowstone National Park with hyperspectral remote sensing data. *Remote sensing of environment,* 121**,** 61-68.

POUTEAU, R., MEYER, J.-Y., TAPUTUARAI, R. & STOLL, B. 2012. Support vector machines to map rare and endangered native plants in Pacific islands forests. *Ecological Informatics,* 9**,** 37-46.

PRANANDA, A. R. A., KAMAL, M. & KUSUMA, D. W. The effect of using different vegetation indices for mangrove leaf area index modelling. IOP Conference Series: Earth and Environmental Science, 2020. IOP Publishing, 012006.

PUDIL, P., NOVOVIČOVÁ, J. & KITTLER, J. 1994. Floating search methods in feature selection. *Pattern recognition letters,* 15**,** 1119-1125.

PYŠEK, P. & RICHARDSON, D. M. 2010. Invasive species, environmental change and management, and health. *Annual review of environment and resources,* 35**,** 25-55.

QIU, S., ZHU, Z. & HE, B. 2019. Fmask 4.0: Improved cloud and cloud shadow detection in Landsats 4–8 and Sentinel-2 imagery. *Remote Sensing of Environment,* 231**,** 111205.

RAIMONDO, D., VON STADEN, L., FODEN, W., VICTOR, J., HELME, N., TURNER, R., KAMUNDI, D. & MANYAMA, P. 2015. National assessment: Red list of South African plants, version 2015.1. *South African National Biodiversity Institute, Pretoria, South Africa*.

RAJAH, P., ODINDI, J., MUTANGA, O. & KIALA, Z. 2019. The utility of Sentinel-2 Vegetation Indices (VIs) and Sentinel-1 Synthetic Aperture Radar (SAR) for invasive alien species detection and mapping. *Nature Conservation,* 35**,** 41.

RÄSÄNEN, A., ELSAKOV, V. & VIRTANEN, T. 2019. Usability of one-class classification in mapping and detecting changes in bare peat surfaces in the tundra. *International Journal of Remote Sensing,* 40**,** 4083-4103.

RAST, M., BEZY, J. & BRUZZI, S. 1999. The ESA Medium Resolution Imaging Spectrometer MERIS a review of the instrument and its mission. *International Journal of Remote Sensing,* 20**,** 1681-1702.

REA, J. & ASHLEY, M. 1976. Phenological evaluations using Landsat—1 sensors. *International Journal of Biometeorology,* 20**,** 240-248.

REED, B. C., BROWN, J. F., VANDERZEE, D., LOVELAND, T. R., MERCHANT, J. W. & OHLEN, D. O. 1994. Measuring phenological variability from satellite imagery. *Journal of vegetation science,* 5**,** 703-714.

REICH, P. B. 1995. Phenology of tropical forests: patterns, causes, and consequences. *Canadian Journal of Botany,* 73**,** 164-174.

REIMANN, C., ARNOLDUSSEN, A., BOYD, R., FINNE, T. E., KOLLER, F., NORDGULEN, Ø. & ENGLMAIER, P. 2007. Element contents in leaves of four plant species (birch, mountain ash, fern and spruce) along anthropogenic and geogenic concentration gradients. *Science of the Total Environment,* 377**,** 416-433.

RICHARDSON, A. D., HUFKENS, K., MILLIMAN, T. & FROLKING, S. 2018. Intercomparison of phenological transition dates derived from the PhenoCam Dataset V1. 0 and MODIS satellite remote sensing. *Scientific reports,* 8**,** 1-12.

RICHARDSON, A. J. & WIEGAND, C. 1977. Distinguishing vegetation from soil background information. *Photogrammetric engineering and remote sensing,* 43**,** 1541-1552.

RIDOLFI, L., LAIO, F. & D'ODORICO, P. 2008. Fertility island formation and evolution in dryland ecosystems. *Ecology and Society,* 13.

RIHAN, W., ZHANG, H., ZHAO, J., SHAN, Y., GUO, X., YING, H., DENG, G. & LI, H. 2021. Promote the advance of the start of the growing season from combined effects of climate change and wildfire. *Ecological Indicators,* 125**,** 107483.

ROBERTS, A. M., TANSEY, C., SMITHERS, R. J. & PHILLIMORE, A. B. 2015. Predicting a change in the order of spring phenology in temperate forests. *Global change biology,* 21**,** 2603-2611.

ROCCHINI, D., ANDREO, V., FÖRSTER, M., GARZON-LOPEZ, C. X., GUTIERREZ, A. P., GILLESPIE, T. W., HAUFFE, H. C., HE, K. S., KLEINSCHMIT, B. & MAIROTA, P. 2015. Potential of remote sensing to predict species invasions: A modelling perspective. *Progress in Physical Geography,* 39**,** 283-309.

ROCHA, A. V. & SHAVER, G. R. 2009. Advantages of a two band EVI calculated from solar and photosynthetically active radiation fluxes. *Agricultural and Forest Meteorology,* 149**,** 1560-1563.

RODRIGUES, A., MARCAL, A. R. & CUNHA, M. PhenoSat—A tool for vegetation temporal analysis from satellite image data. 2011 6th International Workshop on the Analysis of Multi-temporal Remote Sensing Images (Multi-Temp), 2011. IEEE, 45-48.

RODRIGUEZ-GALIANO, V., DASH, J. & ATKINSON, P. M. 2015. Intercomparison of satellite sensor land surface phenology and ground phenology in Europe. *Geophysical Research Letters,* 42**,** 2253-2260.

ROUSE JR, J. 1972. Monitoring the vernal advancement and retrogradation (green wave effect) of natural vegetation.

ROUSE JR, J., HAAS, R., DEERING, D., SCHELL, J. & HARLAN, J. 1974. Monitoring the Vernal Advancement and Retrogradation (Green Wave Effect) of Natural Vegetation.[Great Plains Corridor].

ROUSE, J. W., HAAS, R. H., SCHELL, J. A., DEERING, D. W. & HARLAN, J. C. 1974. Monitoring the vernal advancement and retrogradation (green wave effect) of natural vegetation. *NASA/GSFC Type III Final Report, Greenbelt, Md,* 371.

ROYIMANI, L., MUTANGA, O., ODINDI, J., DUBE, T. & MATONGERA, T. N. 2019. Advancements in satellite remote sensing for mapping and monitoring of alien invasive plant species (AIPs). *Physics and Chemistry of the Earth, Parts A/B/C,* 112**,** 237-245.

RWANGA, S. S. & NDAMBUKI, J. M. 2017. Accuracy assessment of land use/land cover classification using remote sensing and GIS. *International Journal of Geosciences,* 8**,** 611.

RYHERD, S. & WOODCOCK, C. 1996. Combining spectral and texture data in the segmentation of remotely sensed images. *Photogrammetric engineering and remote sensing,* 62**,** 181-194.

SABAT-TOMALA, A., RACZKO, E. & ZAGAJEWSKI, B. 2020. Comparison of support vector machine and random forest algorithms for invasive and expansive species classification using airborne hyperspectral data. *Remote Sensing,* 12**,** 516.

SAKAMOTO, T., WARDLOW, B. D., GITELSON, A. A., VERMA, S. B., SUYKER, A. E. & ARKEBAUER, T. J. 2010. A two-step filtering approach for detecting maize and soybean phenology with time-series MODIS data. *Remote Sensing of Environment,* 114**,** 2146-2159.

SAKAMOTO, T., YOKOZAWA, M., TORITANI, H., SHIBAYAMA, M., ISHITSUKA, N. & OHNO, H. 2005. A crop phenology detection method using time-series MODIS data. *Remote sensing of environment,* 96**,** 366-374.

SANKEY, J. B., WALLACE, C. S. & RAVI, S. 2013. Phenology-based, remote sensing of post-burn disturbance windows in rangelands. *Ecological indicators,* 30**,** 35-44.

SATO, Y., MASHIMO, Y., SUZUKI, R. O., HIRAO, A. S., TAKAGI, E., KANAI, R., MASAKI, D., SATO, M. & MACHIDA, R. 2017. Potential Impact of an Exotic Plant Invasion on Both Plant and Arthropod Communities in a Semi-natural Grassland on Sugadaira Montane in Japan. *Journal of Developments in Sustainable Agriculture,* 12**,** 52-64.

SAYRE, N. F., MCALLISTER, R. R., BESTELMEYER, B. T., MORITZ, M. & TURNER, M. D. 2013. Earth stewardship of rangelands: coping with ecological, economic, and political marginality. *Frontiers in Ecology and the Environment,* 11**,** 348-354.

SCHABER, J. & BADECK, F.-W. 2003. Physiology-based phenology models for forest tree species in Germany. *International journal of biometeorology,* 47**,** 193-201.

SCHNEIDER, L. & GEOGHEGAN, J. 2006a. Land abandonment in an agricultural frontier after a plant invasion: the case of bracken fern in southern Yucatán, Mexico. *Agricultural and Resource Economics Review,* 35**,** 167-177.

SCHNEIDER, L. & GEOGHEGAN, J. 2006b. Land abandonment in an agricultural frontier after a plant invasion: the case of bracken fern in southern Yucatán, Mexico. *Agricultural and Resource Economics Review,* 35**,** 167-177.

SCHNEIDER, L. C. 2004. Bracken fern invasion in southern yucatán: a case for land-change science. *Geographical Review,* 94**,** 229-241.

SCHNEIDER, L. C. 2006. Invasive species and land-use: the effect of land management practices on bracken fern invasion in the region of Calakmul, Mexico. *Journal of Latin American Geography***,** 91-107.

SCHNEIDER, L. C. & FERNANDO, D. N. 2010. An untidy cover: invasion of bracken fern in the shifting cultivation systems of Southern Yucatán, Mexico. *Biotropica,* 42**,** 41-48.

SCHNEIDER, L. C. & INITIATIVE, E. C. 2004. Invasive Species and Common property: The case of bracken fern (Pteridium aquilinum (L.) Kuhn) invasion in the region of Calakmul.

SCHÖLKOPF, B., PLATT, J. C., SHAWE-TAYLOR, J., SMOLA, A. J. & WILLIAMSON, R. C. 2001. Estimating the support of a high-dimensional distribution. *Neural computation,* 13**,** 1443-1471.

SCHWARTZ, M. D., BETANCOURT, J. L. & WELTZIN, J. F. 2012. From Caprio's lilacs to the USA National Phenology Network. *Frontiers in Ecology and the Environment,* 10**,** 324-327.

SCHWARTZ, M. D. & HANES, J. M. 2010. Intercomparing multiple measures of the onset of spring in eastern North America. *international Journal of Climatology,* 30**,** 1614-1626.

SCHWARTZ, M. D. & REED, B. C. 1999. Surface phenology and satellite sensor-derived onset of greenness: an initial comparison. *International Journal of Remote Sensing,* 20**,** 3451-3457.

SELIYA, N., ABDOLLAH ZADEH, A. & KHOSHGOFTAAR, T. M. 2021. A literature review on one-class classification and its potential applications in big data. *Journal of Big Data,* 8**,** 1-31.

SENYANZOBE, J., MULEI, J., BIZURU, E., BOOKS, R., OER, R., SCARDA, R. & TENDERS, R. Environmental and social impacts of Pteridium aquilinum (L.) Kuhn)(Bracken Fern) invasive species growing in Nyungwe Forest, Rwanda. Fifth African Higher Education Week and RUFORUM Biennial Conference 2016," Linking agricultural universities with civil society, the private sector, governments and other stakeholders in support of agricultural development in Africa", Cape Town, South Africa, 17-21 October 2016, 2016. RUFORUM, 147-150.

SEONG, N.-H., JUNG, D., KIM, J. & HAN, K.-S. 2020. Evaluation of NDVI Estimation Considering Atmospheric and BRDF Correction through Himawari-8/AHI. *Asia-Pacific Journal of Atmospheric Sciences*, 1-10.

SEYEDNASROLLAH, B., YOUNG, A. M., HUFKENS, K., MILLIMAN, T., FRIEDL, M. A., FROLKING, S. & RICHARDSON, A. D. 2019. Tracking vegetation phenology across diverse biomes using Version 2.0 of the PhenoCam Dataset. *Scientific data,* 6, 1-11.

SHELESTOV, A., LAVRENIUK, M., KUSSUL, N., NOVIKOV, A. & SKAKUN, S. 2017a. Exploring Google Earth Engine platform for big data processing: Classification of multi-temporal satellite imagery for crop mapping. *frontiers in Earth Science,* 5, 17.

SHELESTOV, A., LAVRENIUK, M., KUSSUL, N., NOVIKOV, A. & SKAKUN, S. Large scale crop classification using Google earth engine platform. 2017 IEEE international geoscience and remote sensing symposium (IGARSS), 2017b. IEEE, 3696-3699.

SHEN, M., PIAO, S., DORJI, T., LIU, Q., CONG, N., CHEN, X., AN, S., WANG, S., WANG, T. & ZHANG, G. 2015. Plant phenological responses to climate change on the Tibetan Plateau: research status and challenges. *National Science Review,* 2, 454-467.

SHEN, M., TANG, Y., DESAI, A. R., GOUGH, C. & CHEN, J. 2014. Can EVI-derived land-surface phenology be used as a surrogate for phenology of canopy photosynthesis? *International Journal of Remote Sensing,* 35, 1162-1174.

SHOKO, C. & MUTANGA, O. 2017. Examining the strength of the newly-launched Sentinel 2 MSI sensor in detecting and discriminating subtle differences between C3 and C4 grass species. *ISPRS Journal of Photogrammetry and Remote Sensing,* 129, 32-40.

SHUCHMAN, R. A., SAYERS, M. J. & BROOKS, C. N. 2013. Mapping and monitoring the extent of submerged aquatic vegetation in the Laurentian Great Lakes with multi-scale satellite remote sensing. *Journal of Great Lakes Research,* 39, 78-89.

SIBANDA, M., MUTANGA, O., DUBE, T., S VUNDLA, T. & L MAFONGOYA, P. 2019. Estimating LAI and mapping canopy storage capacity for hydrological applications in wattle infested ecosystems using Sentinel-2 MSI derived red edge bands. *GIScience & Remote Sensing,* 56, 68-86.

SILLEOS, N. G., ALEXANDRIDIS, T. K., GITAS, I. Z. & PERAKIS, K. 2006. Vegetation indices: advances made in biomass estimation and vegetation monitoring in the last 30 years. *Geocarto International,* 21, 21-28.

SINTAYEHU, D. W., DALLE, G. & BOBASA, A. F. 2020. Impacts of climate change on current and future invasion of Prosopis juliflora in Ethiopia: environmental and socio-economic implications. *Heliyon,* 6, e04596.

SKAKUN, S., JUSTICE, C. O., VERMOTE, E. & ROGER, J.-C. 2018. Transitioning from MODIS to VIIRS: an analysis of inter-consistency of NDVI data sets for agricultural monitoring. *International journal of remote sensing,* 39, 971-992.

SKOWRONEK, S., ASNER, G. P. & FEILHAUER, H. Performance of One-Class Classifiers for Invasive Species Mapping using Hyperspectral Remote Sensing. AGU Fall Meeting Abstracts, 2016. B52A-06.

SKOWRONEK, S., ASNER, G. P. & FEILHAUER, H. 2017. Performance of one-class classifiers for invasive species mapping using airborne imaging spectroscopy. *Ecological Informatics,* 37, 66-76.

SMALL, C. & SOUSA, D. 2019. Spatiotemporal characterization of mangrove phenology and disturbance response: the Bangladesh Sundarban. *Remote Sensing,* 11, 2063.

SOUBRY, I., MANAKOS, I. & KALAITZIDIS, C. Recent Advances in Land Surface Phenology Estimation with Multispectral Sensing. GISTAM, 2021. 134-145.

SSALI, F., MOE, S. R. & SHEIL, D. 2017. A first look at the impediments to forest recovery in bracken-dominated clearings in the African Highlands. *Forest Ecology and Management,* 402, 166-176.

STANIMIROVA, R., CAI, Z., MELAAS, E. K., GRAY, J. M., EKLUNDH, L., JÖNSSON, P. & FRIEDL, M. A. 2019. An empirical assessment of the MODIS land cover dynamics and TIMESAT land surface phenology algorithms. *Remote Sensing,* 11, 2201.

STÖCKLI, R. & VIDALE, P. L. 2004. European plant phenology and climate as seen in a 20-year AVHRR land-surface parameter dataset. *International Journal of Remote Sensing,* 25**,** 3303-3330.

STUDER, S., STÖCKLI, R., APPENZELLER, C. & VIDALE, P. L. 2007. A comparative study of satellite and ground-based phenology. *International Journal of Biometeorology,* 51**,** 405-414.

SUN, H., CHEN, Y., XIONG, J., YE, C., YONG, Z., WANG, Y., HE, D. & XU, S. 2022. Relationships between climate change, phenology, edaphic factors, and net primary productivity across the Tibetan Plateau. *International Journal of Applied Earth Observation and Geoinformation***,** 102708.

SUN, Y., QIN, Q., REN, H., ZHANG, T. & CHEN, S. 2019. Red-edge band vegetation indices for leaf area index estimation from sentinel-2/msi imagery. *IEEE Transactions on Geoscience and Remote Sensing,* 58**,** 826-840.

SUSLICK, K. S. 2001. Encyclopedia of physical science and technology. *Sonoluminescence and Sonochemistry Massachusetts: Elsevier Science Ltd***,** 1-20.

SVINURAI, W., HASSEN, A., TESFAMARIAM, E. & RAMOELO, A. 2018. Performance of ratio-based, soil-adjusted and atmospherically corrected multispectral vegetation indices in predicting herbaceous aboveground biomass in a Colophospermum mopane tree–shrub savanna. *Grass and Forage Science,* 73**,** 727-739.

SYCHOLT, A. 2002. *A Guide to the Drakensberg*, Struik.

SYPHARD, A. D. & FRANKLIN, J. 2010. Species traits affect the performance of species distribution models for plants in southern California. *Journal of Vegetation Science,* 21**,** 177-189.

TAMIMINIA, H., SALEHI, B., MAHDIANPARI, M., QUACKENBUSH, L., ADELI, S. & BRISCO, B. 2020. Google Earth Engine for geo-big data applications: A meta-analysis and systematic review. *ISPRS Journal of Photogrammetry and Remote Sensing,* 164**,** 152-170.

TAN, B., MORISETTE, J. T., WOLFE, R. E., GAO, F., EDERER, G. A., NIGHTINGALE, J. & PEDELTY, J. A. 2010. An enhanced TIMESAT algorithm for estimating vegetation phenology metrics from MODIS data. *IEEE Journal of Selected Topics in Applied Earth Observations and Remote Sensing,* 4**,** 361-371.

TAN, B., MORISETTE, J. T., WOLFE, R. E., GAO, F., EDERER, G. A., NIGHTINGALE, J. & PEDELTY, J. A. 2011. An enhanced TIMESAT algorithm for estimating vegetation phenology metrics from MODIS data. *IEEE Journal of Selected Topics in Applied Earth Observations and Remote Sensing,* 4**,** 361-371.

TANG, J., KÖRNER, C., MURAOKA, H., PIAO, S., SHEN, M., THACKERAY, S. J. & YANG, X. 2016. Emerging opportunities and challenges in phenology: a review. *Ecosphere,* 7.

TAO, F., YOKOZAWA, M., XU, Y., HAYASHI, Y. & ZHANG, Z. 2006. Climate changes and trends in phenology and yields of field crops in China, 1981–2000. *Agricultural and forest meteorology,* 138**,** 82-92.

TASSI, A., GIGANTE, D., MODICA, G., DI MARTINO, L. & VIZZARI, M. 2021. Pixel-vs. Object-Based Landsat 8 Data Classification in Google Earth Engine Using Random Forest: The Case Study of Maiella National Park. *Remote Sensing,* 13, 2299.

TASSI, A. & VIZZARI, M. 2020. Object-oriented lulc classification in google earth engine combining snic, glcm, and machine learning algorithms. *Remote Sensing,* 12**,** 3776.

TAYLOR, R. V., HOLTHUIJZEN, W., HUMPHREY, A. & POSTHUMUS, E. 2020a. Using phenology data to improve control of invasive plant species: A case study on Midway Atoll NWR. *Ecological Solutions and Evidence,* 1**,** e12007.

TAYLOR, R. V., HOLTHUIJZEN, W., HUMPHREY, A. & POSTHUMUS, E. 2020b. Using phenology data to improve control of invasive plant species: A case study on Midway Atoll NWR. *Ecological Solutions and Evidence,* 1**,** 1-7.

TCHAKOUNTÉ, F. & HAYATA, F. 2017. Supervised learning based detection of malware on android. *Mobile Security and Privacy.* Elsevier.

TESTA, S., SOUDANI, K., BOSCHETTI, L. & MONDINO, E. B. 2018. MODIS-derived EVI, NDVI and WDRVI time series to estimate phenological metrics in French deciduous forests. *International journal of applied earth observation and geoinformation,* 64**,** 132-144.

THENKABAIL, P. S. 2015. Remote sensing of land resources: Monitoring, modeling, and mapping advances over the last 50 years and a vision for the future.

THOMPSON, J. A., PAULL, D. J. & LEES, B. G. 2015. Using phase-spaces to characterize land surface phenology in a seasonally snow-covered landscape. *Remote Sensing of Environment,* 166**,** 178-190.

TIAN, F., CAI, Z., JIN, H., HUFKENS, K., SCHEIFINGER, H., TAGESSON, T., SMETS, B., VAN HOOLST, R., BONTE, K. & IVITS, E. 2021. Calibrating vegetation phenology from Sentinel-2 using eddy covariance, PhenoCam, and PEP725 networks across Europe. *Remote Sensing of Environment,* 260**,** 112456.

TIAN, J., WANG, L., YIN, D., LI, X., DIAO, C., GONG, H., SHI, C., MENENTI, M., GE, Y. & NIE, S. 2020. Development of spectral-phenological features for deep learning to understand Spartina alterniflora invasion. *Remote Sensing of Environment,* 242**,** 111745.

TOMASZEWSKA, M. A., NGUYEN, L. H. & HENEBRY, G. M. 2020. Land surface phenology in the highland pastures of montane Central Asia: Interactions with snow cover seasonality and terrain characteristics. *Remote Sensing of Environment,* 240**,** 111675.

TONG, X., TIAN, F., BRANDT, M., LIU, Y., ZHANG, W. & FENSHOLT, R. 2019. Trends of land surface phenology derived from passive microwave and optical remote sensing systems and associated drivers across the dry tropics 1992–2012. *Remote Sensing of Environment,* 232**,** 111307.

TOWERS, P. C., STREVER, A. & POBLETE-ECHEVERRÍA, C. 2019. Comparison of vegetation indices for leaf area index estimation in vertical shoot positioned vine canopies with and without grenbiule hail-protection netting. *Remote Sensing,* 11**,** 1073.

TRAGANOS, D. & REINARTZ, P. 2018. Mapping Mediterranean seagrasses with Sentinel-2 imagery. *Marine pollution bulletin,* 134**,** 197-209.

TRANSON, J., D'ANDRIMONT, R., MAUGNARD, A. & DEFOURNY, P. 2018. Survey of hyperspectral earth observation applications from space in the sentinel-2 context. *Remote Sensing,* 10**,** 157.

TREITZ, P. & ROGAN, J. 2004. Remote sensing for mapping and monitoring land-cover and land-use change-an introduction. *Progress in planning,* 61**,** 269-279.

TSUCHIYA, K., KANEKO, M. & SUNG, S. 2003. Comparison of image data acquired with AVHRR, MODIS, ETM+ and ASTER over Hokkaido, Japan. *Advances in Space Research,* 32**,** 2211-2216.

TURBELIN, A. J., MALAMUD, B. D. & FRANCIS, R. A. 2017. Mapping the global state of invasive alien species: patterns of invasion and policy responses. *Global Ecology and Biogeography,* 26**,** 78-92.

UDELHOVEN, T. 2010. TimeStats: A software tool for the retrieval of temporal patterns from global satellite archives. *IEEE Journal of Selected Topics in Applied Earth Observations and Remote Sensing,* 4**,** 310-317.

ÜSTÜN, B., MELSSEN, W. & BUYDENS, L. 2007. Visualisation and interpretation of support vector regression models. *Analytica chimica acta,* 595**,** 299-309.

VÁCLAVÍK, T. & MEENTEMEYER, R. K. 2012. Equilibrium or not? Modelling potential distribution of invasive species in different stages of invasion. *Diversity and Distributions,* 18**,** 73-83.

VAN DER MEER, F., VAN DER WERFF, H. & VAN RUITENBEEK, F. 2014. Potential of ESA's Sentinel-2 for geological applications. *Remote sensing of environment,* 148**,** 124-133.

VAZ, A. S., KUEFFER, C., KULL, C. A., RICHARDSON, D. M., VICENTE, J. R., KÜHN, I., SCHRÖTER, M., HAUCK, J., BONN, A. & HONRADO, J. P. 2017. Integrating ecosystem services and disservices: insights from plant invasions. *Ecosystem Services,* 23**,** 94-107.

VERHEGGHEN, A., BONTEMPS, S. & DEFOURNY, P. 2014. A global NDVI and EVI reference data set for land-surface phenology using 13 years of daily SPOT-VEGETATION observations. *International Journal of Remote Sensing,* 35**,** 2440-2471.

VESCOVO, L., WOHLFAHRT, G., BALZAROLO, M., PILLONI, S., SOTTOCORNOLA, M., RODEGHIERO, M. & GIANELLE, D. 2012. New spectral vegetation indices based on the near-infrared shoulder

wavelengths for remote detection of grassland phytomass. *International journal of remote sensing,* 33**,** 2178-2195.

VIÑA, A., GITELSON, A. A., NGUY-ROBERTSON, A. L. & PENG, Y. 2011. Comparison of different vegetation indices for the remote assessment of green leaf area index of crops. *Remote Sensing of Environment,* 115**,** 3468-3478.

VINA, A., GITELSON, A. A., RUNDQUIST, D. C., KEYDAN, G., LEAVITT, B. & SCHEPERS, J. 2004. Monitoring maize (Zea mays L.) phenology with remote sensing. *Agronomy Journal,* 96**,** 1139-1147.

VITASSE, Y., DELZON, S., DUFRÊNE, E., PONTAILLER, J.-Y., LOUVET, J.-M., KREMER, A. & MICHALET, R. 2009. Leaf phenology sensitivity to temperature in European trees: Do within-species populations exhibit similar responses? *Agricultural and forest meteorology,* 149**,** 735-744.

VRIELING, A., MERONI, M., DARVISHZADEH, R., SKIDMORE, A. K., WANG, T., ZURITA-MILLA, R., OOSTERBEEK, K., O'CONNOR, B. & PAGANINI, M. 2018. Vegetation phenology from Sentinel-2 and field cameras for a Dutch barrier island. *Remote Sensing of Environment,* 215**,** 517-529.

VRIELING, A., SKIDMORE, A. K., WANG, T., MERONI, M., ENS, B. J., OOSTERBEEK, K., O'CONNOR, B., DARVISHZADEH, R., HEURICH, M. & SHEPHERD, A. 2017. Spatially detailed retrievals of spring phenology from single-season high-resolution image time series. *International journal of applied earth observation and geoinformation,* 59**,** 19-30.

WANG, C., CHEN, J., WU, J., TANG, Y., SHI, P., BLACK, T. A. & ZHU, K. 2017a. A snow-free vegetation index for improved monitoring of vegetation spring green-up date in deciduous ecosystems. *Remote sensing of environment,* 196**,** 1-12.

WANG, C., LI, J., LIU, Q., ZHONG, B., WU, S. & XIA, C. 2017b. Analysis of differences in phenology extracted from the enhanced vegetation index and the leaf area index. *Sensors,* 17**,** 1982.

WANG, F.-M., HUANG, J.-F., TANG, Y.-L. & WANG, X.-Z. 2007. New vegetation index and its application in estimating leaf area index of rice. *Rice Science,* 14**,** 195-203.

WANG, J., YANG, D., DETTO, M., NELSON, B. W., CHEN, M., GUAN, K., WU, S., YAN, Z. & WU, J. 2020. Multi-scale integration of satellite remote sensing improves characterization of dry-season green-up in an Amazon tropical evergreen forest. *Remote Sensing of Environment,* 246**,** 111865.

WANG, S., LU, X., CHENG, X., LI, X., PEICHL, M. & MAMMARELLA, I. 2018. Limitations and challenges of MODIS-derived phenological metrics across different landscapes in pan-Arctic regions. *Remote Sensing,* 10**,** 1784.

WANG, X. & ZHAO, C. 2005. The Application of Image Registration Based on ERDAS IMAGINE Software System. *Power System Engineering,* 21**,** 59-62.

WARDLOW, B. D. & EGBERT, S. L. 2010. A comparison of MODIS 250-m EVI and NDVI data for crop mapping: a case study for southwest Kansas. *International Journal of Remote Sensing,* 31**,** 805-830.

WATSON, C. J., RESTREPO-COUPE, N. & HUETE, A. R. 2019. Multi-scale phenology of temperate grasslands: improving monitoring and management with near-surface phenocams. *Frontiers in Environmental Science,* 7**,** 14.

WEI, H., HEILMAN, P., QI, J., NEARING, M. A., GU, Z. & ZHANG, Y. 2012. Assessing phenological change in China from 1982 to 2006 using AVHRR imagery. *Frontiers of Earth Science,* 6**,** 227-236.

WEISS, E., MARSH, S. & PFIRMAN, E. 2001. Application of NOAA-AVHRR NDVI time-series data to assess changes in Saudi Arabia's rangelands. *International Journal of Remote Sensing,* 22**,** 1005-1027.

WHITE, K., PONTIUS, J. & SCHABERG, P. 2014. Remote sensing of spring phenology in northeastern forests: A comparison of methods, field metrics and sources of uncertainty. *Remote Sensing of Environment,* 148**,** 97-107.

WHITE, M. A., DE BEURS, K. M., DIDAN, K., INOUYE, D. W., RICHARDSON, A. D., JENSEN, O. P., O'KEEFE, J., ZHANG, G., NEMANI, R. R. & VAN LEEUWEN, W. J. 2009. Intercomparison, interpretation, and assessment of spring phenology in North America estimated from remote sensing for 1982–2006. *Global Change Biology,* 15**,** 2335-2359.

WHITESIDE, T. G., BOGGS, G. S. & MAIER, S. W. 2011. Comparing object-based and pixel-based classifications for mapping savannas. *International Journal of Applied Earth Observation and Geoinformation,* 13**,** 884-893.

WILLIAMS, G. & FOLEY, A. 1976. Seasonal variations in the carbohydrate content of bracken. *Botanical Journal of the Linnean Society,* 73**,** 87-93.

WONG, C. Y., D'ODORICO, P., ARAIN, M. A. & ENSMINGER, I. 2020. Tracking the phenology of photosynthesis using carotenoid-sensitive and near-infrared reflectance vegetation indices in a temperate evergreen and mixed deciduous forest. *New Phytologist,* 226**,** 1682-1695.

WU, C., GONSAMO, A., GOUGH, C. M., CHEN, J. M. & XU, S. 2014. Modeling growing season phenology in North American forests using seasonal mean vegetation indices from MODIS. *Remote Sensing of Environment,* 147**,** 79-88.

WU, C., PENG, D., SOUDANI, K., SIEBICKE, L., GOUGH, C. M., ARAIN, M. A., BOHRER, G., LAFLEUR, P. M., PEICHL, M. & GONSAMO, A. 2017. Land surface phenology derived from normalized difference vegetation index (NDVI) at global FLUXNET sites. *Agricultural and Forest Meteorology,* 233**,** 171-182.

XIE, Q., DASH, J., HUANG, W., PENG, D., QIN, Q., MORTIMER, H., CASA, R., PIGNATTI, S., LANEVE, G. & PASCUCCI, S. 2018. Vegetation indices combining the red and red-edge spectral information for leaf area index retrieval. *IEEE Journal of selected topics in applied earth observations and remote sensing,* 11**,** 1482-1493.

XIONG, J., THENKABAIL, P. S., GUMMA, M. K., TELUGUNTLA, P., POEHNELT, J., CONGALTON, R. G., YADAV, K. & THAU, D. 2017. Automated cropland mapping of continental Africa using Google Earth Engine cloud computing. *ISPRS Journal of Photogrammetry and Remote Sensing,* 126**,** 225-244.

XU, K., QIAN, J., HU, Z., DUAN, Z., CHEN, C., LIU, J., SUN, J., WEI, S. & XING, X. 2021. A new machine learning approach in detecting the oil palm plantations using remote sensing data. *Remote Sensing,* 13**,** 236.

XU, X., JI, X., JIANG, J., YAO, X., TIAN, Y., ZHU, Y., CAO, W., CAO, Q., YANG, H. & SHI, Z. 2018. Evaluation of one-class support vector classification for mapping the paddy rice planting area in Jiangsu Province of China from Landsat 8 OLI imagery. *Remote Sensing,* 10**,** 546.

XUE, J. & SU, B. 2017. Significant remote sensing vegetation indices: A review of developments and applications. *Journal of sensors,* 2017.

YAN, D., ZHANG, X., NAGAI, S., YU, Y., AKITSU, T., NASAHARA, K. N., IDE, R. & MAEDA, T. 2019. Evaluating land surface phenology from the Advanced Himawari Imager using observations from MODIS and the Phenological Eyes Network. *International Journal of Applied Earth Observation and Geoinformation,* 79**,** 71-83.

YAN, D., ZHANG, X., YU, Y. & GUO, W. 2016a. A comparison of tropical rainforest phenology retrieved from geostationary (SEVIRI) and polar-orbiting (MODIS) sensors across the Congo Basin. *IEEE Transactions on Geoscience and Remote Sensing,* 54**,** 4867-4881.

YAN, D., ZHANG, X., YU, Y., GUO, W. & HANAN, N. P. 2016b. Characterizing land surface phenology and responses to rainfall in the Sahara desert. *Journal of Geophysical Research: Biogeosciences,* 121**,** 2243-2260.

YANG, T., ALA, M., ZHANG, Y., WU, J., WANG, A. & GUAN, D. 2018. Characteristics of soil moisture under different vegetation coverage in Horqin Sandy Land, northern China. *PLoS One,* 13**,** e0198805.

YANG, X., TANG, J. & MUSTARD, J. F. 2014. Beyond leaf color: Comparing camera-based phenological metrics with leaf biochemical, biophysical, and spectral properties throughout the growing season of a temperate deciduous forest. *Journal of Geophysical Research: Biogeosciences,* 119**,** 181-191.

YAO, R., WANG, L., HUANG, X., GUO, X., NIU, Z. & LIU, H. 2017. Investigation of urbanization effects on land surface phenology in Northeast China during 2001–2015. *Remote Sensing,* 9**,** 66.

YAO, T. & ZHANG, Q. Assessment of terrestrial vegetation dynamics from MODIS fAPAR chl product and land surface model. 2016 IEEE International Geoscience and Remote Sensing Symposium (IGARSS), 2016. IEEE, 1288-1291.

YAPI, T. S., O'FARRELL, P. J., DZIBA, L. E. & ESLER, K. J. 2018. Alien tree invasion into a South African montane grassland ecosystem: impact of Acacia species on rangeland condition and livestock carrying capacity. *International Journal of Biodiversity Science, Ecosystem Services & Management,* 14**,** 105-116.

YETEMEN, O., ISTANBULLUOGLU, E., FLORES-CERVANTES, J. H., VIVONI, E. R. & BRAS, R. L. 2015. Ecohydrologic role of solar radiation on landscape evolution. *Water Resources Research,* 51**,** 1127-1157.

YOKOYAMA, R., SHIRASAWA, M. & PIKE, R. J. 2002. Visualizing topography by openness: a new application of image processing to digital elevation models. *Photogrammetric engineering and remote sensing,* 68**,** 257-266.

YU, X., ZHUANG, D., CHEN, S., HOU, X. & CHEN, H. Vegetation phenology from multi-temporal EOS MODIS data. Weather and Environmental Satellites, 2004. International Society for Optics and Photonics, 185-193.

YUAN, C., QIN, X., QIN, Z. & WANG, R. 2018. Image segmentation based on modified superpixel segmentation and spectral clustering. *The Journal of Engineering,* 2018**,** 1704-1711.

ZALAMEA, P.-C., MUNOZ, F., STEVENSON, P. R., PAINE, C. T., SARMIENTO, C., SABATIER, D. & HEURET, P. 2011. Continental-scale patterns of Cecropia reproductive phenology: evidence from herbarium specimens. *Proceedings of the Royal Society B: Biological Sciences,* 278**,** 2437-2445.

ZEFERINO, L. B., DE SOUZA, L. F. T., DO AMARAL, C. H., FERNANDES FILHO, E. I. & DE OLIVEIRA, T. S. 2020. Does environmental data increase the accuracy of land use and land cover classification? *International Journal of Applied Earth Observation and Geoinformation,* 91**,** 102128.

ZENG, L., WARDLOW, B. D., XIANG, D., HU, S. & LI, D. 2020. A review of vegetation phenological metrics extraction using time-series, multispectral satellite data. *Remote Sensing of Environment,* 237**,** 111511.

ZHANG, D., LAVENDER, S., MULLER, J.-P., WALTON, D., ZOU, X. & SHI, F. 2018a. MERIS observations of phytoplankton phenology in the Baltic Sea. *Science of the total environment,* 642**,** 447-462.

ZHANG, X., FRIEDL, M. A. & SCHAAF, C. B. 2006. Global vegetation phenology from Moderate Resolution Imaging Spectroradiometer (MODIS): Evaluation of global patterns and comparison with in situ measurements. *Journal of Geophysical Research: Biogeosciences,* 111.

ZHANG, X., FRIEDL, M. A., SCHAAF, C. B., STRAHLER, A. H., HODGES, J. C., GAO, F., REED, B. C. & HUETE, A. 2003. Monitoring vegetation phenology using MODIS. *Remote sensing of environment,* 84**,** 471-475.

ZHANG, X., JAYAVELU, S., LIU, L., FRIEDL, M. A., HENEBRY, G. M., LIU, Y., SCHAAF, C. B., RICHARDSON, A. D. & GRAY, J. 2018b. Evaluation of land surface phenology from VIIRS data using time series of PhenoCam imagery. *Agricultural and Forest Meteorology,* 256**,** 137-149.

ZHANG, X., LIU, L. & YAN, D. 2017. Comparisons of global land surface seasonality and phenology derived from AVHRR, MODIS, and VIIRS data. *Journal of Geophysical Research: Biogeosciences,* 122**,** 1506-1525.

ZHANG, X., WANG, J., HENEBRY, G. M. & GAO, F. 2020. Development and evaluation of a new algorithm for detecting 30 m land surface phenology from VIIRS and HLS time series. *ISPRS Journal of Photogrammetry and Remote Sensing,* 161**,** 37-51.

ZHANG, X., YANG, G., XU, X., YAO, X., ZHENG, H., ZHU, Y., CAO, W. & CHENG, T. 2021. An assessment of Planet satellite imagery for county-wide mapping of rice planting areas in Jiangsu Province, China with one-class classification approaches. *International Journal of Remote Sensing,* 42**,** 7610-7635.

ZHANG, X., YE, Y., WANG, W. & WANG, Y. Detection of Land Surface Phenology from New Generation Geostationary Satellites and Its Compassion with Observations from Polar-Orbiting Satellites. AGU Fall Meeting Abstracts, 2019. A34F-03.

ZHANG, Y. & HEPNER, G. F. 2017. Short-Term Phenological Predictions of Vegetation Abundance Using Multivariate Adaptive Regression Splines in the Upper Colorado River Basin. *Earth Interactions,* 21**,** 1-26.

ZHAO, C.-Y., LIU, Y.-Y., SHI, X.-P. & WANG, Y.-J. 2020. Effects of soil nutrient variability and competitor identify on growth and co-existence among invasive alien and native clonal plants. *Environmental Pollution,* 261**,** 113894.

ZHAO, H., YANG, Z., LI, L. & DI, L. 2011. Improvement and comparative analysis of indices of crop growth condition monitoring by remote sensing. *Transactions of the Chinese Society of Agricultural Engineering,* 27**,** 243-249.

ZHAO, P., LU, D., WANG, G., WU, C., HUANG, Y. & YU, S. 2016. Examining spectral reflectance saturation in Landsat imagery and corresponding solutions to improve forest aboveground biomass estimation. *Remote Sensing,* 8**,** 469.

ZHAO, T. X. P., CHAN, P. K. & HEIDINGER, A. K. 2013. A global survey of the effect of cloud contamination on the aerosol optical thickness and its long-term trend derived from operational AVHRR satellite observations. *Journal of Geophysical Research: Atmospheres,* 118**,** 2849-2857.

ZHAO, Y. & CEN, Y. 2013. *Data mining applications with R*, Academic Press.

ZHENG, Y., WU, B., ZHANG, M. & ZENG, H. 2016. Crop phenology detection using high spatio-temporal resolution data fused from SPOT5 and MODIS products. *Sensors,* 16**,** 2099.

ZHOU, J., JIA, L. & MENENTI, M. 2015. Reconstruction of global MODIS NDVI time series: Performance of Harmonic ANalysis of Time Series (HANTS). *Remote Sensing of Environment,* 163**,** 217-228.

ZHU, G., JU, W., CHEN, J. & LIU, Y. 2014. A Novel Moisture Adjusted Vegetation Index (MAVI) to reduce background reflectance and topographical effects on LAI retrieval. *PloS one,* 9**,** e102560.

ZHU, W., CHEN, G., JIANG, N., LIU, J. & MOU, M. 2013. Estimating carbon flux phenology with satellite-derived land surface phenology and climate drivers for different biomes: A synthesis of AmeriFlux observations. *PloS one,* 8**,** e84990.

ZUO, L., LIU, R., LIU, Y. & SHANG, R. 2019. Effect of Mathematical Expression of Vegetation Indices on the Estimation of Phenology Trends from Satellite Data. *Chinese Geographical Science,* 29**,** 756-767.